8-2021

# The Periaqueductal Grey in Opioid Tolerance and Chronic Pain

Akila Ram
*Utah State University*

THE PERIAQUEDUCTAL GREY IN OPIOID TOLERANCE AND CHRONIC PAIN

by

Akila Ram

A dissertation submitted in partial fulfillment
of the requirements for the degree

of

DOCTOR OF PHILOSOPHY

in

Biology

Approved:

| | |
|---|---|
| Erin N. Bobeck, Ph.D.<br>Major Professor | Karen Kapheim, Ph.D.<br>Committee Member |
| Susannah French, Ph.D.<br>Committee Member | Mona Buhusi, Ph.D.<br>Committee Member |
| Timothy Shahan, Ph.D.<br>Committee Member | D. Richard Cutler, Ph.D.<br>Interim Vice Provost of Graduate Studies |

UTAH STATE UNIVERSITY
Logan, Utah

2021

ABSTRACT

The Periaqueductal Grey in Opioid Tolerance and Chronic Pain

by

Akila Ram, Doctor of Philosophy

Utah State University, 2021

Major Professor: Erin N. Bobeck, Ph.D.
Department: Biology

The midbrain ventrolateral periaqueductal gray (vlPAG) is a component of the descending pain modulatory pathway and activation of $\mu$-opioid receptors (MOPr) in this region produces antinociception in mice. The vlPAG is also a site of modulation of opioid tolerance, a phenomenon that emerges as a result of chronic opioid use and necessitates increasing the dose of opioid to achieve desired levels of pain relief. Studies into the mechanism of opioid tolerance have shown that the vlPAG undergoes adaptations in intracellular signaling following long-term opioid use. However, the dynamics of intracellular second messenger signaling in the vlPAG following chronic opioid use have yet to be fully examined. In this thesis, I use the MOPr agonist, morphine to characterize MOPr downstream protein kinase activation and localization patterns in the vlPAG. I first show that key intracellular kinases, Extracellular Signal-Regulated Kinase 1/2 (ERK 1/2), Protein Kinase-C (PKC), and Protein Kinase-A (PKA) are significantly increased in activity following morphine tolerance in both male and female mice. I then examine the behavioral correlates of PKC activity within this brain region. I show that sustained inhibition of PKC activity only within the vlPAG blocks the development of morphine antinociceptive tolerance in mice treated with chronic morphine. I also show that continuous blockade of PKC activity in this brain region enhances morphine antinociception in opioid naive mice. Finally, as long-term opioid use is associated with multiple negative side effects, I explored the role of the receptor GPR171 as a therapeutic target for chronic neuropathic

and inflammatory pain. I show that the GPR171 agonist, MS15203, reduces chronic neuropathic and inflammatory pain in male, but not in female mice. Taken together, this thesis identifies key intracellular signaling alterations within the vlPAG following chronic morphine, identifies the contribution of an individual kinase within this brain region in the development of opioid tolerance, and lends *in vivo* support to a non-opioid therapeutic alternative for chronic pain treatment.

(95 pages)

# PUBLIC ABSTRACT

The Periaqueductal Grey in Opioid Tolerance and Chronic Pain

Akila Ram

Pain is the body's natural warning system to indicate one is in an environment highly detrimental to survival. The body's response to the sensation of pain is to immediately withdraw from this environment, ensuring continued survival. However, when pain lasts beyond the window in which it is useful, it no longer serves as a helpful warning system but instead degrades the quality of life. Chronic pain leads to patients seeking opioids to alleviate their condition and regain control of their lives. A severe negative side effect of the use of opioids to treat chronic pain is the development of tolerance - a condition where, due to prolonged usage of opioids, the body fails to produce the desired levels of pain relief from the opioid dose. This necessitates increasing the dose of opioid and puts one at a greater risk of developing further negative side effects such as dependence and addiction. In the early 1990s we learned that tolerance to opioids, such as the drug morphine, is created and regulated in the brain. Specifically, it is created by adaptations within neurons in a midbrain region called the ventrolateral periaqueductal gray (vlPAG). This thesis has three central objectives - first to delve deeper into the vlPAG to better describe the neuronal adaptations that follow morphine tolerance, second to examine in greater specificity the contributions of a singular protein, Protein Kinase-C, in the development of morphine tolerance and third, to evaluate a novel non-opioid compound as a therapeutic for chronic pain. The studies in this thesis describe the nature and mechanism of adaptations that occur in vlPAG neurons following morphine tolerance and, in addition, describe a sex-specific non-opioid therapeutic for chronic pain.

# ACKNOWLEDGMENTS

Foremost, I want to thank my advisor, Erin Bobeck for mentoring me through my PhD and for helping me grow as a scientist and researcher. I would not be where I am today if not for Erin's leadership.

My sincere thanks to the graduate and undergraduate researchers of the Bobeck lab for their support.

Thank you, Samridhi, Laavanya, and Mathangi for being there for me through the good days and the tough times, and my amazing friends across the country for their relentless support and optimism.

My parents, Ram and Vasu, and my brother Siva, for bearing with me as I moved across the world to get a PhD.

My amazing partner, Siddharth, for all the sacrifices he's made for me and for being a pillar of support through graduate school.

Last but not the least, this thesis was written as the world is on the horizon of emerging out from the COVID-19 pandemic. Thank you to all the healthcare workers and researchers who have made our vaccines possible and given us hope.

CONTENTS

# LIST OF TABLES

# LIST OF FIGURES

# ACRONYMS

| | |
|---|---|
| AC | Adenylyl Cyclase |
| AKIP-1 | A-Kinase Interacting Protein-1 |
| ANOVA | Analysis of Variance |
| AU | Arbitrary Units |
| $\beta$-Arr | $\beta$-Arrestin |
| BSA | Bovine Serum Albumin |
| cAMP | cyclic Adenosine Monophosphate |
| cDNA | complementary Deoxyribonucleic Aicd |
| CFA | Complete Freund's Adjuvant |
| CI | Confidence Interval |
| CIPN | Chemotherapy-Induced Peripheral Neuropathy |
| CTCF | Corrected Total Cell Fluorescence |
| DAMGO | [D-Ala2, N-MePhe4, Gly-ol]-enkephalin |
| ERK 1/2 | Extracellular Signal-Regulated Kinase 1/2 |
| GABA | $\gamma$-amino butyric acid |
| GRK | G-protein Receptor Kinase |
| IHC | Immuno-Histo-Chemistry |
| MOPr | $\mu$-Opioid Receptor |
| PBS | Phosphate Buffered Saline |
| PFA | Paraformaldehyde |
| PKA | Protein Kinase-A |
| PKC | Protein Kinase-C |
| qRT-PCR | quantitative Real-Time Polymerase Chain Reaction |
| RNA | Ribonucleic Acid |
| RVM | Rostral Ventromedial Medulla |
| SEM | Standard Error of Mean |
| vlPAG | ventrolateral Periaqueductal Gray |

# CHAPTER 1

# INTRODUCTION

The ongoing opioid crisis in the United States has spurred efforts to develop safer analgesics and to better understand the neural mechanisms of opioid tolerance and addiction. It is imperative to recognize the intracellular and circuit level changes that occur during the transition from analgesia to tolerance, so they may be addressed before the symptoms of dependence develop.

## The ventrolateral periaqueductal gray

A core component of the central mechanism of descending pain modulation pathway is the ventrolateral periaqueductal gray (vlPAG). While the PAG in its entirety is subdivided into regions essential for behavior ranging from arousal to defensive evasion, the ventrolateral region has been specifically implicated in its role to produce antinociception [1, 2]. The neurons of the vlPAG that project to the rostral ventromedial medulla mediate this behavioral effect. These neurons are primarily inhibitory GABA-ergic neurons, along with a small fraction of excitatory glutamatergic and dopaminergic D2 neurons [3, 4]. Endogenous opioid peptides such as enkephalins have been shown to act on the vlPAG neurons, producing pain relief in situations such as stress-induced analgesia [5]. The presence of opioid receptors, including the $\mu$-opioid receptor, facilitates the antinociceptive function of the vlPAG.This particular brain region is special interest in the study of opioid-induced pain relief as intracellular adaptations within the vlPAG neurons facilitate the development of opioid tolerance [6].

## Opioid tolerance

Opioids, such as morphine and fentanyl, act as powerful pain-relieving agents in the short term. However, continued usage of these drugs produces adaptations within the descending pain modulatory system, decreasing the ability of the drug to produce pain relief. This necessitates increasing the dosage of the opioid to achieve the required level of pain relief so the patient may not

experience a decline in quality of life. However, as opioids also act at multiple targets in the body, including the gastrointestinal system and the reward pathway in the brain, increasing the dose of opioids creates imbalances of these physiological functions [7]. To develop better targeted therapies that produce lasting pain relief without disrupting other physiological systems, the changes that are produced in the vlPAG neurons as a result of chronic opioid exposure must first be elucidated. There is substantial evidence that the intracellular signaling pathway at the $\mu$-opioid receptor is altered following exposure to chronic morphine.

## Intracellular signaling at the $\mu$-opioid receptor

The $\mu$-opioid receptor (MOPr) is a member of the Class A family of G-protein coupled receptors, wherein its primary characteristic is its multipass transmembrane structure with seven subunits [8]. The intracellular C-terminal tail of the receptor is coupled with a heterotrimeric G-protein, including an inhibitory G-protein, the G$\beta$ and G$\gamma$ subunits. Within the vlPAG, MOPr is primarily expressed in GABA-ergic neurons that project to the medulla. Activation of the MOPr via agonists such as morphine, inhibits the release of GABA from these projections neurons, thereby disinhibiting the neurons of the medulla and resulting in antinociception at the spinal cord [9].

The development of antinociceptive tolerance to opioids has been linked to MOPr-dependent changes within the vlPAG. At the circuitry level, opioid tolerance is the term given to the physiological state when activation of the MOPr does not produce adequate disinhibition of the medullary neurons. This occurs when the activation of MOPr in the vlPAG projection neurons does not sufficiently inhibit the release of GABA, owing to a dysregulated communication from the receptor to the neurotransmitter vesicle [10]. While the precise nature of these adaptations is under intense scrutiny, there is considerable evidence to suggest that following persistent activation of the MOPr, there is an agonist-dependent upregulation of intracellular signaling, such as greater permeability of potassium channels and increased cyclic AMP signaling [11]. In addition to these changes, positive or negative modulation of protein kinase activity has been hypothesized to be a medium through which the receptor signaling is dysregulated after opioid tolerance.

The MOPr signals via the G-protein pathway following activation by its agonists. The G$\alpha$ subunit

initiates a signaling cascade which begins with the inhibition of enzymatic activity of Adenylyl Cyclase (AC). This leads to the inhibition of the kinase Protein Kinase-A. In the interim, the MOPr is phosphorylated by a kinase such as Protein Kinase-C (PKC) or G-protein Receptor Kinase (GRK) to terminate further G-protein dependent signaling and desensitize the receptor. This process results in the recruitment of a scaffolding protein, $\beta$-Arrestin, to recruit the cellular endocytosis machinery to internalize the receptor [12]. There is considerable evidence that following persistent MOPr activation by morphine, there is a shift in the signaling system from a G-protein dependent to a predominantly $\beta$-Arrestin ($\beta$-Arr) dependent pathway [13, 14]. A characteristic of a $\beta$-Arr-dependent pathway is the activation of Extracellular Signal-Regulated Kinase (ERK 1/2). Following the assembly of the endocytosis machinery within a clathrin-coated pit, the C-terminal tail of the MOPr protrudes outside the endocytic vesicle and is associated with $\beta$-Arr [15]. This system enables persistent signaling of the MOPr via $\beta$-Arr long after the receptor is no longer on the surface.

## Extracellular Signal-Regulated Kinase

ERK 1/2 is a kinase that is essential regulator for neurodevelopment such as memory consolidation, synaptic regulation, and for initiating further signaling cascades [16, 17]. Following activation of the MOPr by an agonist, ERK 1/2 activation depends on the biased nature of the agonist. Certain agonists such as fentanyl, produce rapid antinociception and are efficient at recruiting $\beta$-Arr to the receptor. ERK 1/2 can thus be activated acutely by fentanyl. On the other hand, morphine is a weak recruiter of $\beta$-Arr and does not produce ERK 1/2 activation at an acute timepoint [18]. Interestingly, there is recent evidence to show that following chronic morphine treatment, there is a shift in MOPr signaling from a G-protein dependent to a $\beta$-arr dependent pathway [19]. If this were the case, chronic morphine treatment would produce antinociceptive tolerance when measured at the behavioral level and also ERK 1/2 activation when measured at the cellular level in the vlPAG.

## Protein Kinase-A

PKA is activated when the repressor subunits of the enzyme bind to cAMP and dissociate from the holoenzyme, thus freeing the catalytic subunit [20]. PKA has been reported to contribute

to the dampening of GABA inhibition seen in vlPAG neurons following morphine tolerance [10]. Following exposure to chronic morphine, it has been reported that AC undergoes a superactivation event caused by a switching of the G$\alpha$ protein from an inhibitory to an excitatory facilitator [21]. While this result has been previously shown in in-vitro culture and ex-vivo slice preparations, this result has not yet been shown in native tissue from the vlPAG.

## Protein Kinase-C

PKC is a downstream kinase activated by the G$\beta$ and G$\gamma$ subunits of the MOPr following activation by an agonist [22]. Conventional isoforms of PKC have been reported to phosphorylate the MOPr after activation by morphine, but not fentanyl [23]. This effect is an example of the G-protein bias of the morphine at the MOPr. Further, dominant-negative PKC and phosphorylation-deficient MOPr have been shown to be insensitive to the acute effects of morphine in that the receptor signaling was not terminated and PKC was unable to phosphorylate the receptor [24, 25]. However, the nature of PKC activation, particularly within the vlPAG, following chronic morphine has remained unexplored.

## The multiple facets of chronic pain

Chronic pain is a severe painful sensation that persists long after the initial injury or trauma has healed. It is a growing public health concern in the united states and contributes to a decreased quality of life for the patient in addition to lost time and wages in the economy due to the patients' ill health. The current opioid epidemic in the united states, which has been the center of multiple legal battles and humanitarian crises has largely been brought about by the overprescription of opioids for chronic pain [26]. The crux of the crisis stems from the fact that while opioids are remarkable at alleviating pain at the short-term, extended use of opioids for months without a plan to taper off the usage results in disastrous consequences for the patient [27]. In patients with chronic pain, alternative therapies are needed to address the source of pain in addition to using supplemental opioids to manage breakthrough pain. Further, while we have coined the umbrella term, chronic pain, the pathophysiology of this condition differs upon the source of pain.

In addition to the highly debilitatory nature of chronic pain, there is further reporting that females are disproportionally affected by chronic pain. This includes higher incidences of reporting of migraines and fibromyalgia [28, 29]. Further, females are very likely to be prescribed opioids for the treatment of chronic pain and develop rapid dependence and addiction these drugs [30]. This is an increasing problem in the study of pain particularly as a majority of historical research into the central and peripheral mechanisms regulating pain and antinociception were performed in male animals [31].

## Non-opioid treatment of chronic pain

Armed with our new knowledge of the opioid receptor structure and function and with the help of computations tools to identify and predict functions of recently discovered receptor systems, the field can make vast progress into developing pain therapeutics that are not derived from opioid narcotics [32]. These new classes of drugs can be developed to target the $\mu$, $\kappa$, or $\delta$ opioid receptors or a heteromer thereof, in a way that minimizes its interaction with the reward circuit [33, 34]. Alternatively, the drug can target any of several non-opioid physiological targets that participate in antinociception, thereby avoiding interactions with opioid receptors altogether [35, 36].

One such target for the non-opioid treatment of chronic pain is the receptor, GPR171. A recently deorphanized neuropeptide receptor, GPR171 was initially characterized for its role in the hypothalamus to promote feeding upon activation [37, 38]. Along with the observation that its mRNA is widely expressed in the mouse brain, closer investigation showed that it is present in the vlPAG on the same neurons that express the MOPr [39, 40]. An exploratory study in the Bobeck lab showed that the systemic administration of the GPR171 agonist, MS15203, enhanced morphine antinociception on acute thermal pain tests. Further preliminary investigation by the laboratory into the dynamics of GPR171 expression in other pain modalities indicated that chronic neuropathic pain decreased protein levels of this receptor within the vlPAG. Capitalizing on this pain-dependent modulation of GPR171 levels, we explored the role of this receptor in modulating hypersensitivity and allodynia in chronic pain modalities in both males and females.

In the first study, intracellular kinase activation and localization patterns within the vlPAG were evaluated in male and female mice. The activity of G-protein and $\beta$-Arr-dependent second messenger kinases – ERK 1/2, PKC, and PKA – is elevated within the vlPAG following morphine tolerance. These kinases also displayed treatment-dependent localization patterns within the vlPAG that inform the specific adaptations created in vlPAG neurons following morphine tolerance.

In the second study, the contribution of Protein Kinase-C (PKC) activity in the development of morphine tolerance was examined. PKC association with the MOPr was quantified within the vlPAG following multiple paradigms of morphine treatment. It is noted that in addition to elevated pPKC levels in the vlPAG, the activated PKC co-localizes with the MOPr in the vlPAG extensively after morphine tolerance. Intra-PAG administration of a PKC inhibitor compound, Gö-7874, prevented the development of antinociceptive tolerance towards morphine. Further, inhibition of PKC activity enhanced the antinociceptive effect of morphine in opioid-naïve mice.

In the third study, the therapeutic potential of the receptor GPR171 was evaluated. A synthetic agonist of the receptor, compound MS15203, was injected systemically over 5 consecutive days in male and female mouse models of chronic neuropathic or inflammatory pain. When administered in male mice experiencing either modality of chronic pain, MS15203 reduced both neuropathic and inflammatory pain. However, it was found that females undergoing chronic pain did not experience a reduction in thermal or mechanical hypersensitivity in response to the GPR171 agonist compound. This study reports a sexual dimorphism in analgesic properties of GPR171.

# CHAPTER 2

# MORPHINE-INDUCED KINASE ACTIVATION AND LOCALIZATION IN THE PERIAQUEDUCTAL GRAY OF MALE AND FEMALE MICE

## 2.1 Introduction

Opioids, such as morphine, while being highly effective in the treatment of acute pain, have adverse consequences if consumed long-term. One such consequence of chronic morphine use is the development of antinociceptive tolerance where a particular dose ceases to relieve pain over time, thus leading to dose escalation to achieve desired levels of pain relief. *In-vitro* and *in-vivo* studies have indicated that the ventrolateral periaqueductal gray (vlPAG) of the midbrain regulates the development of opioid antinociceptive tolerance [10, 41, 42, 43]. Neurons in the vlPAG project to the rostral ventromedial medulla (RVM), which then synapse onto the dorsal horn of the spinal cord. Activation of the vlPAG by pharmacological or electrophysiological methods disinhibits the RVM, which subsequently blocks incoming pain signals received by the spinal cord from peripheral nociceptors [1, 4, 44]. Upon repeated exposure to opioids, the vlPAG has decreased ability to produce antinociception and disinhibit the neurons of the RVM [42]. While the behavioral and electrophysiological outcomes of opioid tolerance have been well established, there is not a clear consensus on the intracellular adaptations within the vlPAG.

Molecular studies have evaluated $\mu$-opioid receptor-induced G protein and $\beta$-arrestin intracellular signaling pathways and have revealed that chronic morphine induces distinct signaling patterns compared to other opioids [45, 46]. These signaling changes have been implicated in the development of opioid tolerance [47, 48]. Furthermore, vlPAG inhibition of G protein-activated enzymes, such as adenylyl cyclase (AC), c-Jun N-terminal kinase, and protein kinase-C (PKC) leads to a reduction in the development of morphine tolerance [10, 48**?** ]. Conversely, inhibition of the $\beta$-arrestin-dependent proteins, ERK 1/2 and GRK, leads to greater tolerance or no change in tolerance

to morphine [14**?** ] respectively. However, these studies have predominantly been conducted in male rodents despite known sex differences in opioid-induced antinociception and tolerance. Typically, these sex differences manifest as reduced antinociception in females when comparing the same dose of opioids in males, which has been linked to neuroanatomical differences within the descending pain pathway. These include a greater density of $\mu$-opioid receptors (MOPr) within the vlPAG and more opioid sensitive projection neurons from vlPAG to RVM in males [49, 50]. However, intracellular protein-specific alterations in the vlPAG of females have not been studied in detail and the community lacks a clear comparison of paradigm-specific sex differences in vlPAG intracellular signaling.

The goal of the current study is to bridge the gap in knowledge regarding the intracellular kinase signaling profile within the vlPAG following acute and chronic morphine treatment in both male and female mice. Overall, we find similar patterns of morphine-induced activation of several key kinases in both sexes, but the magnitude of expression is typically greater in males. Furthermore, we find that kinases downstream of $\beta$-arrestin are colocalized to endosomes only after chronic morphine, whereas G-protein associated kinases are localized to the nucleus.

## 2.2 Materials and Methods

### 2.2.1 Animals

Adult male and female C57BL/6CS mice (Charles River Laboratories, CA), 6-8 weeks old and weighing 18-26 g at the start of the study were used in behavioral and immunofluorescence experiments. Food and water were available *ad libitum*, except during testing. Mice were housed (four to five per cage) in a humidity and temperature-controlled room with a 12-hour light/dark cycle (off at 1900). All procedures were performed during the light cycle and in accordance with the Guide for the Care and Use of Laboratory Animals adopted by the National Institutes of Health. The animal procedures were approved by the Utah State University Institutional Care and Use Committee (Protocol #2775).

### 2.2.2 Study design

This study was not pre-registered. Mice were assigned to treatment groups by block randomization, where equal numbers of morphine or saline-treated mice were present. Enumeration of the nuclear punctae in the pPKA analysis was manually performed by experimenters blinded to the drug treatments. The experimenter was not blinded to the drug treatments during behavior testing, automated image analysis, or statistical analysis. No calculations were performed to predetermine sample size. The study was designed to be exploratory. No exclusion criteria were pre-determined and no animals were excluded in the experiments performed.

### 2.2.3 Drug treatment:

Subjects were administered morphine sulfate (West-Ward Pharmaceuticals) dissolved in 0.9% saline (10 mg/kg in a volume of 10 ml/kg i.p.). For acute morphine treatment, the animals were administered a single dose of morphine 30 minutes before brain collection. For chronic morphine treatment, the animals were administered morphine twice daily, for a total of 9 doses. This particular dose was selected since it is the half-maximal antinociceptive dose (ED50) that also leads to behavioral tolerance in various strains of male C57BL/6 mice [51, 52, 53]. The subjects' brains were collected 30 minutes following the final dose of morphine or saline. This time point has been previously shown to correspond with peak MAP kinase (eg. ERK 1/2) activation [54] and morphine antinociception [40].

### 2.2.4 Thermal nociception assays

Male and female mice were habituated to room temperature apparatus and were handled daily for 3 days prior to the study. Nociception was assessed using the hot plate (Harvard Apparatus, Holliston, MA) and warm-water tail flick (Thermo Scientific, Waltham, MA) assays. For the hot plate assay, mice were placed on a heated surface with the temperature adjusted to 52. Time to the first sign of nociception, such as paw licking or jump response, on the hot plate was recorded. The cut-off period for this assay was 60 seconds to minimize tissue damage. For the tail flick assay, mice were gently restrained and the distal third of their tails were immersed in a water bath set to

50. The latency in tail withdrawal was recorded and a cut-off period of 20 seconds was maintained to prevent tissue damage.

Male and female mice were administered morphine (10 mg/kg i.p.) or 0.9% saline (10 ml/kg i.p.) twice daily for a total of 9 injections. All animals were tested on the hot plate and tail flick assays prior to drug administration to assess baseline scores. The post-drug testing took place 30 min following drug administration on days 1, 3, and 5; where day 1 is the first day of drug treatment. Morphine antinociceptive tolerance was assessed by a return to baseline thresholds as previously established [53, 55]. Following the behavioral study, the mice were classified as chronic morphine- or saline-treated animals and their brains were isolated for immunofluorescence analysis. A subset of mice in each treatment group were injected with the drug treatment protocol without the behavioral testing mentioned above.

### 2.2.5 Immunofluorescence staining and digital image acquisition

Animals were deeply anesthetized using isofluorane and transcardially perfused with 4% paraformaldehyde (PFA). Isofluorane was selected as the anesthetic as the circulatory system of the mouse must be functional for successful transcardial perfusion. Their brains were post-fixed in 4% PFA for 1 hour following which they were stored in 1x PBS until further processing. Sectioning was performed on a vibratome (Leica Biosystems, Germany) and 50 µm sections containing the vlPAG were selected for immunofluorescence analysis. The sections were first incubated in sodium borohydride (1% in PBS) to expose the epitopes. Subsequently, they were permeabilized with Triton-X 100 (Sigma-Aldrich, St. Louis, MO), blocked with normal goat serum (5% in PBS), and incubated overnight in primary antibodies in their appropriate buffer [1% BSA (Sigma) and 3% Triton X-100 (Sigma) in PBS]. The following day, the slices were washed in PBS and incubated for 2 hours in diluted secondary antibodies in 1% BSA in PBS. The antibodies were sourced from Cell Signaling Technology (Rabbit anti-pERK 1/2 Cat. 4370S 1:200; Rabbit anti-pPKC Cat. 38938S 1:400; Rabbit anti-pPKA substrate Cat. 9621S 1:200), Abcam (Goat anti-Eea1 Cat. 208942 1:200), Life Technologies (Goat anti-Rabbit A594 Cat. A11037 1:1000; Donkey anti-Goat A488 Cat. A11055

1:1000) and Jackson ImmunoResearch (Donkey anti-Rabbit A594 Cat. 711-586-152 1:1000 ). Following a second incubation with the fluorophore-conjugated antibody and subsequent PBS washes, the slices were briefly (5 mins) incubated in DAPI, washed with PBS and mounted with an anti-fade (ProLong Diamond Anti-Fade, Life Technologies) on a glass slide. Confocal images of coronal sections comprising of the rostrocaudal axis of the vlPAG as, defined by the mouse brain atlas [56], were acquired on a Zeiss LSM 710 confocal microscope (Carl Zeiss Microscopy, Germany) at Utah State University's microscopy core facility. Microscope hardware information and laser settings for each fluorophore are detailed in Supplementary Note 1.

### 2.2.6 Image processing and fluorescence quantification

Fluorescence intensities of individual kinases were calculated from unedited images while correcting for local background fluorescence. Briefly, for each image of the vlPAG hemisphere that was analyzed, 10 regions corresponding to either pERK 1/2, Eea1, pPKC or pPKA substrate were selected that encompass the entire cell body. Three regions corresponding to local background were also selected for each image. This process was performed for the left and right vlPAG hemispheres and repeated across three coronal sections per subject. On average, 20-30 images per condition were analyzed depending on the kinase, treatment group, sex, and type of analysis performed. Each IHC image containing one hemisphere of the vlPAG was analyzed as an independent measurement to account for the structural and functional heterogeneity of the PAG columns [57, 58, 59] in addition to controlling for the laterality of antinociception in the PAG [60, 61]. We broadly assessed kinase activation in the vlPAG without filtering cell-type specificity, as was performed previously [62, 63]. Following automated image thresholding, fluorescence intensities and relevant parameters were measured with ImageJ (NIH). The corrected total cell fluorescence (CTCF) was calculated for each cell from the integrated density measurement using the formula: CTCF = Integrated Density – (Area of selection x background mean fluorescence). The fluorescence intensities were measured in Arbitrary Units (AU).

For statistical analyses, average CTCF values of each image in a treatment group were normalized to the average of the saline control group of the specific sex using the formula: Y = [(Y-K)/K]*100, where Y is the individual data point and K is the overall average of the saline group for the particular sex and kinase. As there were differences in the saline groups between males and females, we performed this normalization to better compare morphine-induced kinase activity. Colocalization of pERK 1/2 and Eea1, imaged using red and green fluorescent channels respectively, was represented as the Pearson's correlation coefficient and was calculated using the JACoP plugin in ImageJ. This was done in order to automate the analysis in an unbiased manner. The plugin measures overlap between the red and green fluorescent channels with the Pearson's coefficient (r) being the output. A coefficient of 1 is indicative of total overlap while a coefficient of 0 implies no overlap. This method to quantify colocalization of Eea1 with other proteins has been used previously using immunofluoresence in cells [62]. Representative images from all experiments were processed using the Iterative Deconvolve 3D macro in ImageJ to enhance signal and remove fluorescent artifacts. All images were processed through 5 deconvolution cycles.

### 2.2.7 Statistical analysis:

Morphine antinociceptive tolerance in male and female mice was analyzed using two independent two-way ANOVAs. The main effects tested were drug treatment and time. To compare the acute effects of morphine across sexes, t-tests were performed on the thermal latencies of male and female mice administered with a single dose of morphine (10 mg/kg). Sex was not included as a factor in fluorescence quantification or behavior analysis as male and female mice were not concurrently tested. All fluorescence quantification data are expressed as violin plots showing the frequency distribution of pooled CTCF values representative of each hemisphere. The median value along with the 25th and 75th quartiles are indicated within each violin. Normality was measured using a D'Agonstino & Pearson normality test and variance was measured using Spearman's test for heteroscedasticity. The data met the assumptions of normal distribution and homogenous variance. No statistical test for outliers were performed. Statistical analyses including unpaired t-tests, one- and two-way ANOVA followed by post-hoc tests, and graphing were performed using Graph-

Pad Prism 8 (GraphPad, San Diego, CA). Microsoft Excel (Microsoft, Redmond, WA) was used to calculate CTCF values. The number of subjects and specific statistical analyses used in each experiment are indicated in the text.

## 2.3 Results

### 2.3.1 Sex differences in the development of antinociceptive tolerance

Given the large body of literature pertaining to sex differences in morphine action, we sought to assess the development of morphine tolerance in male and female mice using a 5-day treatment paradigm (Fig. 2.1A). We administered systemic morphine (10mg/kg i.p.) twice-daily over the course of 5 days. In males (n=5/group), morphine produced statistically significant antinociception on the hot plate (Time [$F(3,24) = 13.77$, $p<0.0001$]; Treatment [$F(1,8) = 7.583$, $p<0.5$]; Time x Treatment [$F(3, 24) = 7.07$, $p<0.01$]) and tail flick assays (Time $F(3,24) = 11.8$, $p<0.0001$]; Treatment [$F(1,8) = 26.35$, $p<0.001$]; Time x Treatment [$F(3, 24) = 18.08$, $p<0.0001$]) compared to saline controls as measured by a repeated measures two-way ANOVA. A Bonferroni's post-hoc analysis revealed that male mice treated with morphine returned to baseline latency on the hot plate (Bonferroni $p>0.05$, morphine group baseline vs Day 5; Fig. 2.1B), which is indicative of the development of antinociceptive tolerance to morphine. However, the male mice did not return to baseline latency by Day 5 on the tail flick assay (Bonferroni $p<0.001$, morphine group baseline vs Day 5; Fig. 2.1C). Morphine produced statistically significant antinociception in females (n=5-6/group) on the hot plate (Time [$F(1.8, 16.2) = 12.82$, $p<0.001$]; Treatment [$F(1,9) = 31.22$, $p<0.001$]; Time x Treatment [$F(3, 27) = 9.5$, $p<0.001$]) and tail flick assays (Time [$F(3,24) = 11.8$, $p<0.0001$]; Treatment [$F(1,9) = 36.27$, $p<0.0001$]; Time x Treatment [$F(3, 27) = 14.78$, $p<0.0001$]) as measured by a repeated measures two-way ANOVA. A Bonferroni's post-hoc analysis revealed that the morphine-treated females went on to develop tolerance on the hot plate (Bonferroni $p>0.05$) and tail flick (Bonferroni $p>0.05$) tests by Day 5 in comparison to their baseline on Day 0. There was no sex difference in the acute effect of morphine on either the hot plate (Morphine-Male vs Morphine-Female, Day 1, unpaired t-test $p>.05$) or tail flick assays (Morphine-Male vs Morphine-Female,

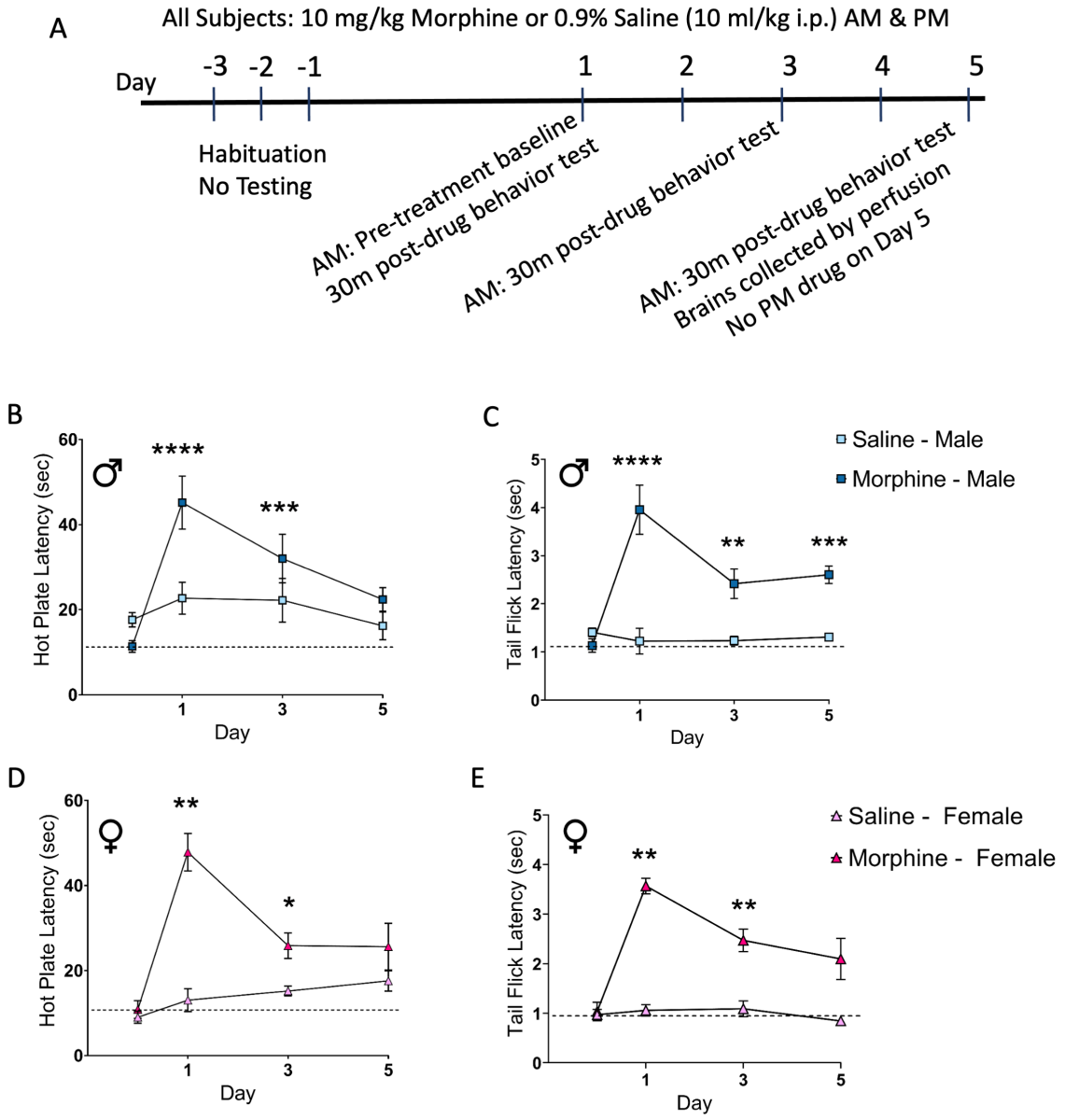


Fig. 2.1: Chronic morphine produces differences in antinociceptive tolerance in male and female mice. (A) An illustrative timeline of the experimental design of the behavioral testing and chronic morphine or saline treatment paradigm. Male mice (n=5/group) treated with morphine (10 mg/kg) developed tolerance on the hot plate (B) but not the tail flick (C) assay. Female mice (n=5-6/group) treated with morphine developed antinociceptive tolerance to morphine by Day 5 of the experiment on both the hot plate (D) and tail flick (E) assays. Two-way ANOVA with Bonferroni's post-hoc test. *$p<0.05$, **$p<0.01$, ***$p=0.0001$ indicate significant differences compared to the treatment group baseline.

Day 1, unpaired t-test $p>.05$). Mice of both sexes that were treated with saline did not display any change in thermal latency over the course of the study.

### 2.3.2 Chronic morphine activates endosome-lined ERK 1/2 in the vlPAG

We subsequently set out to assess the activation pattern and localization of ERK 1/2 within the vlPAG after acute and chronic morphine treatment. We show that morphine treatment produced statistically significant elevation of pERK 1/2 levels in the vlPAG of both males (n=10 images from 6 mice/group) [$F(2, 24) = 21.88$, $p<0.0001$] and females (n=10 images from 5 mice/group) [$F(2, 19) = 4.8$, $p<0.05$] as measured by two independent one-way ANOVAs. A Tukey's post-hoc test revealed that following acute morphine treatment (10mg/kg), there is a moderate increase in pERK 1/2 activation only in males ( 44% increase vs Saline, Tukey $p<0.01$; Fig. 2.2A and 2.2B) but not females (Tukey $p>0.05$; Fig. 2.2A and 2.2C). The post-hoc analysis further revealed that following chronic morphine for 5 days, both males (97% increase vs Saline, Tukey $p<0.0001$; Fig. 2.2B) and females (51% increase vs Saline, Tukey $p<0.01$; Fig. 2.2C) show highly elevated levels of pERK 1/2 in the vlPAG compared to the saline controls. See Table 1 for a summary of sex differences found for all kinases.

To determine whether this ERK 1/2 activity was occurring within endosomes of the vlPAG of these animals, we performed co-staining of pERK 1/2 with a marker for the early endosome, Early Endosome Antigen1 (Eea1, Fig. 2.2D). As we did not observe any sex differences in Eea1 signal, we pooled the data from males and females for further analysis (n=6 images from 5 mice/group). We note that fluorescence signal from the endosomal marker increases following morphine tolerance [$F(2, 19) = 7.24$, $p<0.05$] as measured by a one-way ANOVA, but a Tukey's post-hoc analysis revealed that the increase is relative only to acute morphine (36% increase vs Acute Morphine, Tukey $p<0.05$; Fig. 2.2E).

We next evaluated co-localization of pERK 1/2 and Eea1 signals to calculate an overlap score indicated by the Pearson's coefficient (r). We found that there is a statistically significant overlap

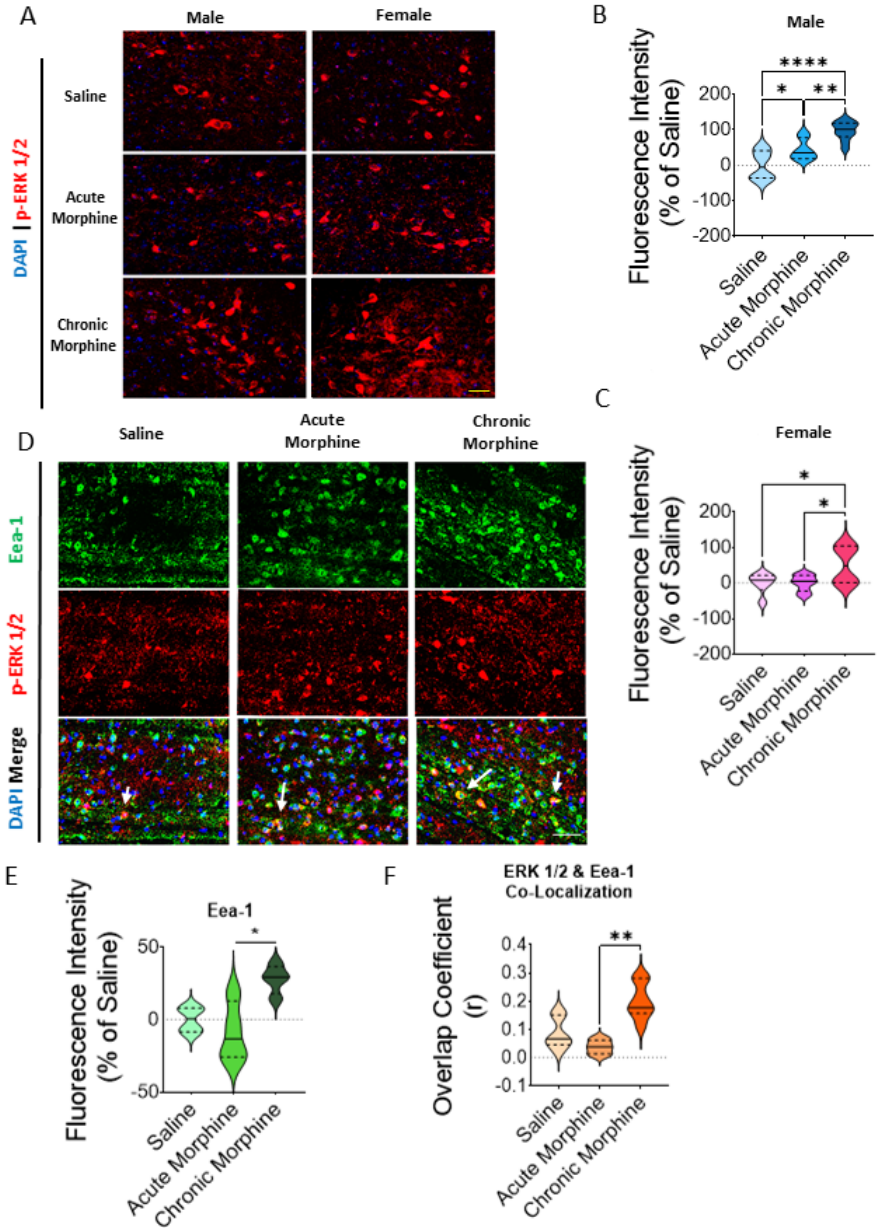


Fig. 2.2: Chronic morphine elevated levels of pERK 1/2 in the vlPAG which colocalizes with the endosome. (A) 20x Confocal images of the vlPAG stained for pERK 1/2 (red) and counterstained with DAPI (black). Male (n=5/group) and female (n=5/group) mice were treated with either 1 injection of morphine (10 mg/kg, i.p.) for the acute paradigm or 9 injections of morphine or saline for the chronic morphine and saline paradigms respectively. Quantification of fluorescence signal indicates that chronic morphine significantly elevated pERK 1/2 levels in the vlPAG in both males (n=10 images from 6 mice/group) (B) and females (n=10 images from 5 mice/group) (C), however acute morphine treatment increased pERK 1/2 only in males. (D) Representative 20x confocal images of male vlPAG sections co-stained with pERK 1/2 (red) and Eea1 (green) and counterstained with DAPI (black). (E) Eea1 fluorescence quantification (n=5/group) indicates that the signal is increased in chronic morphine compared to acute morphine. (F) Quantification of pERK 1/2 and Eea1 signal colocalization as measured by the Pearson's coefficient. Kruskal-Wallis test (ERK-Eea1 colocalization only), One-way ANOVA & Tukey's post-hoc test *p<0.05, **p<0.01, ***p=0.0001. Scale bars = 50 $\mu$m.

between the pERK 1/2 and Eea1 signal as measured by a Kruskal-Wallis test. A Dunn's post-hoc analysis revealed that the median difference in signal intensity is higher in chronic morphine animals (Dunn's $p<0.01$ vs acute morphine; Fig. 2.2F) indicating that the enhanced ERK 1/2 signaling in the vlPAG following morphine tolerance is likely originating at the endosome.

### 2.3.3 Chronic morphine activates Protein Kinase-C in the vlPAG

We next assessed the activation pattern of pPKC within the vlPAG after acute and chronic morphine treatment. We show that morphine treatment produced statistically significant elevation of pPKC levels in the vlPAG of both males (n=10 images from 5 mice/group) [$F(2, 21) = 13.34$, $p<0.001$] and females (n=15 images from 5 mice/group) [$F(2, 28) = 8.1$, $p<0.01$] as measured by a one-way ANOVA. A Tukey's post-hoc test revealed that pPKC levels remained unchanged in males (Tukey $p>0.05$; Fig. 2.3A and 2.3B and females (Tukey $p>0.05$; Fig. 2.3A and 2.3C) following acute morphine. However, chronic morphine treatment resulted in a statistically significant increase in pPKC activation in the vlPAG in males (102% increase vs Saline, Tukey $p<0.0001$ vs saline Fig. 2.3B) and females (57% increase vs Saline, Tukey $p<0.01$ vs saline Fig. 2.3A and 2.3C).

### 2.3.4 Chronic morphine activates Protein Kinase-A in the vlPAG

We next assessed the activation pattern and localization of phosphorylated PKA substrates within the vlPAG after acute and chronic morphine treatment. We show that morphine treatment produced statistically significant alterations of PKA substrate phosphorylation in males (n=10 images from 6 mice/group) [$F(2,21) = 10.9$, $p<0.0001$] and females (n=8 images from 5 mice/group) [$F(2,19) = 8.53$, $p<0.01$] as measured by two one-way ANOVAs. A Tukey's post-hoc analysis revealed that the signal intensity of phosphorylated PKA substrates in males increased following acute morphine treatment (95% increase vs Saline, Tukey $p<0.01$ acute morphine vs saline; Fig. 2.4A and 2.4B) which was similar to the pattern after chronic morphine (115% increase vs Saline, Tukey $p<0.001$ chronic morphine vs saline, ns chronic morphine vs acute morphine; Fig 4A and B). On the other hand, a Tukey's post-hoc analysis in females revealed that acute morphine treatment did not elevate PKA substrate phosphorylation (Tukey $p>0.05$ saline vs acute morphine; Fig. 2.4A and

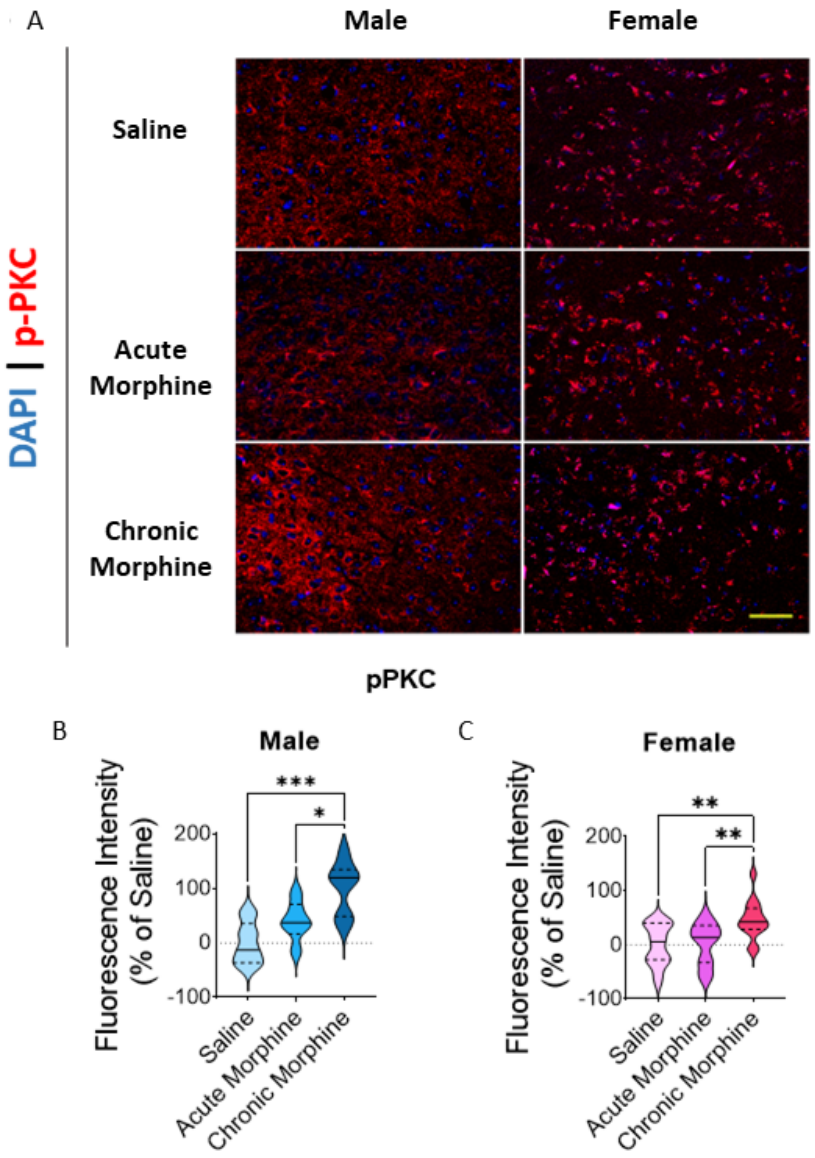


Fig. 2.3: Chronic morphine increased levels of pPKC in the vlPAG. (A) 20x Confocal images of the vlPAG stained for pPKC (red) and counterstained with DAPI (black). Quantification of fluorescence signal indicated that chronic morphine significantly elevated pPKC levels in the vlPAG in both males (B) (n=10 images from 5 mice/group) and females (C) (n=15 images from 5 mice/group). One-way ANOVA and Tukey's post-hoc test *p<0.05, **p<0.01, ***p<0.0001. Scale bar = 50 µm.

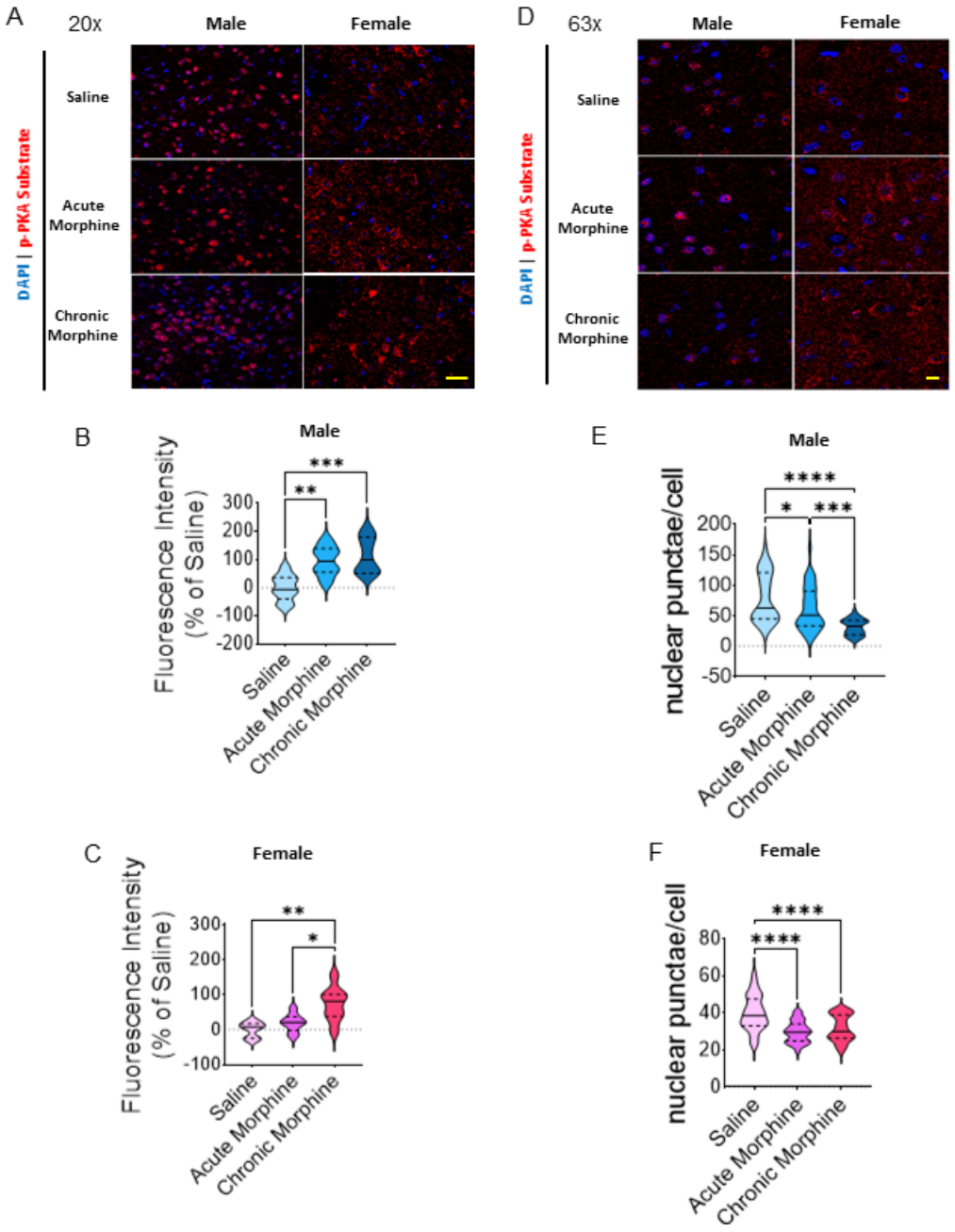


Fig. 2.4: Chronic morphine elevated global levels of pPKA substrate in the vlPAG but resulted in fewer nuclear translocations of the substrate. (A) Representative 20x confocal images of the vlPAG stained for pPKA substrate (red) and counterstained with DAPI (black). Quantification of fluorescence signal indicates that chronic morphine significantly elevated pPKC substrate levels in the vlPAG in both males (B) (n=10 images from 6 mice/group) and females (C) (n=8 images from 5 mice/group). (D) Representative 63x confocal images of nuclei of vlPAG neurons indicating nuclear punctae of pPKA substrates. Quantifications of pPKA substrate nuclear punctae in male (E) and female (F) vlPAG show a reduction in punctae following acute morphine which is further reduced in males after chronic morphine. One-way ANOVA and Tukey's post-hoc test *$p<0.05$, **$p<0.01$, ***$p<0.001$, ****$p<0.0001$. Scale bar = 50 µm (20x) and 10 µm (63x).

| Kinase | Sex | Acute Morphine | Chronic Morphine |
|---|---|---|---|
| **ERK 1/2** | Males | ↑ | ↑↑ |
| | Females | No change | ↑↑ |
| **PKC** | Males | No change | ↑↑ |
| | Females | No change | ↑↑ |
| **PKA** | Males | ↑ | ↑ |
| | Females | No change | ↑↑ |

Table 2.1: Differential kinase expression patterns after acute and chronic morphine in male and female mice. ↑ indicates significant difference from saline, ↑↑ indicates significant difference from saline and acute morphine.

2.4C) and chronic morphine treatment resulted in marked elevation of PKA substrate phosphorylation (74% increase vs Saline, Tukey $p<0.01$ saline vs chronic morphine, $p<0.05$ chronic morphine vs acute morphine; Fig. 2.4A and 2.4C). This elevation of pPKA substrate phosphorylation following chronic morphine treatment is indicative of AC superactivation in the vlPAG following persistent MOPr stimulation.

Over the course of our pPKA substrate analysis, we noticed that there was a remarkable localization of signal as nuclear punctae. Following manual enumeration of the punctae, we showed that there was a significant difference in pPKA substrate nuclear punctae numbers between morphine treatments in both males [$F(2, 113) = 19.97$, $p<0.0001$] and females [$F(2, 191) = 36.66$, $p<0.0001$] using a one-way ANOVA. A Tukey's post-hoc analysis revealed that following acute morphine treatment, there was a significant decrease in the number of nuclear punctae in both males (Tukey $p<0.05$ acute morphine vs saline; Fig. 2.4D and 2.4E) and females (Tukey $p<0.0001$ acute morphine vs saline; Fig. 2.4D and 2.4F). With continued exposure to morphine, the number of pPKA substrate nuclear punctae decreased in males (Tukey $p<0.001$ chronic morphine vs acute morphine, $p<0.0001$ chronic morphine vs saline; Fig. 2.4D and 2.4E), but not females (Tukey $p<0.0001$ chronic morphine vs saline, $p>0.05$ chronic morphine vs acute morphine; Fig. 2.4D and 2.4F). While it is not immediately apparent how the nuclear transport of these proteins is impacted by morphine exposure, this result adds another dimension to the spatiotemporal dynamics of PKA activity.

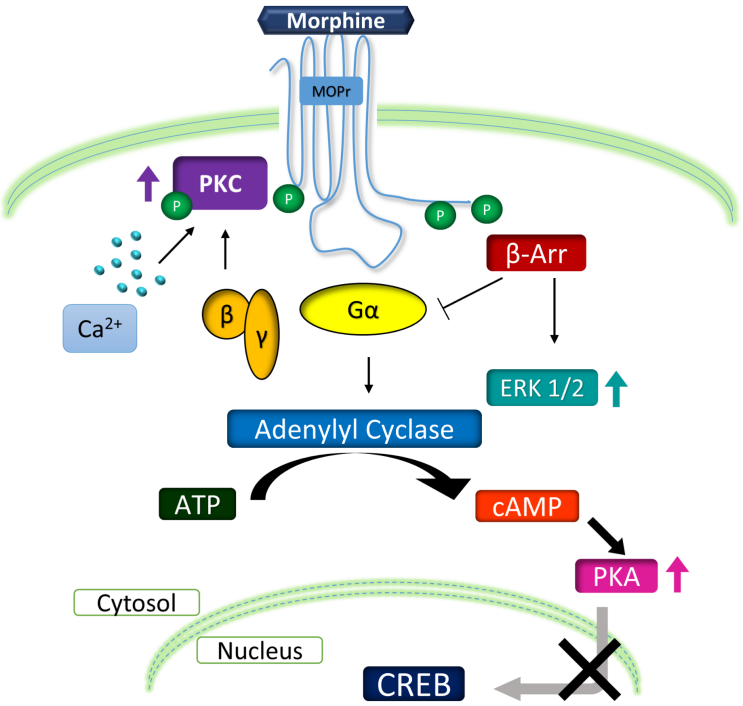


Fig. 2.5: Chronic morphine alters intracellular signaling pathways within the vlPAG. Activated forms of the kinases ERK 1/2, PKC, and PKA are elevated in the mouse vlPAG after 5 days of repeated morphine injections. ERK 1/2 is activated as a consequence of $\beta$-arrestin recruitment. PKC is activated via the $\beta\gamma$ subunits of the G protein. PKA is activated as a result of adenylyl cyclase superactivation following prolonged G$\alpha_i$ stimulation.

## 2.4 Discussion

The current study shows that the protein kinases ERK 1/2, PKC, and PKA are activated in the vlPAG following repeated morphine. Our conclusions follow an immunofluorescence-based assessment of kinase activation and localization in the vlPAG, which has not been possible with other molecular approaches. The elevation in signaling by activated kinases in chronic morphine-treated animals demonstrates that morphine tolerance can be mapped onto a region of the brain that modulates antinociception. We found a similar degree of tolerance development in males and females with the exception of males on the tail flick assay. This correlates with a similar pattern of kinase activation and localization in the vlPAG following repeated morphine injections despite differences found after acute morphine. This suggests that the behavioral manifestation of long-term morphine treatment is regulated by the interaction of multiple signaling systems including, but

not limited to, the MAP kinase, PKC, and AC-PKA pathways as illustrated in Fig. 2.5.

### 2.4.1 Extracellular Signal-Regulated Kinase 1/2

G protein-coupled receptors including MOPr engage the $\beta$-arrestin pathway in an agonist-dependent manner to facilitate internalization and recycling of the receptor which is vital to ensure continued sensitivity to opioids [64]. Previous studies have indicated that chronic morphine administration activates ERK 1/2 in the vlPAG [14, 63] and in the VTA [65] of rats, with direct consequences to the antinociceptive and rewarding effects of morphine, respectively. Further, studies have shown that opioid-induced ERK 1/2 activity in the vlPAG is internalization-dependent [19, 66], strongly indicating the involvement of $\beta$-arrestin. Our study extends this literature by showing that systemic administration, not just intra-vlPAG, can activate ERK 1/2 in the vlPAG of mice. An interesting observation that has not been shown previously is that we found ERK 1/2 was activated following acute morphine in males by 44% compared to saline treatment. However, the kinase was not significantly increased in acute morphine treated females. Previous studies have found that acute morphine injection into the vlPAG of rats does not activate ERK 1/2 [14]. Our observations may be attributed to differences in the model organism or route of administration. Further, various opioids produce differential ERK 1/2 activation within the vlPAG. For instance, pERK 1/2 activation within the vlPAG occurs following acute DAMGO injections but not following morphine or fentanyl [14, 19, 67].

Several GPCRs, including MOPr, can continue to signal via $\beta$-arrestin after having been localized to the endosomal compartment following internalization [15, 68]. The phosphorylated C-terminal tail of the GPCR is located outside the periphery of the clathrin-coated endosome, making $\beta$-arrestin accessible to the cytosolic compartment [69, 70]. Using quantifiable co-localization assays, we demonstrated significant overlap of pERK 1/2 and the early endosomal marker Eea1. Taken together, the increase in pERK 1/2 activity coupled with the elevated co-localization of the kinase with the endosome leads us to infer that the MOPr in the vlPAG can continue to signal via the $\beta$-arrestin-ERK 1/2 pathway after chronic morphine treatment, a phenomenon that is described in

multiple opioid receptors [71, 72].

Our results support the existing hypothesis that following long-term MOPr agonism, there is a shift in ERK 1/2 activation from a G-protein-dependent pathway to a $\beta$-arrestin-dominant system [13, 67]. Inhibition of ERK 1/2 within the vlPAG increases the magnitude of morphine tolerance [14], suggesting that its activity is a compensatory measure that counteracts morphine antinociceptive tolerance.

### 2.4.2 Protein Kinase-C

In the morphine-MOPr system, Protein Kinase-C (PKC) is activated by the $\beta\gamma$ subunits of G-proteins via the phosphoinositide 3-kinase (PI3K) cascade [22, 73]. Activated PKC is known to phosphorylate the MOPr to facilitate desensitization of the receptor and terminate G-protein signaling following morphine administration [66, 74, 75**?** ]. Further, as PKC interacts with the MOPr, the receptor is not rapidly internalized and recycled. This leads to an extended duration where the receptor is unresponsive to further exposure to morphine. This cellular phenomenon has been shown to contribute to the reduction in opioid antinociception [12, 76, 77, 78]. Intra-PAG and intracerebroventricular inhibition of PKC has been shown to reduce the development of acute and chronic tolerance to morphine [47, 79**?** ], emphasizing the role of the kinase in regulating morphine antinociception. In addition to the behavioral outcomes, PKC inhibitors have been shown to decrease opioid receptor desensitization in cellular models and interact with ion channels such as TRPV1 to modulate MOPr activity and antinociception [80, 81]. The current study utilizes antibodies that recognize phosphorylated motifs of conventional PKC subtypes ($\alpha$, $\beta$, and $\gamma$). These PKC isoforms have been demonstrated to mediate morphine tolerance [66, 82], making the assessment of their activity and localization valuable. While the studies inhibiting PKC were performed *in vivo*, many of the fundamental studies evaluating agonist-specific PKC activity were performed *in vitro* [83, 84**?** ]. Here, we use native tissue from a wild-type mouse strain to show that PKC activation is increased in the vlPAG via phosphorylation of its Ser-Thr sites. We also note that pPKC levels are not significantly altered after acute morphine treatment in both sexes, but are elevated following

chronic morphine treatment. In an average cell, chronic morphine treatment increases PKC activation in males by 102% and in females by 57% compared to the respective sex-specific control. This pattern suggests an underlying mechanism by which long-term morphine induces elevated PKC activation within the vlPAG which may contribute to the development of antinociceptive tolerance.

### 2.4.3 Protein Kinase-A

PKA is a ubiquitous downstream modulator of G protein-coupled receptors that is activated by the enzyme AC. As a result of activating the MOPr, the inhibitory G-protein that is coupled to the receptor inhibits AC and PKA activity. In this study, PKA activation was assessed by proxy via antibodies targeting its phosphorylated substrates as antibodies targeting total PKA would not provide information about enzyme activity. In our results, we found an interesting localization pattern, where phosphorylated PKA substrates are a) present in the nuclei of the vlPAG cells and b) altered in number depending on the duration of morphine exposure. We note that the total pPKA substrate signal is greatest in our chronic morphine treated mice, with males displaying a 115% increase and females displaying a 74% increase in PKA activity in the vlPAG compared to the sex-specific saline controls. Our analysis further shows that these chronic morphine-treated animals also have the least number of nuclear punctae of pPKA substrate. Sustained morphine treatment *in-vitro* has been shown to result in a phenomenon known as cAMP superactivation [21, 85]. This delayed compensatory response to the effects of morphine has been postulated to contribute to opioid tolerance and dependence [86, 87]. As sustained PKA activity is also directly responsible for maintaining cellular tolerance to opioids, intervening in cAMP superactivation is a possible avenue to ensure longer-acting opioid responsiveness. Inhibition of this pathway (AC or PKA) has been shown to reverse morphine tolerance [10, 47] further implicating that alterations of this signaling pathway regulates tolerance.

While PKA nuclear translocation has been shown to be facilitated by A-Kinase Interacting Protein-1 (AKIP1), accounting for PKA activity inside the nucleus [20, 88], we are yet unsure if this is modulated by opioid receptor agonists. While previous studies that correlate PKA superac-

tivation with cellular tolerance were performed *in-vitro*, our results provide a corroboration of the hypothesis that enhanced PKA activity within the vlPAG is associated with antinociceptive tolerance to morphine.

### 2.4.4 Sex-Differences in Morphine Tolerance

In the current study, we have shown that male and female mice develop rapid antinociceptive tolerance to repeated injections of morphine. This data is similar to what has been shown previously in rats [89, 90]. Some studies have indicated that female rodents require higher doses of morphine compared to males to produce equivalent analgesia [91]. We note that in our study, 10 mg/kg morphine produced comparable analgesia in terms of thermal latencies in both males and females. Previous studies have attributed sex differences in opioid antinociception and tolerance to differences in MOPr density, number of projections within the descending pathway, microglia activity, and interactions with estrogen and the estrogen receptor. Here we have taken this a step farther to show that the molecular correlates of tolerance development to morphine can be attributed to an increase in pERK 1/2, pPKC, and pPKA substrate signaling in the vlPAG in both sexes.

We note that the males in our study developed antinociceptive tolerance on only the hot plate but not on the tail flick assay. The hot plate test is a supraspinal measure of nociception, whereas the tail flick assay is a spinal reflex. We attribute this discrepancy to the differential development of opioid tolerance as a result of MOPr expression and immune microenvironments at the spinal and supraspinal levels [92, 93, 94]. Taken together, the spinal cord engages intracellular signaling pathways and immune responses that differ from that of the vlPAG. The interaction of the immune microenvironment with opioids such as morphine has been previously reviewed in Ref. [6].

Previous studies have focused on only males to evaluate intracellular kinases after morphine treatment [14, 63, 95, 96]. To our knowledge, this is the first study to directly compare males to females using quantification of kinase activity specifically within the vlPAG, which is challenging to accomplish with conventional protein quantification methods given the size of the vlPAG in mice.

We note the absence of a significant increase in ERK 1/2 activation in females after acute morphine. On the other hand, following chronic morphine, females displayed an elevated pERK 1/2 signal similar to the males. This effect indicates comparable levels of $\beta$-arrestin signaling in males and females after chronic morphine. As this signaling pathway has been associated with internalization of the receptor [12, 53], this increase in pERK 1/2 activity in females suggests that they are may display similar levels of receptor internalization as males after chronic morphine treatment. A summary of the sex differences of each kinase can be found in Table 1.

The current study found no sex differences in the pattern of PKC activity. The absence of a short-term change in PKC activity levels suggests that while chronic morphine preferentially activates PKC, acute morphine may engage a different kinase to terminate MOPr signaling. Previous reports have shown that estradiol does not contribute to MOPr desensitization via PKC in the presence of the opioid peptide DAMGO [97, 98, 99]. This supports our observation that the presence of estrogen does not alter morphine- and MOPr-dependent PKC activity.

Female mice show no change in PKA activity after acute morphine treatment, similar to the effect seen with ERK 1/2 and PKC. Females show superactivation of AC and reduced nuclear transport of phosphorylated PKA substrates only after chronic morphine. On the other hand, male mice display elevated PKA activity immediately following acute morphine treatment, which remains steadily elevated through morphine tolerance. This effect can be attributed to the method of chronic opioid treatment, where morphine injections are repeated by a delay of several hours. This can result in multiple cycles of cellular withdrawal and subsequently a self-compensatory effect to prevent further AC activation. While estradiol and chronic morphine have both been shown enhance hypothalamic PKA activation in guinea pigs [97, 100], it is yet unclear if they both contribute synergistically to PKA activation within the vlPAG. Further, there is evidence that activated PKA substrates can localize to distinct intracellular compartments [88]. However, the role of estrogen in mediating their nuclear transport remains to be established. Current evidence points to immuno-modulatory effects of morphine and estrogen in contributing to sex differences [91] in opioid effects. The sex

differences in kinase activity following morphine may also contribute to the behavioral differences that are commonly seen in morphine antinociception and tolerance. Further studies are required to collect evidence of cross-talk between the estradiol-estrogen receptor and MOPr-AC signaling systems in the vlPAG.

In conclusion, our results demonstrate that chronic intermittent morphine treatment results in the enhanced activation of several protein kinases within the vlPAG that are downstream of the MOPr in male and female mice. The activation of these kinases can serve to enhance morphine tolerance (PKC and PKA) or compensate for tolerance (ERK 1/2).

# Supplementary Material: Microscope and Laser Settings

| Equipment Settings | 20x | 63x |
|---|---|---|
| **Objectives** | Plan-Apochromat 20x/0.8 M27 | Plan-Apochromat 40x/1.40 Oil DIC M27 |
| **Pinhole** | 47µm | 47µm |
| **Pixel dwell** | 1.58 µs | 1.58 µs |
| **Z-depth** | n/a | 25 µm |

Table 2.2: Equipment settings for 20x and 63x objectives

| Laser Settings | A594 | DAPI | A488 |
|---|---|---|---|
| **Filters** | 585-734 nm | 410-579 nm | 495-592 nm |
| **Digital offset** | (-130) – (-95) | (-162) – (-182) | (-93) – (-42) |
| **Digital gain** | 1.0 | 1.0 | 1.0 |
| **Master gain** | 911 – 1032 | 816 | 770 – 824 |
| **Averaging** | line 8 | line 8 | line 8 |
| **Laser power** | 2% | 2% | 2% |

Table 2.3: Laser settings for fluorophore detection

# CHAPTER 3

# INHIBITION OF PROTEIN KINASE-C WITHIN THE VENTROLATERAL PERIAQUEDUCTAL GRAY COUNTERACTS THE DEVELOPMENT OF MORPHINE ANTINOCICEPTIVE TOLERANCE

## 3.1 Introduction

The midbrain ventrolateral periaqueductal gray (vlPAG) is a component of the descending pain modulatory system and exerts pro- or anti-nociceptive effects following input from higher cerebral centers. It is of particular interest in the study of pain systems as it is a site of action of endogenous and exogenous mu opioid agonists. Additionally, the vlPAG governs the development of opioid antinociceptive tolerance, a phenomenon where repeated administration of an opioid ceases to produce adequate pain relief. Tolerance results in a necessity to escalate the dose of the opioid administered, leading to deleterious side effects such as dependence and addiction.

Current efforts to understand opioid action in the vlPAG include studies that characterize intracellular signaling cascades within this brain region. Opioid painkillers, such as morphine, bind to $\mu$-opioid receptors (MOPr) in the vlPAG. Following repeated opioid exposure, multiple cellular and molecular adaptations occur within this brain region, which can be interpreted as molecular signatures of behavioral changes. Intracellular kinases that participate in the MOPr signaling pathway are of particular interest since manipulation of MOPr-downstream kinases can indeed have behavioral outcomes.

Previous *in vitro* studies have shown that PKC phosphorylates Ser-Thr sites in the activated MOPr, leading to desensitization of the receptor [23, 24]. PKC-dependent desensitization has been shown to be the predominant cellular mechanism when the MOPr is stimulated by morphine, but not high-potency agonists. These studies hypothesize that this particular mechanism is inefficient at

enabling rapid MOPr internalization and recycling to the membrane, thereby contributing to morphine tolerance *in vitro* [83]. However, whether PKC interacts with MOPr after morphine agonism within the vlPAG *in vivo* is unknown.

PKC is also of particular interest within the MOPr pathway *in vivo*. The kinase has been shown to interact with $\mu$, $\delta$, and $\kappa$ opioid receptors to modulate stress and analgesia behaviors across different brain regions [82, 101, 102]. In particular, PKC activity has been shown to enable antinociceptive tolerance towards partial MOPr agonists such as morphine. Conversely, PKC is ineffective at reducing tolerance to repeated administrations of the more potent MOPr agonist, DAMGO [24, 103]. While previous studies on PKC have inhibited conventional PKC isoforms in the CNS to modulate behavioral morphine tolerance, the specific role of PKC within the vlPAG to modulate this effect has not been described [104].

We hypothesize that Protein Kinase-C activity in the vlPAG plays a critical role in the development of morphine antinociceptive tolerance. We found that repeated inhibition of PKC specifically within the vlPAG prevents the development of morphine tolerance. In addition, we note that inhibition of PKC activity within the vlPAG enhances the antinociceptive effect of morphine in opioid-naïve mice. Our findings establish that PKC activity within the vlPAG contributes to the development of morphine antinociceptive tolerance.

## 3.2 Materials and Methods

### 3.2.1 Animals

Adult male C57BL/6 mice (Charles River Laboratories, CA), 6-8 weeks old and weighing 18-26 g at the start of the study were used in the study. Food and water were available ad libitum, except during testing. Mice were housed (four to five per cage) in a humidity and temperature-controlled room with a 12-hour light/dark cycle (off at 1900). All procedures were performed in accordance with the Guide for the Care and Use of Laboratory Animals adopted by the National Institutes

of Health and were approved by the Institutional Animal Care and Use Committee of Utah State University (Protocol no. 2775).

### 3.2.2 Drugs

Morphine sulphate (West Ward, Inc.) was obtained as 8 mg/ml stock and different dosages (10, 8, 4.4, 2 & 1 mg/kg) were prepared by diluting with sterile 0.9% saline. Go-7874 (Cat. 365252, Sigma-Aldrich) was dissolved in 10% DMSO and 16nmols were cumulatively administered per animal over 8 microinjections. This particular concentration of the PKC inhibitor was selected as it was previously shown to prevent the development of morphine tolerance when injected into the cerebrospinal fluid [47]. Animals were pre-treated by microinjection of either the PKC inhibitor or DMSO vehicle (0.2 $\mu$l/session) 15 mins prior to systemic injection of morphine (10mg/kg) or saline. This dose of morphine was selected as it has been reported to produce rapid antinociceptive tolerance after repeated injections [40].

### 3.2.3 Stereotaxic surgery

Briefly, animals were anaesthetized with a mixture of ketamine (100 mg/ml) and xylazine (20 mg/ml, Akorn, Inc.) in sterile 0.9% saline, injected intraperitoneally (i.p.) at a dose of 10 ml/kg. The animal was then placed in a stereotaxic apparatus (Stoelting and Kopf). The skull was exposed by an incision of the scalp followed by application of povidone iodide (Betadine). A small craniotomy was made using a hand drill at the region of interest. Stereotaxic coordinates (AP: -4.8, DV: -0.6, ML:-2.3 from bregma) as described previously [56, 105] were used to lower the guide cannula into the vlPAG. Two small bone anchor screws (Cat. 51457, Stoelting) were implanted away from the cannulation site to provide support for the cranial plaster (Stoelting). A stylet was placed in the implanted cannula to prevent blockage. Guide cannula (4 mm) and stylets (4 mm) were made in-house using a 25g syringe needle (Exel Inc.) and a metal wire (Small Parts, Inc.) respectively. Injectors to deliver the drug through the guide cannula were made in-house using a metal wire (Small Parts, Inc) trimmed to a length of 5 mm, which is 1 mm beyond the guide cannula. Mice were placed in a clean cage near a gentle heat source until recovered from anesthesia and then pair-

housed housed in the animal facility. Their health was monitored by assessing grooming and weight daily during the course of their recovery and behavioral testing. Behavioral tests were performed after at least 10 days of recovery. At the conclusion of the behavioral study, cresyl violet (Sigma) was microinjected into the cannula and animals were euthanized by CO2 inhalation. The animals' brains were isolated, sectioned to 100 um thickness on a vibratome (Leica) and microinjection location was examined using a brightfield microscope (Keyence BZ-X810).

### 3.2.4 Intra-vlPAG microinjection

Over the course of recovery from stereotaxic surgery, animals were handled daily to acclimatize them to the experimenter and to prevent occlusion of the cannula by fluid clots. For microinjection of the PKC inhibitor or vehicle, animals were gently restrained and the injector was lowered through the guide cannula. The injector was set up to be connected to a $1\mu$l syringe (Hamilton) using flexible tubing. The syringe plunger was depressed at a rate of $0.1\mu$l/30s for a total of $0.2\mu$l/session. Following microinjection of the appropriate volume of drug or control solution, the injector was left in place for another 30s to prevent backflow.

### 3.2.5 Behavior testing

Following complete recovery from surgery, mice were tested on the hot plate and tail flick assays to obtain their baseline thermal nociceptive thresholds. On Day 1 of the study, the effect of the PKC inhibitor on acute morphine administration was assessed. Briefly, following pre-treatment with Gö-7874 or 10% DMSO, animals were injected with either morphine (10mg/kg, i.p.) or 0.9% saline (10ml/kg, i.p.). 30m following the morphine or saline treatment, the animals' thermal latencies were assessed on the hot plate and tail flick tests. The animals were not subjected to further behavioral tests until Day 5. On Day 5 of the study, the animals were subjected to a morphine dose-response paradigm, during which the subjects were challenged with log-normal increasing doses of morphine and tested on their thermal nociceptive thresholds.

### 3.2.6 Immunofluorescence staining and confocal microscopy

Immunofluorescence staining was performed as described previously [40]. Briefly, the mice

were deeply anesthetized using isofluorane and transcardially perfused with 4% paraformaldehyde (PFA). Their brains were post-fixed in 4% PFA for 1 hour following which they were stored in 1x PBS until further processing. Sectioning was performed on a vibratome (Leica Biosystems, Germany) and 50 $\mu$m sections containing the vlPAG were selected for immunofluorescence analysis. The sections were first incubated in sodium borohydride (1% in PBS) to expose the epitopes and reduce autofluorescence caused by the fixative. Subsequently, they were permeabilized with Triton-X 100 (Sigma-Aldrich, St. Louis, MO), blocked with normal goat serum (5% in PBS), and incubated overnight in primary antibodies in their appropriate buffer [1% BSA (Sigma) and 3% Triton X-100 (Sigma) in PBS]. The following day, the slices were washed in PBS and incubated for 2 hours in diluted secondary antibodies in 1% BSA in PBS. The antibodies were sourced from Cell Signaling Technology (Rabbit anti-pPKC Cat. 38938S 1:400), Neuromics (Guinea Pig anti-MOPr Cat. GP10106 1:200) and Life Technologies (Goat anti-Rabbit A594 Cat. A11037 1:1000; Goat anti-Guinea Pig A647 Cat. A21450 1:1000). Following a second incubation with the fluorophore-conjugated antibody and subsequent PBS washes, the slices were briefly (5 mins) incubated in DAPI, washed with PBS and mounted with an anti-fade (ProLong Diamond Anti-Fade, Life Technologies) on a glass slide. Confocal images of coronal sections comprising of the rostrocaudal axis of the vlPAG as, defined by the mouse brain atlas [56], were acquired on a Zeiss LSM 710 confocal microscope (Carl Zeiss Microscopy, Germany) at Utah State University's microscopy core facility.

### 3.2.7 Quantification of fluorescence intensity and signal overlap

Fluorescence intensities of individual kinases were calculated from unedited images while correcting for local background fluorescence. Briefly, for each image of the vlPAG hemisphere that was analyzed, 10 regions corresponding to either pPKC or MOPr were selected that encompass the entire cell body. Three regions corresponding to local background were also selected for each image. This process was performed for the left and right vlPAG hemispheres and repeated across three coronal sections per subject. Each IHC image containing one hemisphere of the vlPAG was analyzed as an independent measurement to account for the structural and functional heterogeneity of the PAG columns [57, 58, 59] in addition to controlling for the laterality of antinociception in the

PAG [60, 61]. We broadly assessed kinase activation in the vlPAG without filtering cell-type specificity, as was performed previously [62, 63]. Following automated image thresholding, fluorescence intensities and relevant parameters were measured with ImageJ (NIH). The corrected total cell fluorescence (CTCF) was calculated for each cell from the integrated density measurement using the formula: CTCF = Integrated Density – (Area of selection x background mean fluorescence). The fluorescence intensities were measured in Arbitrary Units (AU).

For statistical analyses, average CTCF values of each image in a treatment group were normalized to the average of the saline control group of the specific sex using the formula: Y = [(Y-K)/K]*100, where Y is the individual data point and K is the overall average of the saline group for the particular sex and kinase. As there were differences in the saline groups between males and females, we performed this normalization to better compare morphine-induced kinase activity. Colocalization of pERK 1/2 and Eea1, imaged using red and green fluorescent channels respectively, was represented as the Pearson's correlation coefficient and was calculated using the JACoP plugin in ImageJ. This was done in order to automate the analysis in an unbiased manner. The plugin measures overlap between the red and green fluorescent channels with the Pearson's coefficient (r) being the output. A coefficient of 1 is indicative of total overlap while a coefficient of 0 implies no overlap. This method to quantify colocalization of Eea1 with other proteins has been used previously using immunofluoresence in cells [62]. Representative images from all experiments were processed using the Iterative Deconvolve 3D macro in ImageJ to enhance signal and remove fluorescent artifacts. All images were processed through 5 deconvolution cycles.

### 3.2.8 Statistical Analysis

Results are presented as mean ± standard error of mean (SEM). Statistical analyses of behavioral studies were performed using a repeated measures two-way analysis of variance (ANOVA) combined with Bonferroni's post-hoc test. Ninety-five percent confidence intervals (CI) were used to compare individual ED50 values following a significant ANOVA. Statistical analyses of qRT-PCR data and fluorescence quantification were performed using a one-way ANOVA combined with

a Tukey's post-hoc test. Normality of data was evaluated using the D-Agostino and Pearson test. Experimenters were not blinded to drug treatment over the course of the study. Morphine treatment produces marked hyperlocomotion in mice and Gö-7874 possesses a strong orange hue, making blinding impractical for the experimenter. All graphing and statistical analyses were performed using Prism 9.0 (GraphPad, San Diego, CA).

## 3.3 Results

### 3.3.1 Activated Protein Kinase-C is co-localized with the $\mu$-opioid receptor in the ventrolateral PAG following morphine tolerance

Previous *in vitro* studies have suggested that morphine-induced activation of the MOPr causes recruitment of PKC to the receptor for phosphorylation. Receptor phosphorylation results in the termination of G-protein signaling and is considered to be the first step in receptor desensitization and internalization. In order to determine if PKC associates with MOPr in the vlPAG following morphine treatment, we performed co-staining for pPKC and MOPr in brain slices of mice treated with acute or chronic morphine (Fig. 3.1A). We quantified the intensity of MOPr fluorescence in the vlPAG of saline, acute morphine, and chronic morphine treated animals. A one-way ANOVA indicated significant differences in MOPr fluorescence intensity between these treatment groups ($F(2, 149) = 16.15$, $p<0.0001$). A Tukey's post-hoc analysis revealed that the fluorescence signal intensity is highest in chronic morphine-treated animals (Saline vs Chronic Morphine $p<0.0001$; Acute Morphine vs Chronic Morphine $p<0.001$; Fig. 3.1B, C). This indicates that following chronic morphine, there appears to be an increase in the protein levels of the MOPr in the vlPAG. We then analyzed the overlap between the two pPKC and MOPr signals and computed a Pearson's correlation coefficient. A non-parametric comparison of the signal overlap score indicated significant differences between the median scores of the groups (Kruskal-Wallis test, $p<0.0001$). A Dunn's multiple comparisons analysis revealed that the median difference in signal intensity is higher in chronic morphine treated animals (Saline vs Chronic Morphine, $p<0.0001$; Acute Morphine vs Chronic Morphine, $p<0.01$), indicating that the activated PKC is associated with the MOPr to a greater degree in these mice (Fig

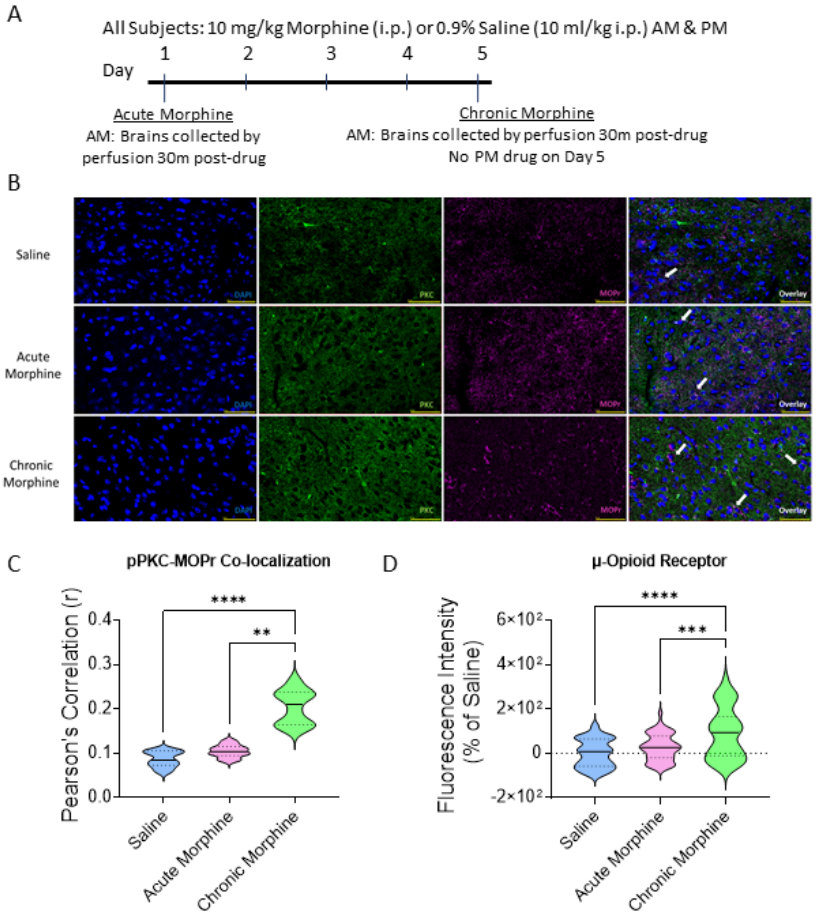


Fig. 3.1: Activated Protein Kinase-C is co-localized with the $\mu$-opioid receptor in the ventrolateral PAG following morphine tolerance. (A) Representative 20x images of the vlPAG stained for pPKC (green), MOPr (magenta) and DAPI (blue) (B) Quantification of immunofluorescence signal from MOPr. (C) Quantification of signal overlap between pPKC and MOPr channels. One-way ANOVA with Bonferroni's post-hoc test and Kruskal-Wallis test with Dunn's multiple comparisons, $**p<0.01$, $***p<0.001$, $****p<0.0001$. Scale bar = 50$\mu$m

3.1B, D).

### 3.3.2 Acute Protein Kinase-C inhibition does not affect morphine antinociception

We proceeded to locally inhibit PKC activity by unilaterally implanting a cannula over the vlPAG to deliver the PKC inhibitor, Gö-7874 (see Fig. 3.2A for a timeline). Only mice that had injection sites located within or directly adjacent to the ventrolateral PAG were included in analysis as good placements (Fig. D) In order to assess if acute inhibition of PKC had any effect on the antinociceptive effect of morphine, we tested the mice on the hot plate and tail flick assays following the microinjection and drug treatment. A two-way ANOVA indicated significant differences in thermal latencies in both the hot plate (Time $F(2, 33.23) = 287.3$, $p<0.0001$; Treatment $F(3, 17) = 17.45$, $p<0.0001$; Time x Treatment $F(6,34) = 94.85$, $p<0.0001$) and tail flick (Time $F(2, 22.74) = 55.89$, $p<0.0001$; Treatment $F(3, 18) = 9.01$, $p<0.0001$; Time x Treatment $F(6,36) = 15.63$, $p<0.0001$) tests. A Tukey's post-hoc analysis of the hot plate or tail flick tests revealed that there were no differences in thermal latencies between treatment groups prior to the commencement of the PKC inhibition paradigm ($p>0.05$). The post-hoc analysis also revealed that following acute morphine treatment, the thermal latencies of the mice were significantly different compared to the baseline of the respective group in both the hot plate and tail flick tests (Tukey's $p<0.05$). However, there were no differences in thermal latencies on the hot plate or tail flick tests between groups that were pre-treated with Vehicle or Gö-7874 (Tukey's $p>0.05$). Thus, acute treatment with the PKC inhibitor, Gö-7874 does not alter the antinociceptive effects of morphine, producing comparable antinociception as the Vehicle control.

### 3.3.3 Inhibition of Protein Kinase-C within the vlPAG prevents the development of morphine antinociceptive tolerance

On Day 5 of the study, the development of morphine tolerance was assessed in mice. Baseline hot plate and tail flick latencies were measured prior to the morphine dose-response test. A one-way ANOVA indicated that on Day 5 of the study, the thermal threshold baselines of the groups were not significantly different from each other on both the hot plate ($F(3, 19) = 2.99$, $p>0.05$) and tail

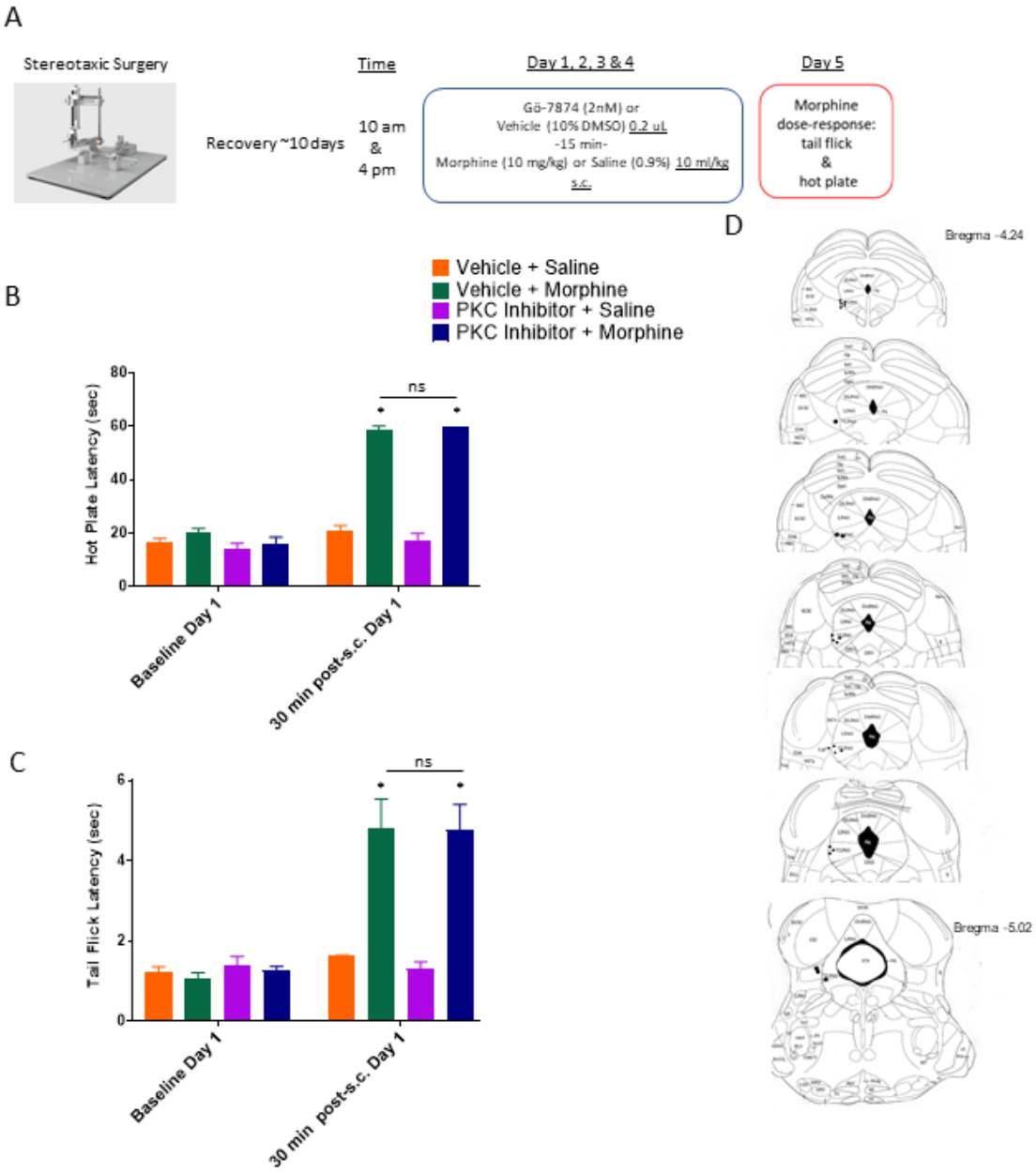


Fig. 3.2: Acute Protein Kinase-C inhibition does not affect morphine antinociception. (A) A pictorial timeline of the intra-vlPAG PKC inhibition paradigm. (B) Hot plate and (C) Tail flick latencies of mice on Day 1 of the study. The mice were first microinjected with the PKC inhibitor or vehicle. 15 minutes later, they were given a subcutaneous injection of morphine or saline. Acute antinociceptive effects of morphine were tested 30 mins after the s.c. injection. (D) Representative images of the rostro-caudal axis of the ventrolateral PAG depicting intra-vlPAG cannula placements.

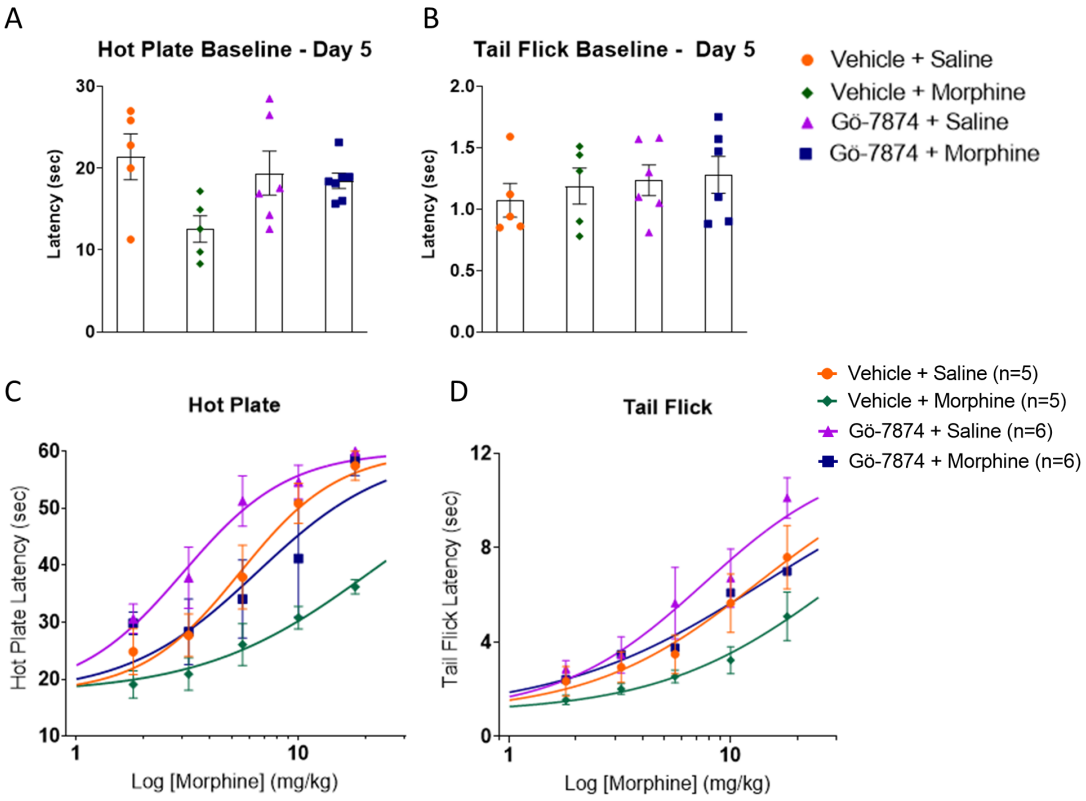


Fig. 3.3: Inhibition of Protein Kinase-C within the vlPAG prevents the development of morphine antinociceptive tolerance. (A) Hot plate and (B) Tail flick baselines prior to the morphine dose-response test. (C) Hot plate and (D) Tail flick latencies of mice over the course of a morphine dose-response to test the development of antinociceptive tolerance.

flick ($F(3, 19) = 0.38$, $p>0.05$) tests. Repeated morphine treatment caused a significant rightward shift in the morphine dose-response curve on Day 5 on the hot plate ($F(3, 117) = 32.9$; Fig. 3.3C) and the tail flick ($F(3, 117) = 9.63$; Fig. 3.3D ) tests, indicating the development of antinociceptive tolerance. Repeated pre-treatment of the Protein Kinase-C inhibitor, Gö-7874, preceding each morphine injection did not cause this rightward shift, revealing that PKC inhibition within the vlPAG prevented the development of morphine antinociceptive tolerance. This is numerically quantified as measured by the ED50 values of morphine on the hot plate and tail flick tests (see Table 3.1). Further, pre-treatment with Gö-7874 enhanced morphine antinociception, producing a leftward shift in morphine-naïve mice compared to vehicle-treated controls in both hot plate and tail flick tests (Fig. 3.3 C and D; Table 3.1).

| | Vehicle + Saline | Vehicle + Morphine | Gö-7874 + Saline | Gö-7874 + Morphine |
|---|---|---|---|---|
| **Hot Plate** | 5.45 ±0.61# | 21.01 ±4.81∗ | 3.02 ±0.33∗# | 6.5 ±0.74# |
| **Tail Flick** | 13.19 ±2.44# | 30.59 ±7.51∗ | 7.59 ±1.12∗# | 13.97 ±2.95# |

Table 3.1: ED50 values for morphine on the hot plate and tail flick test after intra-vlPAG microinjection. Data are presented as Morphine ED50 values ± C.I. (mg/kg). * - statistically significant from vehicle + saline, # - statistically significant from vehicle + morphine; C.I.: confidence interval.

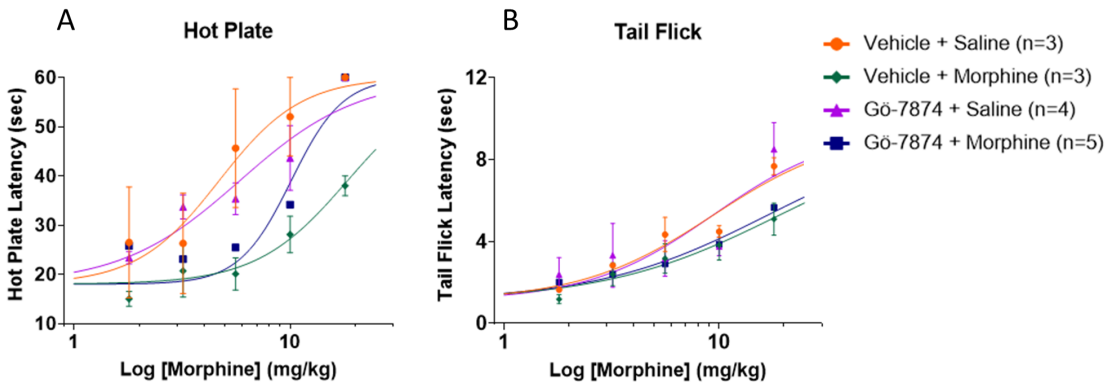


Fig. 3.4: Non-vlPAG inhibition of Protein Kinase-C does not prevent the development of morphine antinociceptive tolerance. (A) Hot plate and (B) Tail flick latencies of mice over the course of a morphine dose-response to test the development of antinociceptive tolerance.

### 3.3.4 Non-vlPAG inhibition of Protein Kinase-C does not prevent the development of morphine antinociceptive tolerance

We sought to determine the specific role of the vlPAG in modulating PKC-dependent morphine antinociceptive tolerance. Following morphine dose-response testing on Day 5, cannula implantation sites were visualized. Mice that had non-vlPAG directed injection sites were grouped according to their treatment groups and were analyzed separately. Mice pre-treated with Vehicle + Morphine displayed a significantly higher rightward shift in the dose response curve on the hot plate (Fig. 3.4A) and tail flick (Fig. 3.4B) tests, indicative of the development of antinociceptive tolerance. An analysis of variance indicated significant differences in ED50 values of morphine in the hot plate ($F(3, 88 = 6.73$, $p<0.001$) and tail flick test ($F(3, 88) = 3.71$, $p<0.05$). On the hot plate and tail flick tests, there were no significant differences between the morphine ED50 values for Vehicle + Saline treated mice and the Gö-7874 + Saline treated mice (see Table 3.2). This indicates that non-vlPAG

targeted microinjection of PKC inhibitor did not enhance morphine antinociception in opioid-naïve mice. Further, there were no significant differences between the morphine ED50 values of the Vehicle + Morphine treated mice and the Gö-7874 + Morphine treated mice (Table 3.2). This indicates that non-vlPAG targeted microinjection of the PKC inhibitor did not prevent the development of antinociceptive tolerance to morphine in this group of mice.

| | **Vehicle + Saline** | **Vehicle + Morphine** | **Gö-7874 + Saline** | **Gö-7874 + Morphine** |
|---|---|---|---|---|
| **Hot Plate** | 4.69 $\pm$1.09# | 18.44 $\pm$3.34$*$ | 5.85 $\pm$1.5# | 10.12 $\pm$0.97$*$# |
| **Tail Flick** | 9.40 $\pm$0.93# | 19.13 $\pm$4.27$*$ | 9.38 $\pm$2.08# | 16.86 $\pm$2.77$*$ |

Table 3.2: ED50 values for morphine on the hot plate and tail flick test after non-targeted intra-vlPAG microinjection. Data are presented as Morphine ED50 values $\pm$ C.I. (mg/kg). * - statistically significant from vehicle + saline, # - statistically significant from vehicle + morphine; C.I.: confidence interval

## 3.4 Discussion

In this current study, we found that MOPr receptor immunostaining is increased after morphine tolerance and it is co-localized with phosphorylated PKC. Inhibition of PKC activity within the ventrolateral periaqueductal gray (vlPAG) reduces the development of tolerance to the antinociceptive effects of morphine. Further, microinjection of the PKC inhibitor, Gö-7874, within this brain region enhances the antinociceptive effect of morphine in opioid-naïve animals. Taken together, this study demonstrates the importance PKC activity within the PAG in driving morphine antinociceptive tolerance.

The PAG is a highly heterogeneous brain region divided into distinct spatial regions with specialized functions. The vlPAG encompasses the greatest number of neurons that project to the medulla and modulate descending pain. As a region enriched in MOPr, this brain region is a key component of endogenous opioid signaling. In addition to its role in channeling antinociceptive input to medulla, the vlPAG is also independently capable of producing antinociception via electrical or pharmacological stimulation. Interestingly, repeated pharmacological stimulation of the vlPAG

via microinjection of opioid agonists can produce antinociceptive tolerance as measured by a decrease in potency and efficacy of the agonist [106]. Thus, the vlPAG is a critical gatekeeper in the continued efficacy of opioids in pain relief and repeated opioid receptor activity in this brain region is a contributor to antinociceptive tolerance. In order to validate advances in pain therapeutics, we require a precise understanding of the mechanisms by which adaptations in the vlPAG contribute to macroscopic behavioral changes following opioid tolerance.

The development of morphine antinociceptive tolerance can also occur following repeated systemic injection of morphine [6]. On acute pain tests, this is manifested as a reduction in latency compared to opioid-naïve mice to thermal noxious stimuli following repeated treatment with the opioid. While electrophysiological and behavioral studies have examined the contribution of the PAG in morphine antinociceptive tolerance, the contribution of intracellular signaling kinases towards this effect has not been fully clarified [10, 19]. Protein Kinase-C is a particularly interesting candidate for inquiry into the intracellular mechanisms of morphine tolerance as it is reported to phosphorylate the morphine-activated MOPr and contributes to its delayed internalization and recycling in a cellular model [83].

The appearance of pPKC around the periphery of vlPAG neurons co-localizing with MOPr suggests that the kinase is actively phosphorylating the receptor following morphine agonism. This result has been previously shown in vitro where phosphorylation-deficient PKC was unable to associate with the MOPr after morphine-stimulation (REF). Further, electrophysiological studies looking at rat Locus Ceuruleus neurons have indicated that PKC-dependent phosphorylation of the MOPr produces desensitization of the receptor, contributing to opioid tolerance [81]. Interestingly, while there is a reported loss of function of the MOPr following morphine tolerance, our immunofluorescence data indicates that the protein levels are increased specifically within the vlPAG. Previous studies have suggested a down-regulation of MOPr protein levels in the mouse brainstem and in cell culture following opioid tolerance [107, 108]. However, other studies have shown an upregulation of MOPr mRNA across the brain including within in the PAG and an enhancement in MOPr lev-

els at forebrain synaptic sites [109, 110]. Our observation is in agreement with these latter reports suggesting that within the PAG, morphine tolerance over 5 days produces an upregulation of MOPr protein levels that is associated with activated conventional isoforms of PKC.

PKC exists in multiple isoforms, including conventional and atypical isoforms. While these are all expressed in the central nervous system [82], we elected to apply the conventional isoform inhibitor, Gö-7874. Previous studies using this inhibitor have shown that intra-cerebroventricular injection of this compound can reinstate antinociception in morphine pelleted mice [82, 111]. In addition, a study using a non-specific GRK/PKC inhibitor within the vlPAG blocks morphine tolerance development [18]. Several leading hypotheses propose that PKC works endogenously to produce tolerance to morphine [112]. The desensitization of the morphine-activated MOPr through PKC-dependent phosphorylation is not a strong recruiter of the internalization system. As the receptor recycling lags behind, other systems step in to produce intracellular adaptations, one of which manifests as behavioral tolerance to the antinociceptive effects of opioids [113]. Our work expands on these studies and implicates the conventional PKC isoforms within the vlPAG in regulating morphine tolerance.

The ED50 of morphine is varied across the hot plate and tail flick tests, indicating differences in supraspinal and spinal antinociception. An interesting divergence in the physiology of morphine tolerance emerges when comparing the hot plate and tail flick morphine ED50 values in the Vehicle + Morphine treated mice (Table 3.1. It appears that to achieve equivalent antinociception at the spinal level as measured by the tail flick test, a 10-fold higher dose of morphine is needed in comparison to supraspinal antinociception as measured by the hot plate test. Previous studies have indeed noted a higher dose of morphine is required to produce equivalent antinociception on the tail flick test compared to the hot plate, attributable to both the route of delivery of the opioid and the local density of opioid receptors [82].

A remarkable outcome of this study is the observation that repeated treatment with the PKC

inhibitor in opioid-naïve mice resulted in a significant decrease in the ED50 of morphine on the hot plate test. This suggests that preemptive inhibition of PKC activity can enhance the antinociceptive ability of morphine at both the spinal and the supraspinal levels. It can be hypothesized that PKC inhibition in the vlPAG contributes to the enhancement of morphine antinociception in opioid naïve mice, while preventing the development of morphine tolerance in mice treated chronically with the opioid. This observation also raises interesting questions about the distribution of PKC expression in the CNS and their relative contribution to the development of opioid antinociceptive tolerance, which is deserving of further investigation.

The development of opioid tolerance is particularly deleterious in clinical considerations as the physician must increase the prescribed dose of opioid to achieve desired levels of pain relief, placing the patient at an increased risk for developing opioid use disorder. Here, we show that the antinociceptive tolerance to morphine is regulated by the kinase PKC within the ventrolateral periaqueductal gray. Further research into the mechanisms of PKC activity within the vlPAG are needed to decouple the effects of antinociceptive tolerance and morphine dependence. In addition, as females have been reported to develop a lesser degree of antinociceptive tolerance than males [114], the contribution of PKC activity to these sex differences also warrants exploration.

# CHAPTER 4

# GPR171 ALLEVIATES CHRONIC NEUROPATHIC AND INFLAMMATORY PAIN IN MALE, BUT NOT FEMALE MICE

## 4.1 Introduction

Chronic pain is growing public health concern with over 50 million adults in the United States having suffered from the condition since 2016 [115]. Globally, nearly 2 billion people have been affected by chronic pain conditions, emphasizing the need for extensive research and development of efficacious therapeutics [116]. Despite the progress made in studying the causal and therapeutic mechanisms of chronic pain, the inclusion of female cohorts in pain studies is limited [31, 117]. Several reports have highlighted the existence of sex differences in the pathology of chronic pain [118, 119, 120, 121]. Indeed, females have been reported to experience more severe and persistent pain than males in postoperative settings leading to reduced levels of physical activity [122]. In addition, the estrus stage of females has also been implicated in their pain sensitivity and their responsiveness to opioid analgesics [91, 123]. However, the long-term use of opioid analgesics for the treatment of chronic pain has profound negative side effects and has been shown to have limited effectiveness in the daily management of chronic pain [27]. Given these substantial issues with usage of opioids, we sought to look beyond this class of drugs to identify efficacious therapeutics for chronic pain.

G-protein coupled receptors (GPCRs) and their dysregulation is implicated in a wide range of pathologies, including chronic pain [124, 125, 126]. However, only 34% of FDA-approved drugs target GPCRs, highlighting the yet untapped potential of the GPCR family to be therapeutic targets [127, 128]. One particularly promising target of interest for novel pain therapeutics is the G-protein coupled receptor, GPR171, and its endogenous ligand, BigLEN. The peptide BigLEN is derived from the neuropeptide precursor ProSAAS. The precursor peptide, in turn, has been shown to be

upregulated in the cerebrospinal fluid of patients with fibromyalgia and within the periaqueductal gray in a rodent model of opioid-induced hyperalgesia [129, 130]. The receptor, GPR171, and its endogenous ligand, BigLEN, are widely expressed through the brain including the periaqueductal gray (PAG) [40, 131]. This particular brain region is situated in the descending pain modulatory pathway and is a site of action for a range of antinociceptive drugs including opioids and cannabinoids [132, 133]. Previous studies exploring the role of GPR171 in acute pain showed that agonism of the receptor via systemic administration of the synthetic agonist, compound MS15203, led to an increase in the antinociceptive effect of systemic morphine administration [40].

We explored the role of GPR171 in chronic neuropathic and inflammatory pain in male and female mice. The therapeutic potential of the GPR171 agonist compound, MS15203, was assessed via repeated once-daily systemic (10 mg/kg i.p.) injections. We found that the compound MS15203 reduced the duration of chronic neuropathic and inflammatory pain in male mice, but not female mice. While we found no alterations in gene expression levels of ProSAAS or GPR171 in the PAG of male or female mice, we found that CIPN produces a decrease in GPR171 protein levels in vlPAG of male mice. We note that following MS15203 treatment, the GPR171 protein levels in male mice with neuropathic pain recovered and were indeed elevated compared to untreated controls. Our findings demonstrate a sexually dimorphic receptor system in chronic pain and establish a role for the recently deorphanized receptor GPR171 in the reduction of chronic pain in male mice.

## 4.2 Materials and Methods

### 4.2.1 Animals

102 Adult male and female C57BL/6CS mice (Charles River Laboratories, CA), 6-8 weeks old and weighing 18-26 g at the start of the study were used in the study. Food and water were available ad libitum, except during testing. Mice were housed (four to five per cage) in a humidity and temperature-controlled room with a 12-hour light/dark cycle (off at 1900). All behavior testing took place during the light cycle. For the female cohorts, estrus stage was determined by obtaining

a vaginal lavage daily starting 5 days prior to the start of the study. A lavage was also obtained daily over the course of the study. All procedures were performed in accordance with the Guide for the Care and Use of Laboratory Animals adopted by the National Institutes of Health and were approved by the Institutional Animal Care and Use Committee of Utah State University (Protocol 2775).

### 4.2.2 CFA-induced inflammatory pain

Animals were very briefly anesthetized with isofluorane (99.9%, inhaled; Fluriso, VetOne) and restrained in order to access the plantar surface of the hind paw. Complete Freund's Adjuvant (CFA, Cat.F5881, Sigma-Aldrich) was injected under the epidermis into the plantar surface of both hind paws using a 27G needle (20 $\mu$l/paw) as described previously [134]. Animals in the control group received light isofluorane anesthesia alone without manipulation of their hind paws to prevent inflammation from the injection procedure. Drug administration commenced 24h following CFA injection.

### 4.2.3 Assessment of inflammatory pain in mice

A plantar test was performed as previously described [135] to assess inflammatory pain. Briefly, the subjects were placed in plexiglass enclosures on top of a glass platform. The animals were acclimatized to the testing chamber for 3 days prior to the start of the study (1 hour/session). On each testing day, the animals were acclimatized in the testing chamber for 20 minutes, or until cessation of exploratory behavior. A radiant heat source (IITC, Cat. 390) was applied to the plantar surface of the hind paw and the time to a nocifensive response was recorded. A cut-off time of 20 seconds was enforced to avoid potential injury due to tissue damage. Two trials were performed on each hindpaw to obtain the average reaction time per paw and a third reaction time was obtained if the preceding two values differed by 2s or more. Both left and right hindpaws were tested and their average thermal latency was considered for statistical analysis. Baseline latencies were established prior to injection of CFA. Following CFA injection on Day 0, the plantar test took place on Days 1, 3, and 5, where Day 0 marks the injection of CFA and Day 1 is 24h following CFA injection.

### 4.2.4 Chemotherapy-induced peripheral neuropathy

Paclitaxel (Sigma-Aldrich, MO, USA) was diluted in a vehicle comprising of Cremphor (Sigma-Aldrich, MO, USA)/90% ethanol/ 0.9% saline in a 1:1:18 ratio, and administered intraperitoneally (i.p.; 4 mg/kg) to mice on four alternate days (cumulative dose 16 mg/kg) to induce neuropathy as described previously [33, 136]. The control group received four injections of the vehicle (10 mL/kg). As paclitaxel can be present in animal excreta, bedding of mice used in this study was treated as a biohazard and disposed according to University guidelines.

### 4.2.5 Assessment of mechanical allodynia in mice

The von Frey filament test was performed as previously described [33] to assess allodynia in mice. Briefly, all mice (vehicle- and paclitaxel-treated) were placed in plexiglass enclosures mounted onto a testing platform containing a metal, perforated floor (Stoelting Co., Wood Dale, IL, USA). Animals were acclimatized to the testing chamber for 3 days prior to the start of the study (1 hour/session). On each testing day, the animals were acclimatized in the testing chamber for 20 minutes, or until cessation of exploratory behavior. Mechanical allodynia was assessed in male mice by applying von Frey filaments to the midplantar region of both hindpaws for approximately 2s per stimulus using calibrated filaments (Touch Test kit, Cat.NC12775-99, North Coast Medical). All trials began with the 1g filament and proceeded using an up-down trial design. Both right and left hindpaws were tested and their average mechanical threshold was considered for statistical analysis. A sudden paw withdrawal, flinching, or paw licking was regarded as a nocifensive response. A negative response was followed by the use of a larger filament. For assessment of mechanical allodynia in females, an electronic von Frey device (Ugo Basile, Italy; Cat.38450) was used as the allodynic females' mechanical thresholds were lower than the detectable range of the manual filaments. Paw mechanical withdrawal thresholds are expressed as a percentage of baseline values, where the baseline represents von Frey thresholds prior to paclitaxel or vehicle treatment.

### 4.2.6 Drug treatment

GPR171 agonist (MS15203, a gift from Dr. Sanjai Pathak) was dissolved in sterile 0.9% saline

(1 mg/ml). Mice in the Paclitaxel- and CFA-induced chronic pain studies were randomly assigned, by block randomization, into four treatment groups: pain + MS15203, pain + saline, no pain + MS15203, and no pain + saline. Mice in the MS15203 treatment group received 10 mg/kg i.p. as this dose was previously shown to produce an increase in hot plate thermal latency when co-administered with morphine [40]. To evaluate the effect of MS15203 on chronic neuropathic pain, the animals were administered with one dose of either MS15203 or saline, once daily for 5 days starting on Day 15. To evaluate the effect of MS15203 on chronic inflammatory pain, the animals were administered with one dose of either MS15203 or saline, once daily for 5 days starting 24h following induction of inflammatory pain.

### 4.2.7 Immunofluorescence staining and microscopy

Immediately following the final behavioral testing, a subset of the subjects ( 3/group) were deeply anesthetized using isofluorane and transcardially perfused with 4% paraformaldehyde (PFA). Their brains were post-fixed in 4% PFA for 1 hour and then were stored in 1x PBS at 4°C until further processing. Sectioning was performed on a vibratome (Leica Biosystems, Germany) and 50 $\mu$m sections containing the vlPAG were selected for immunofluorescence analysis. The sections were first incubated in sodium borohydride (1% in PBS) to expose the epitopes and decrease autofluorescence from aldehydes. Subsequently, they were permeabilized with Triton-X 100 (3%, Sigma-Aldrich), blocked with normal goat serum (5% in PBS), and incubated overnight in primary antibodies in their appropriate buffer (1% BSA (Sigma-Aldrich) in PBS). The following day, the slices were washed in PBS and incubated for 2 hours in diluted secondary antibodies in 1% BSA in PBS. The antibodies were sourced from GeneTex (Rabbit anti-GPR171, Cat.GTX108131, 1:400) and Life Technologies (Goat anti-Rabbit A594, Cat.A11037, 1:1000). Following subsequent PBS washes, the slices were briefly (5 mins) incubated in DAPI, washed with PBS and mounted with an anti-fade (ProLong Diamond Anti-Fade, Cat.P36961, Invitrogen) on a glass slide. Representative images of coronal sections containing the vlPAG, as defined by the mouse brain atlas [56], were acquired on a Zeiss LSM 710 confocal microscope (Carl Zeiss Microscopy, Germany) at Utah State University's microscopy core facility.

### 4.2.8 Quantification of immunofluorescence

Quantification of GPR171-fluorescence was performed using ImageJ (NIH) on automatically thresholded images as previously described [137, 138]. Up to 5 images of the vlPAG representative of both left and right hemispheres and across different rostro-caudal positions were analyzed per animal per group. They were analyzed as independent measurements to account for the structural and functional heterogeneity of the PAG [58, 59, 60, 61]. Ten cells in the field of view were randomly selected along with three areas representing background fluorescence. The fluorescence from GPR171 signal was calculated using the formula for Corrected Total Cell Fluorescence (CTCF) (Integrated Density – (area of selection$\times$mean background fluorescence)). The measurements have been presented in arbitrary units (AU).

### 4.2.9 Quantitative RT-PCR

Immediately following the final behavioral testing, a subset of the subjects (3-5/group) were euthanized by decapitation and the periaqueductal gray was dissected and snap-frozen on dry ice. The tissue samples were stored at -80°C until further processing. RNA was extracted from the tissues using Trizol (Cat. 15596026, Invitrogen) and RNeasy Plus Mini Kit (Cat. 74136, Qiagen) following the manufacturer's instructions. The eluted RNA was quantified using a Qubit 4 fluorometer (Invitrogen). cDNA was prepared using the Maxima first-strand synthesis kit for qRT-PCT (Cat. K1642, Thermo-Fisher) following the manufacturer's instructions. Samples were prepared using SYBR green (iTaq Universal SYBR Green Supermix, Cat. 1725121, Bio-Rad, CA) for gene expression analysis on a real-time thermocycler (CFX384 Touch, Bio-Rad). Custom primers as described previously [38] were used for GAPDH, GPR171, and ProSAAS (Integrated DNA Technologies). The synthesized cDNA was assayed in triplicate and analyzed using the $2\Delta\Delta$Ct method. Here, Ct indicates the cycle number at which the fluorescence signal crosses an arbitrary threshold within the exponential phase of the amplification curve. To calculate $\Delta\Delta$Ct, we used the formula $\Delta\Delta Ct = \{(Ct_{\text{target:treated sample}} - Ct_{\text{GAPDH:treated sample}}) - (Ct_{\text{target:control sample}} - Ct_{\text{GAPDH:control sample}})\}$. The value of the control sample was set to 100% and all samples were evaluated with respect to the control. Negative control reactions were performed to ascertain contaminant-free cDNA synthesis

and primer specificity was evaluated using melt curve analyses. The primer sequence information can be found in the supplementary material (Table S1).

### 4.2.10 Statistical Analysis

Results are presented as mean ± standard error of mean (SEM). Statistical analyses of behavioral studies were performed using a repeated measures two-way analysis of variance (ANOVA) combined with Bonferroni's post-hoc test. Normality of data was evaluated using the D-Agostino and Pearson test. Statistical analyses of qRT-PCR data and fluorescence quantification were performed using a one-way ANOVA combined with a Tukey's post-hoc test. Experimenters were blinded to drug treatment (saline and MS15203), but not to the pain state during behavioral studies and statistical analysis. All graphing and statistical analyses were performed using Prism 9.0 (GraphPad, San Diego, CA).

## 4.3 Results

### 4.3.1 GPR171 agonist does not reduce chronic inflammatory pain in female mice

We used a model of CFA-induced inflammatory pain to study the effect of GPR171 agonism on pain relief (Fig. 4.1A). In females, (n=6-8/group), intra-plantar CFA injection produced inflammatory pain and associated thermal hypersensitivity as measured by a plantar test. The estrus stage did not impact the subjects' thermal thresholds (Fig. 4.5A). A repeated measures two-way ANOVA indicated significant differences in thermal thresholds over the course of the study (Time [F (3.159, 88.44) = 36.78, p<0.0001]; Treatment [F (3, 28) = 14.57, p¡0.0001]; Time x Treatment [F (12, 112) = 8.211, p¡0.0001]). A Bonferroni's post-hoc test revealed that the female mice developed thermal hypersensitivity 24 hours following the CFA insult (Fig. 4.1B: Day 1, Control + Saline vs CFA + Saline or CFA + MS15203, p¡0.001) which persisted through the duration of the study (Fig. 4.1B: Day 5 post-drug, Control + Saline vs CFA + Saline, p<0.0001). However, the Bonferroni's post-hoc analysis revealed that despite chronic (once-daily) treatment with MS15203, there was no change in the thermal latency of female mice with inflammation-induced hypersensitivity (Fig. 4.1B: Day

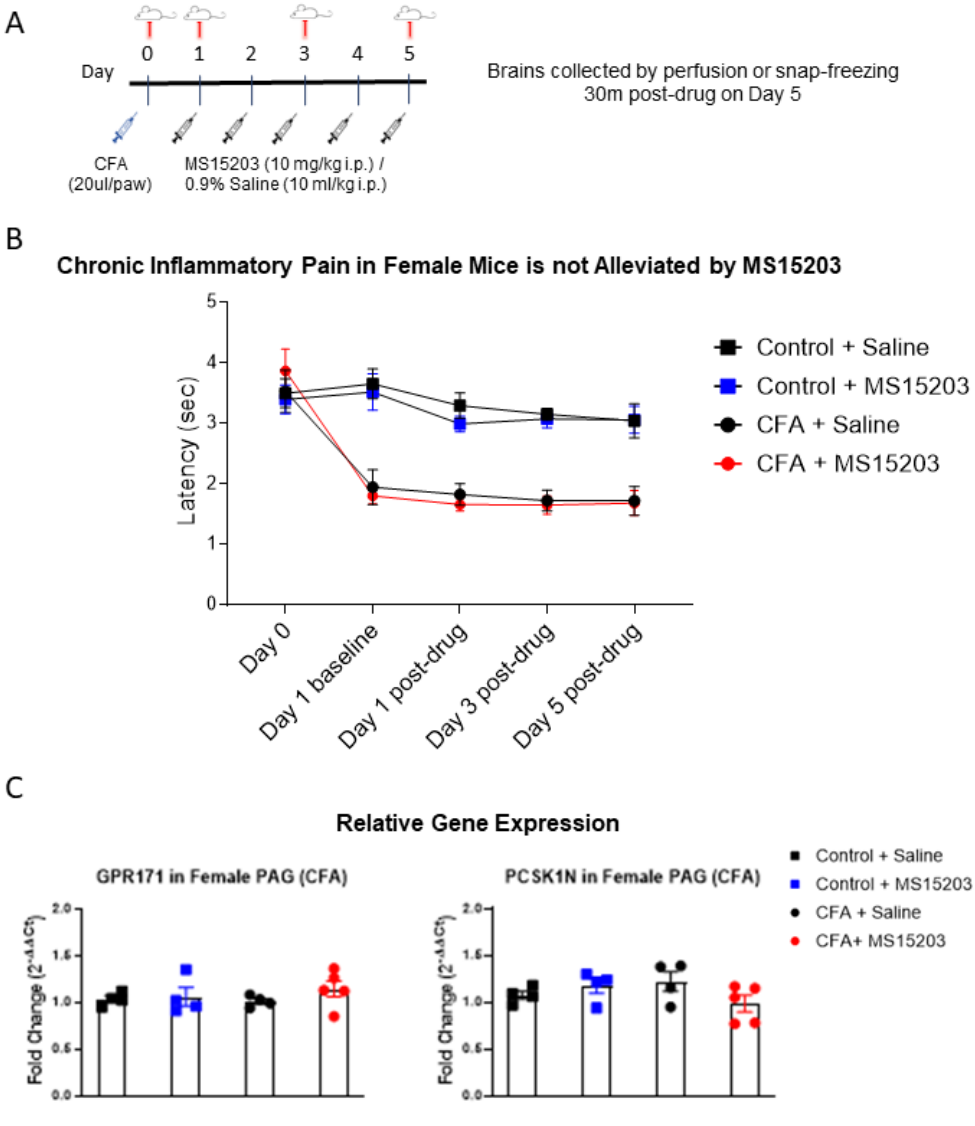


Fig. 4.1: GPR171 agonist does not reduce chronic inflammatory pain in female mice. (A) An illustrative timeline describing the experimental design of CFA-induced inflammatory pain followed by MS15203 treatment. (B) Female mice (n=6-8/group) injected with CFA in their hind paws developed rapid thermal hypersensitivity as measured by a plantar test. Chronic treatment with MS15203 failed to reduce inflammatory pain as noted by the persistence of thermal hypersensitivity through Day 5. Repeated measured two-way ANOVA with Bonferroni's post-hoc test. (C) Analysis of gene expression changes within the periaqueductal gray (PAG) reveals that the transcript levels of GPR171 and its endogenous ligand, PCSK1N, are unchanged in female mice (n=4-5/group) irrespective of inflammatory pain status or MS15203 treatment. One-way ANOVA with Tukey's post-hoc test.

5 post-drug, CFA + Saline vs CFA + MS15203, $p>0.05$). MS15203 treatment alone did not alter the thermal latencies of females in the Control group.

We then performed qRT-PCR on dissected whole periaqueductal gray (PAG) tissue from a subset of females (n=4-5/group) to evaluate gene expression changes in GPR171 or its endogenous ligand, PCSK1N (Fig. 4.1C). The PAG is a critical modulator of antinociception within the descending pain pathway and is a site of action of endogenous opioid activity [50, 59]. A one-way ANOVA indicated no significant differences between treatment groups on evaluation of GPR171 (Treatment $F(3, 13) = 0.71$, $p>0.05$) or PCSK1N (Treatment $F(3, 13) = 1.68$, $p>0.05$) expression in the PAG.

### 4.3.2 GPR171 agonist reduces chronic inflammatory pain in male mice

We performed a similar experimental paradigm as Fig. 4.1A to evaluate the analgesic properties of GPR171 in male mice. In males, (n=5-6/group), intra-plantar CFA injection produced inflammatory pain and thermal hypersensitivity on the plantar test. A repeated measures two-way ANOVA indicated significant differences in thermal thresholds over the course of the study (Time [$F(3.025, 57.48) = 19.48$, p¡0.0001]; Treatment [$F(3, 19) = 27.08$, $p<0.0001$]; Time $\times$ Treatment [$F(12, 76) = 7.417$, $p<0.0001$]). Similar to the females, the male mice injected with CFA developed thermal hypersensitivity 24 hours later as revealed by a Bonferroni's post-hoc test (Fig. 4.2A: Day 1, Control + Saline vs CFA + Saline or CFA + MS15203, $p<0.0001$). The Bonferroni's post-hoc analysis also revealed that acute MS15203 did not improve thermal latencies in CFA-treated male mice (Fig. 4.2A: Day 1 post-drug, Control + Saline vs CFA + MS15203, $p<0.01$). However, 3 days of once-daily MS15203 treatment increased thermal latencies of male mice and this improvement was sustained through the 5-day chronic treatment paradigm (Fig. 4.2A: Day 3 post-drug, CFA + Saline vs CFA + MS15203, $p<0.05$ and Day 5 post-drug, CFA + Saline vs CFA + MS15203, $p<0.001$).

We performed immunofluorescence staining and quantification of GPR171 in the PAG of male

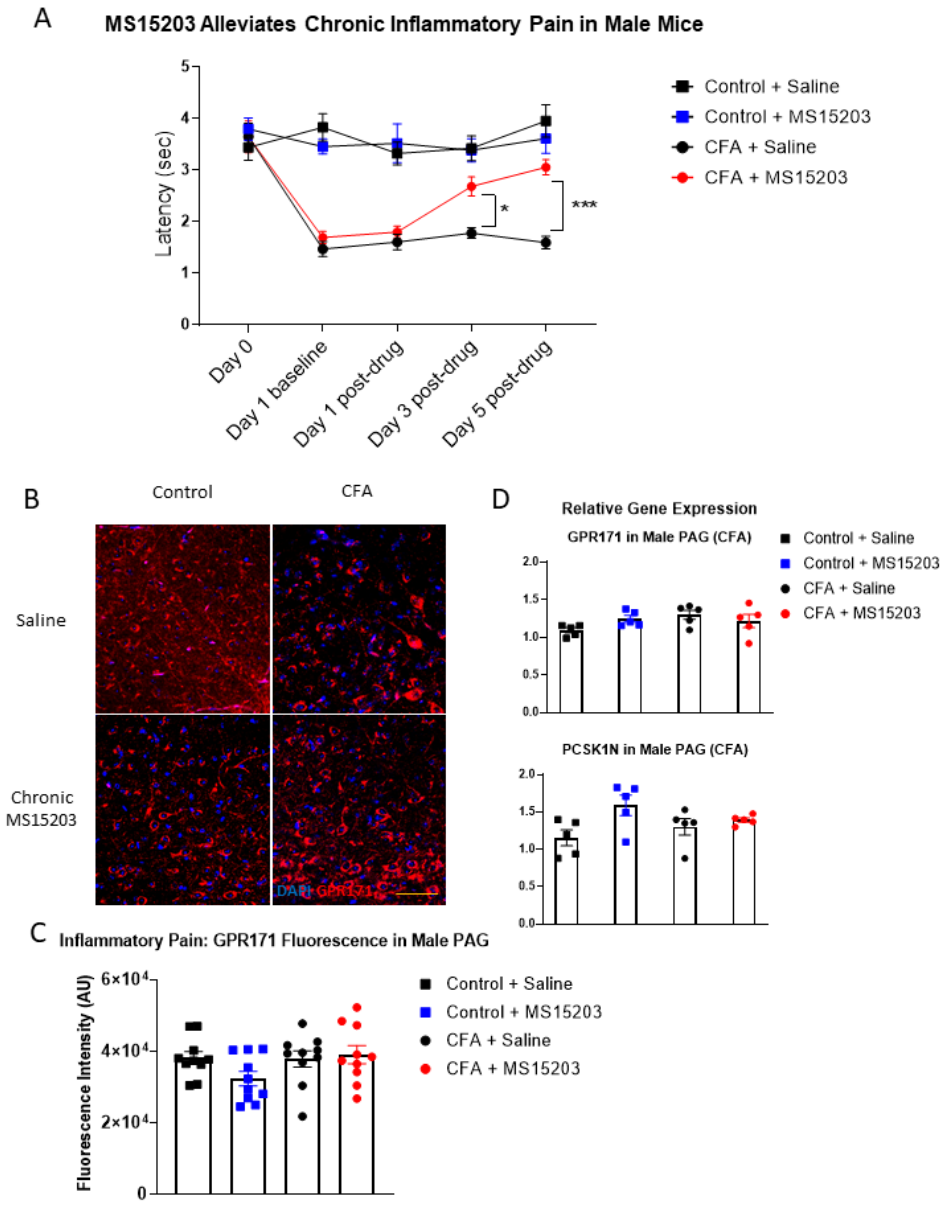


Fig. 4.2: GPR171 agonist reduces chronic inflammatory pain in male mice. (A) Male mice (n=5-6/group) injected with CFA in their hind paws developed rapid thermal hypersensitivity as measured by a plantar test. Chronic treatment with MS15203 alleviated inflammatory pain by Day 3 of the treatment and the analgesia was ongoing through Day 5 as measured by an increase in thermal latencies on the plantar test. Repeated measured two-way ANOVA with Bonferroni's post-hoc test. (B) Fluorescence immunostaining and (C) quantification of GPR171 signal show that the protein levels of GPR171 are unchanged in the ventrolateral PAG (vlPAG) of male mice (n=10-12 images each from 2 mice/group). (D) Analysis of gene expression changes within the PAG reveals that the transcript levels of GPR171 and its endogenous ligand, PCSK1N, are unchanged in male mice (n=4-5/group). One-way ANOVA with Tukey's post-hoc test. ****p$<$0.0001. Scale bar = 50 $\mu$m.

mice to visualize receptor localization and evaluate GPR171 protein levels within the ventrolateral PAG (vlPAG) (Fig. 4.2: C, D). A one-way ANOVA of fluorescence intensities indicated no significant differences between treatment groups on quantification of GPR171 protein levels in the vlPAG (Treatment $F(3, 36) = 1.97$, $p>0.05$).

We then performed qRT-PCR on dissected whole PAG from males to evaluate gene expression changes in GPR171 and PCSK1N (Fig. 4.2B). A one-way ANOVA indicated no significant differences between treatment groups on evaluation of GPR171 (Treatment $F(3, 16) = 2.06$, $p>0.05$) or PCSK1N (Treatment $F(3, 16) = 3.07$, $p>0.05$) expression in the PAG.

### 4.3.3 GPR171 agonist does not alleviate chronic neuropathic pain in female mice

We employed a model of chemotherapy-induced peripheral neuropathy (CIPN) to study the effects of GPR171 agonist treatment on chronic pain (Fig. 4.3A). In females (n=6-7/group), paclitaxel produced allodynia as assessed by an electronic von Frey sensor. The estrus stage did not impact the subjects' mechanical thresholds (Fig. 4.5B). A repeated measures two-way ANOVA indicated significant differences in mechanical thresholds over the course of the study (Time [$F(3.77, 98) = 63.87$, $p<0.0001$]; Treatment [$F(3, 26) = 44.36$, $p<0.0001$]; Time x Treatment [$F(15, 130) = 12.54$, $p<0.0001$]). A Bonferroni's post-hoc test revealed that the female mice developed allodynia by Day 5 following the first dose of paclitaxel (Fig. 4.3B: Day-5, Vehicle + Saline vs Paclitaxel + Saline or Paclitaxel + MS15203, $p<0.001$). Allodynia was maintained through the duration of the study and was ongoing on Day 15 prior to the initiation of pharmacological intervention (Fig. 4.3B, Day - 15, Vehicle + Saline vs. Paclitaxel + Saline or Paclitaxel + MS15203, $p<0.0001$). We then tested the effect of MS15203 at both acute (30min) and chronic (5 days) dosing paradigms. A Bonferroni's post-hoc analysis revealed that neither acute nor chronic MS15203 treatment increased the mechanical thresholds of Paclitaxel + MS15203-treated females (Fig. 4.3B: Day 15 post-test and Day 20, Vehicle + Saline vs Paclitaxel + MS15203, $p<0.0001$). The compound MS15203 alone did not have any effect in vehicle-treated female mice.

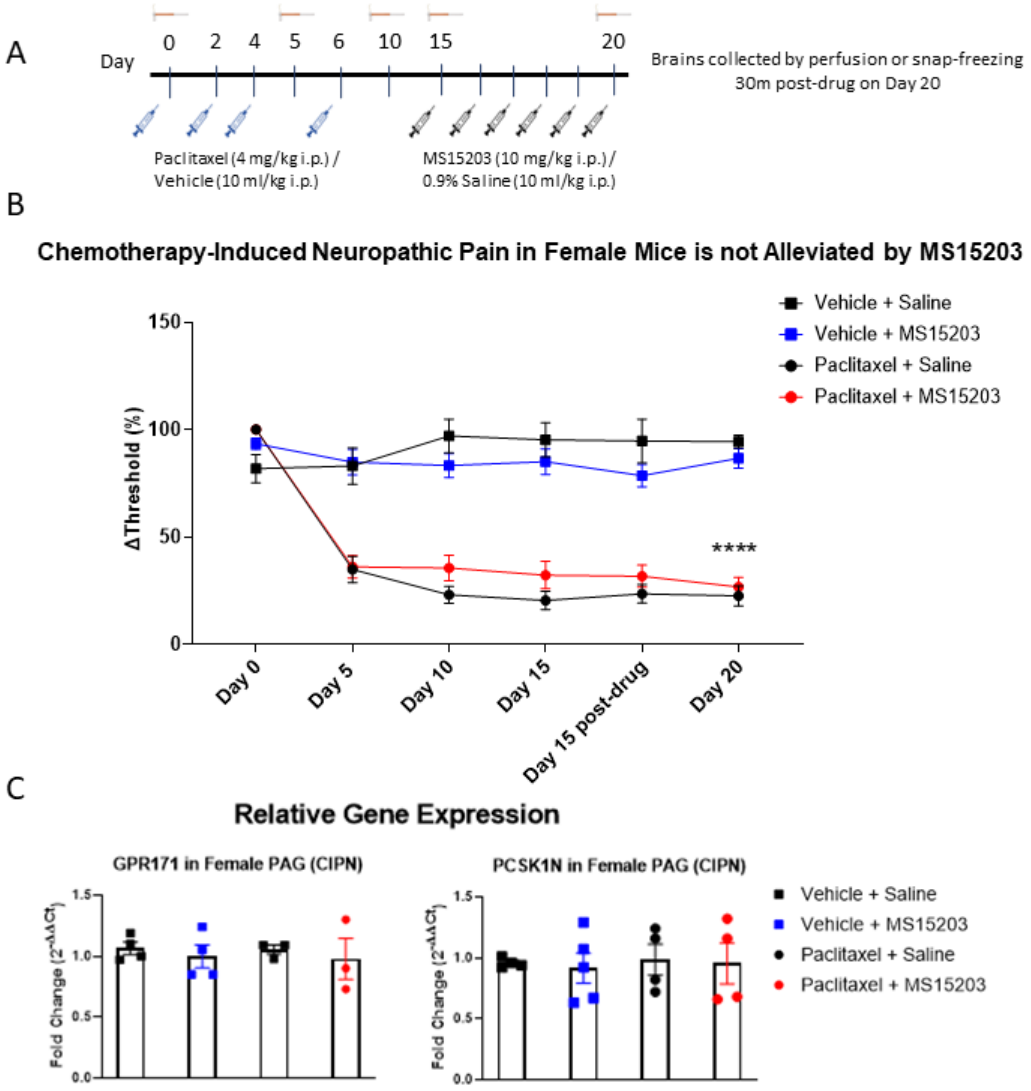


Fig. 4.3: GPR171 agonist does not reduce chronic neuropathic pain in female mice. (A) An illustrative timeline describing the experimental design of chemotherapy-induced peripheral neuropathy followed by MS15203 treatment. (B) Female mice (n=6-7/group) treated with paclitaxel (16 mg/kg cumulative, i.p.) developed allodynia by Day 5 of the study as measured by the von Frey test. Chronic treatment with MS15203 from Day 15 through Day 20 failed to reduce allodynia as noted by the persistence of mechanical hypersensitivity through Day 20. Repeated measures two-way ANOVA with Bonferroni's post-hoc test. (C) Analysis of gene expression changes within the periaqueductal gray (PAG) reveals that the transcript levels of GPR171 and its endogenous ligand, PCSK1N, are unchanged in female mice (n=4-5/group) irrespective of neuropathic pain status or MS15203 treatment. One-way ANOVA with Tukey's post-hoc test.

We proceeded to perform qRT-PCR on dissected PAG from female mice (4-5/group) to assess whether gene expression levels of GPR171 and its endogenous ligand PCSK1N are altered following neuropathic pain and MS15203 treatment. A one-way ANOVA revealed that the expression levels of GPR171 are unchanged in the PAG of female mice irrespective of pain condition or MS15203 treatment ($F(3,13) = 0.572$, $p>0.05$). Similarly, the expression levels of PCSK1N were also unchanged in the PAG of female mice across pain conditions or MS15203 treatment ($F(3,13) = 0.076$, $p>0.05$).

### 4.3.4 GPR171 agonist reduces chronic neuropathic pain in male mice

We performed a similar experimental paradigm as Fig. 4.3A using male mice to assess the anti-allodynic effect of MS15203. In males (n=6-7/group), paclitaxel produced allodynia as assessed by manual von Frey filaments using the up-down method. A repeated measures two-way ANOVA indicated significant differences in mechanical thresholds over the course of the study (Time [$F(3.31, 92.71) = 38$, $p<0.0001$]; Treatment [$F(3, 28) = 82.53$, $p<0.0001$]; Time x Treatment [$F(15, 140) = 13.36$, $p<0.0001$]). A Bonferroni's post-hoc test revealed that the male mice developed allodynia by Day 5 following the first dose of paclitaxel (Fig. 4.4A: Day-5, Vehicle + Saline vs Paclitaxel + Saline or Paclitaxel + MS15203, $p<0.001$). Allodynia was maintained through the duration of the study and was ongoing on Day 15 prior to the initiation of pharmacological intervention (Fig. 4.4A, Day - 15, Vehicle + Saline vs Paclitaxel + Saline or Paclitaxel + MS15203, $p<0.0001$). We then tested the effect of MS15203 at both acute (30min) and chronic (5 days) dosing paradigms. A Bonferroni's post-hoc analysis revealed that acute MS15203 treatment did not alter the mechanical thresholds of male mice in neuropathic pain (Fig. 4.4A: Paclitaxel + MS15203 vs Paclitaxel + Saline, Day 15 baseline vs post-test, Bonferroni $p>0.05$). However, following 5 days of repeated dosing, MS15203 treatment increased the mechanical thresholds of mice in neuropathic pain compared to their saline-treated counterparts (Fig. 4.4A: Paclitaxel + MS15203 vs Paclitaxel + Saline, Day 20, Bonferroni $p<0.05$). The compound MS15203 alone did not have any effect in vehicle-treated male mice.

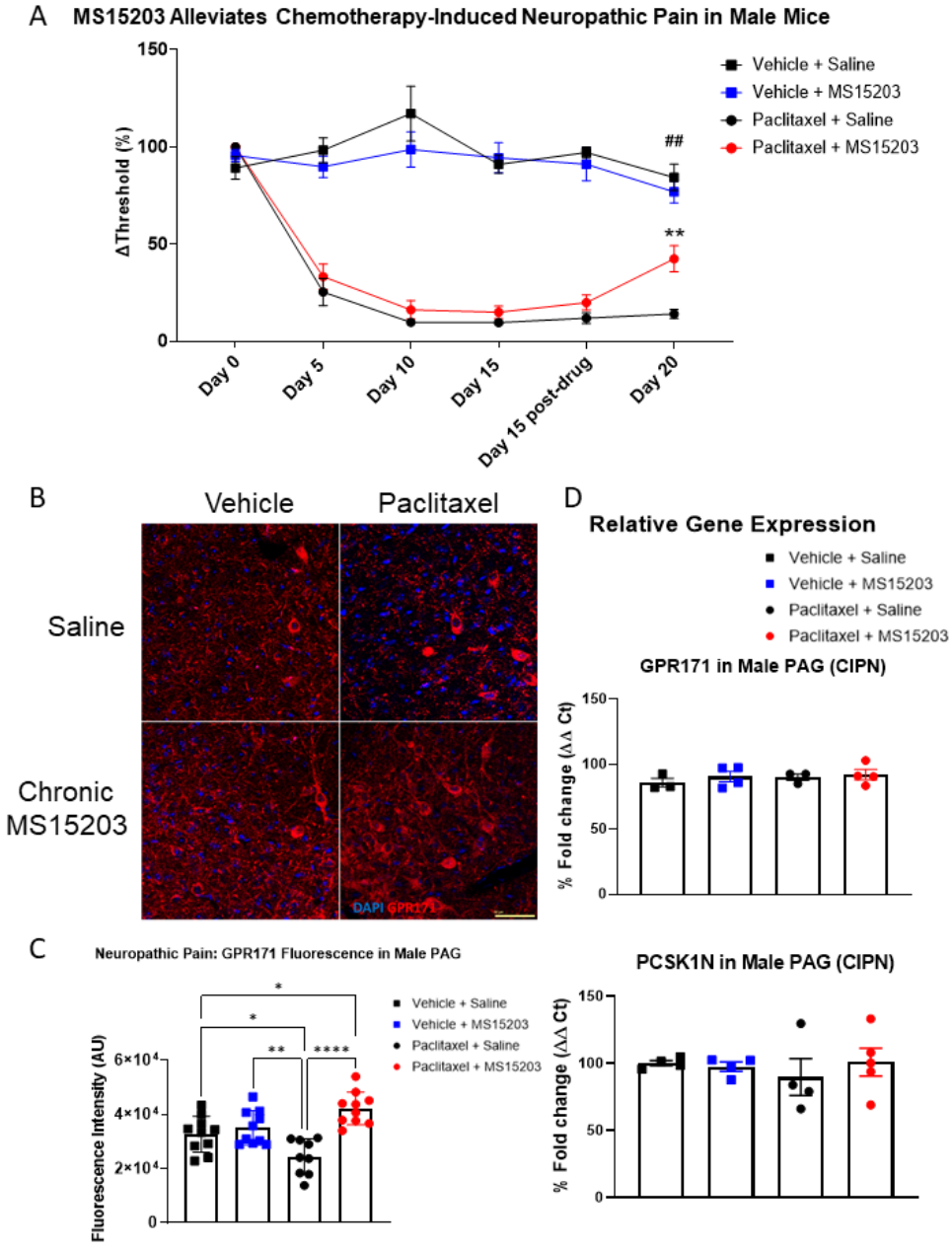


Fig. 4.4: GPR171 agonist reduces chronic neuropathic pain in male mice. (A) Male mice (n=6-7/group) treated with paclitaxel (16 mg/kg cumulative, i.p.) developed allodynia by Day 5 of the study as measured by the von Frey test. Chronic, but not acute, treatment with MS15203 reduced the duration of allodynia as noted by the significant increase in mechanical thresholds compared to Paclitaxel + Saline treated mice. Repeated measures two-way ANOVA with Bonferroni's post-hoc test. (B) Fluorescence immunostaining and (C) quantification of GPR171 signal show that protein levels of GPR171 are decreased following neuropathic pain and chronic treatment with MS15203 results in an increase of GPR171 in the vlPAG (10-12 images each from 2 mice/group). (D) Analysis of gene expression changes within the PAG reveals that the transcript levels of GPR171 and its endogenous ligand, PCSK1N, are unchanged in male mice (n=4-5/group) irrespective of neuropathic pain status or MS15203 treatment. One-way ANOVA with Tukey's post-hoc test. *$p<0.05$, **$p<0.01$, ****$p<0.0001$. Scale bar = 50 $\mu$m.

We performed immunostaining for the receptor GPR171 and quantified fluorescence intensity within the ventrolateral PAG (vlPAG) (Fig. 4.4B,C). Intriguingly, a one-way ANOVA of the fluorescence intensities revealed significant differences between the groups ($F(3,35) = 10.15$, $p<0.0001$). A Tukey's post-hoc test revealed that neuropathic pain resulted in a significant decrease of GPR171 immunostaining compared to vehicle-treated controls (Fig. 4.4D: Vehicle + Saline vs Paclitaxel + Saline, Tukey's $p<0.05$). Further, the post-hoc analysis revealed that following chronic MS15203 treatment, there was a rescue effect and, in fact, the levels of GPR171 were elevated compared to the vehicle-treated controls (Fig. 4.4D: Vehicle + Saline vs Paclitaxel + MS15203, Tukey's $p<0.05$).

We proceeded to perform qRT-PCR on dissected PAG from male mice to assess whether gene expression levels of GPR171 and PCSK1N are altered following neuropathic pain and MS15203 4.4D). A one-way ANOVA revealed that the expression levels of GPR171 are unchanged in the PAG of male mice irrespective of pain condition or MS15203 treatment ($F(3,13) = 0.572$, $p>0.05$). Similarly, the expression levels of PCSK1N were also unchanged in the PAG of male mice across pain conditions or MS15203 treatment ($F(3,13) = 0.076$, $p>0.05$).

## 4.4 Discussion

The current study establishes that the receptor GPR171 is a promising target for the treatment of chronic pain in males. A synthetic agonist for the receptor, MS15203, decreases the duration of both allodynia caused by neuropathic pain and thermal hypersensitivity caused by inflammatory pain in male mice. Interestingly, MS15203 does not reduce allodynia nor thermal pain in female mice using the same dose administered in males. Further, although GPR171 receptor immunostaining is unaltered in males after chronic inflammation, neuropathic pain induces a decrease in GPR171 protein levels which is rescued following chronic MS15203 treatment. The gene expression levels of GPR171 and its endogenous ligand, PCSK1, are unaltered in the PAG. Further, while GPR171 activation is recognized to promote food intake [37], we note that our 5-day treatment did not result in significant alterations in the subjects' weights (Fig. 4.6A-D).

The development of CFA-induced inflammatory pain occurs over a biphasic response time. The initial course of inflammation occurs over the first 24 hours, followed by persistent pain lasting over the course of a week. We report here that systemic administration of the compound MS15203 decreases the duration of CFA-induced inflammatory pain, in a sex-dependent manner, after 3 days of treatment following the initial inflammatory phase. We also note that while this reduction of chronic pain is sustained over the course of the study in male mice, female mice do not display any reduction of thermal hypersensitivity over the course of the study. In previous studies assessing therapeutic options for chemotherapy-induced neuropathic pain, we noted that mechanical allodynia is most pronounced by Day 15 of the study and persists through 30 days [33]. We assessed allodynia following 5 days of once-daily MS15203 treatment (10 mg/kg i.p.). We report here that systemic administration of the compound MS15203 decreases the duration of paclitaxel-induced peripheral neuropathy and associated allodynia after 5 days of treatment in male mice. While the pathophysiology of sex differences in neuropathic pain induced by chemotherapy is unclear, it is indeed a remarkable observation that the GPR171 activation did not promote alleviation of allodynia in females in chronic neuropathic pain.

The absence of changes in ProSAAS or GPR171 mRNA indicate that a 5-day, once-daily treatment regimen does not alter receptor or ligand gene expression in the brain although the drug does exert a physiological effect at this timescale. A recent study showed that peripheral sensory neurons contribute to the pain relief seen with GPR171 activation [139]. While this observation explains alterations at the peripheral level in addition to spinal sensitization to chronic pain, the role of alterations in PAG connectivity and excitability is well established in the context of chronic pain paradigms [140, 141, 142]. The absence of gene expression changes of GPR171 or PCSK1N within the PAG, while observing a modulation of protein levels is indeed a remarkable observation. We postulate that the transcript levels obtained from whole dissected PAG are not representative of the protein levels within the local vlPAG region, a highly variable relationship that has been reviewed previously [143]. The decrease in GPR171 protein levels in the vlPAG following neuropathic pain is comparable to reports of decreased mu opioid receptor availability following chronic pain [144].

We previously found synergistic antinociceptive effects of MS15203 with morphine, indicating the receptors could also be similar in their physiological modulation.

GPR171 is an inhibitory G$\alpha_{i/o}$ coupled receptor which inhibits cAMP production [37]. Based on our study showing GPR171 in GABA neurons in the PAG, we hypothesize that activation of GPR171 leads to a decrease in GABA release [40]. This in turn leads to antinociception by excitation of output neurons in the medulla. In addition, GPR171 is found in the dorsal root ganglion and alleviates inflammatory pain following intrathecal administration of a GPR171 agonist, presumably by inhibiting TRP ion channels [139]. Since we administered the agonist systemically, it is likely that it is working within the central and peripheral nervous system to alleviate pain. In addition, the increase in the endogenous ligand ProSAAS, seen in circulating CSF of fibromyalgia patients, is likely a consequence of adaptations towards restoring GPR171 signaling as we have observed a decrease in brain-specific GPR171 receptor expression in males with neuropathic pain [129]. The lack of alleviation of neuropathic or inflammatory pain in females following chronic MS15203 treatment warrants further investigation. Previous studies have indicated that C57BL/6 mice display stable pain behaviors across estrus stages [145, 146]. It is plausible that the dose of agonist administered (10mg/kg, i.p.) was insufficient to produce a physiological response in females. Further, there is considerable evidence of heightened immune activation in females at both central and peripheral sensory processing regions, which contribute to mechanical and thermal hypersensitivity [91, 147, 148, 149]. The heightened microglial activation in the PAG in females has been shown to reduce morphine-induced antinociception [150]. While there is a paucity of studies examining immune interactions with GPR171 activity, the possibility of the immune microenvironment modulating GPR171-dependent analgesic activity cannot be ruled out. Further, studies with female mice have reported that the sex-specific differences in chronic pain are driven in part by the action of hormones and are peripherally regulated by TRP channels [145, 151]. As GPR171 exerts its peripheral effects via TRP channels on sensory afferents in male mice, the microenvironment in this region can be postulated to contribute to the observed sex differences [139]. Further, as the gene encoding GPR171 is located on chromosome 3 of the mouse, the observed differences in behavior

cannot be attributed to sex chromosome-linked causes. Indeed, sex differences in antinociception have been found in other systems such as the fatty acid-derived resolvin D5, that was able to produce antinociception in males with neuropathic or inflammatory pain, but not in females [152]. Our findings thus identify GPR171 not only as a novel target for the treatment of chronic inflammatory and neuropathic pain, but also one that displays sexual dimorphism in pain regulation.

Chronic inflammatory and neuropathic pain present public health concerns without efficacious treatment options. Our findings suggest that the receptor GPR171 is a therapeutic target for the treatment of multiple modalities of chronic pain in a sex-dependent manner and its agonist, MS15203, can be used to treat chronic pain.

# Supplementary Material

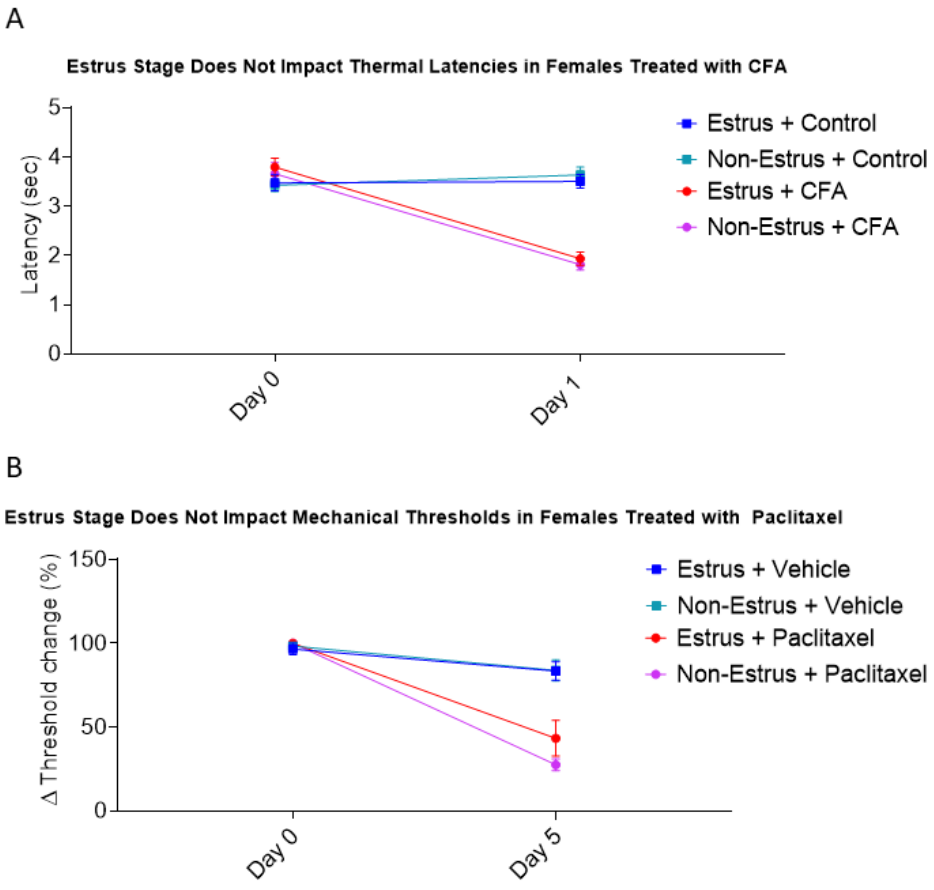


Fig. 4.5: Estrus stage does not impact baseline thresholds of female mice. Female mice do not show significant differences in their A) thermal thresholds or B) mechanical thresholds on Day 0 of the chronic pain studies. Two-way repeated measures ANOVA indicated significant differences in the thresholds of the mice in inflammatory or neuropathic pain. However, a Bonferroni's post-hoc test revealed that there were no differences in the baseline thresholds of mice in their respective studies.

| Name of Gene Target | Forward Primer Sequence | Reverse Primer Sequence |
|---|---|---|
| **GAPDH** | TGAAGGTCGGTGTGAACG | CAATCTCCACTTTGCCACTG |
| **GPR171** | CTGGCGGTGTCTAATTTGT | GTTTTCTTCCAGAGGCTTGCTC |
| **GPR171** | AGTGTATGATGATGGCCC | CCCTAGCAAGTACCTCAG |

Table 4.1: Primer sequences for quantitative RT-PCR.

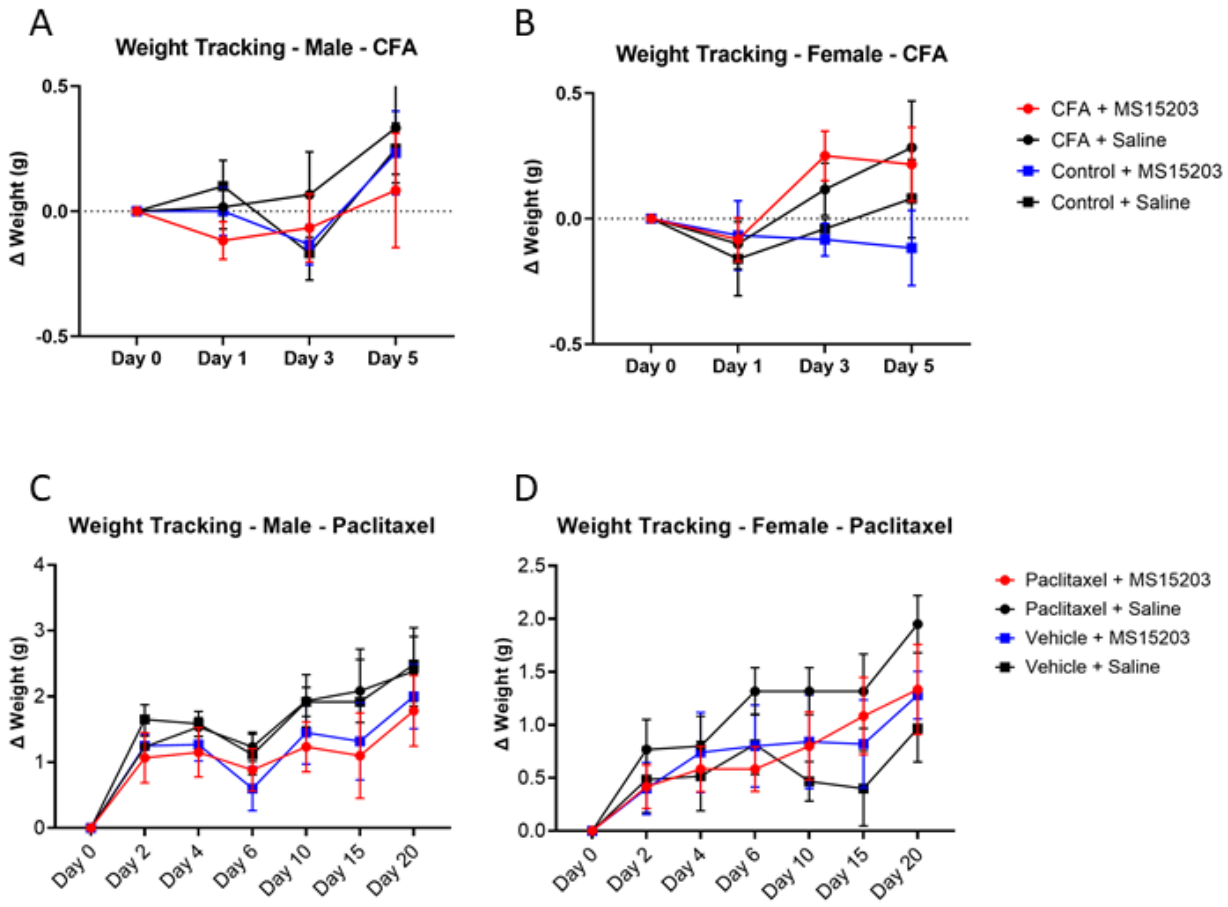


Fig. 4.6: MS15203 treatment does not produce significant weight gain in male or female mice. Once-daily injection of MS15203 (10mg/kg, i.p.) for 5 days does not produce significant weight grain in male (A, C) or female (B, D) mice. A two-way repeated measures ANOVA indicated significant differences in weight changes in mice in the chemotherapy-induced peripheral neuropathy (CIPN) study. However, a Bonferroni's post-hoc test revealed that there were no significant differences in weight changes between Day 15 and Day 20 of the study, the duration in which the mice received MS15203.

# CHAPTER 5

# GENERAL DISCUSSION

This thesis lays the groundwork in clarifying how chronic opioid treatment is manifested at the intracellular signaling level. Through multiple levels of analysis including molecular, cellular, and behavioral studies, this thesis provides substantial evidence of elevated levels of intracellular protein kinases following morphine tolerance. In a step further, this thesis has also included female cohorts where possible, a group that has been underrepresented in studies of opioid neuropharmacology. Alongside the advances made in our basic understanding of the neurobiology of opioid tolerance, this thesis also explores the therapeutic potential of a novel G-protein Coupled Receptor (GPCR) in the treatment of chronic pain. Pre-clinical translational studies such as the one in this thesis provide a foundation on which therapeutic leads are evaluated for drug development.

The opioid crisis in the United States traces its history to the 1980s, much before deadly mortality rates that brought this issue to the forefront in the 2010s. The subject of multiple documentaries and lawsuits, the opioid crisis has largely been borne from the over-marketing and over-prescription of synthetic opioids for non-critical pain patients [153]. In addition to the downplayed risks of dependence to these opioids, the prescribing physicians and pharmacies were largely remiss in a plan to taper usage, leading to rampant misuse.

As opioids were primarily prescribed for the management of pain in patients, the scientific community sought to decouple the analgesic property of opioids from their negative side effects. To achieve this decoupling, it was postulated that following activation of the μ-opioid receptor by its agonist, the G-protein-dependent pathway contributed to analgesia whereas the $\beta$-Arrestin-dependent pathway contributed to the negative effects such as respiratory depression – the most common cause of overdose deaths [53]. While this theory did not ultimately hold water, it opened an intriguing dimension in the study of the intracellular signaling in opioid neuropharmacology [154]. The intracel-

lular signatures of signaling pathway dynamics in the brain following $\mu$-opioid receptor activation have been largely understudied although they contribute to the physiological effects of the opioid drug. This thesis has made large strides in understanding these complex cellular processes *in vivo*.

In the realm of neurobiology of opioid analgesia, the ventrolateral periaqueductal gray (vlPAG) is particularly important for the continued analgesic effect of the drug. While this brain region is not actively involved in opioid-induced reward, it is a critical regulator of opioid antinociceptive tolerance – a phenomenon wherein repeated and persistent use of an opioid results in a decreased ability of the particular dose to provide desired pain relief. Repeated microinjections of opioids into the vlPAG, but not other reward-related areas produces antinociceptive tolerance [41]. However, not all opioids are created equally, with some opioids preferentially activating G-protein signaling while others are biased towards the $\beta$-Arrestin pathway [155]. This dimorphism adds another layer of complexity to our understanding of opioid receptor signaling, such that while ultimately the behavioral output is antinociception, the intracellular signaling, and probably the mechanism of tolerance are varied depending upon the opioid studied.

Morphine, a prototypical opioid narcotic and a partial agonist of the μ-opioid receptor, acts on the μ-opioid receptors in the vlPAG to produce antinociception. Chronic treatment with morphine produces antinociceptive tolerance on acute thermal pain tests. Early investigation into the role of the vlPAG in regulating this behavior effect showed that morphine tolerance is associated with elevated levels of $\beta$-Arrestin-dependent ERK signaling in this brain region. Further, cellular studies showed elevated levels of the G-protein downstream kinases, Protein Kinase-A (PKA) and Protein Kinase-C (PKC). However, the activation patterns of PKC and PKA have not been clarified in native tissue and have remained poorly understood in females.

In Chapter 2 of this thesis, quantification of immuno-fluorescence is applied to draw conclusions about the levels of protein activation in the vlPAG. This particular brain region is restrictively small in mice such that dissecting the vlPAG and extracting total protein from the tissue would not

yield assayable sample without pooling across multiple animals. In order to better compare inter-individual differences and gain and understanding of intracellular signaling dynamics specifically within the vlPAG, quantitative immunofluorescence was selected as the most appropriate methodology. In doing so, the activation levels of the kinases ERK 1/2, PKC, and PKA were found to be the highest in chronic morphine-treated male and female mice, as compared to mice that were treated with saline or acute morphine. In addition, following acute morphine treatment, only the levels of ERK 1/2 were significantly elevated in the vlPAG. This study also showed that activated ERK 1/2 was present within the endosomes of only the chronic morphine-treated mice, indicating a role for $\beta$-Arrestin in internalizing the MOPr after long-term opioid treatment. Intriguingly, this study added substantial evidence to the postulate that following chronic morphine treatment, there is a shift in ERK 1/2 activation from a G-protein-dependent pathway to a $\beta$-Arrestin-dependent pathway, thus acting as an indicator of intracellular adaptations that occur in the vlPAG [14, 67].

As Chapter 2 of this thesis provides the basic framework for clarifying alterations in kinase signaling following morphine tolerance, Chapter 3 of the thesis focuses on a specific kinase, PKC, which is elevated following chronic morphine treatment. This kinase is recruited to the receptor to drive desensitization after morphine-induced activation of the MOPr. Interfering with PKC signaling would potentially drive other redundancies to phosphorylate the receptor and initiate the receptor recycling process. Chapter 3 of this thesis describes efforts to target PKC activity and observe behavioral modulation of morphine antinociceptive tolerance.

In Chapter 3 of the thesis, the specific contribution of PKC activity in the vlPAG towards the development of antinociceptive tolerance to morphine was examined in great detail. Targeted delivery of the PKC inhibitor Gö-7874 into the vlPAG was achieved through stereotaxic cannula implantation and repeated drug delivery. While one dose (2nM) of PKC inhibitor did not have an effect of morphine activity, repeated administration of the inhibitor (16nM cumulative) within the vlPAG was able to prevent the development of antinociceptive tolerance to repeated systemic administration of morphine. Further, in this section, the critical nature of the vlPAG was explicitly

demonstrated as non-targeted inhibition of PKC did not affect the degree of tolerance to morphine.

This work is significant as it contributes to our understanding of kinase-dependent modulation of MOPr activity within the vlPAG. Based on this work, it can be postulated that the inhibition of PKC drives a different kinase to terminate G-protein signaling and effectively recycle the receptor to sustain morphine antinociceptive activity. This has far-reaching clinical implications. By prolonging the window in which morphine produces pain relief, it obviates the necessity to increase the dose of morphine in opioid-tolerant patients. To pursue this avenue further, it would be of interest to test the behavioral consequences of PKC inhibition following the development of opioid tolerance. This would provide the community with more information about the critical role of PKC in the temporal regulation of MOPr recycling.

Given the broad range of negative side effects associated opioid use, it is indeed a worthwhile endeavor to seek alternative pharmacological interventions to address chronic pain. The primary motivation behind Chapter 4 of this thesis is the proof-of-concept validation that the non-opioid GPCR, GPR171, is a therapeutic target for chronic pain. The identification of GPR171 as an inhibitory GPCR that enhances the antinociceptive effects of morphine in acute pain tests, in addition to being present in the same vlPAG neurons as the MOPr, was a pharmacological similarity to the MOPr that drove the curiosity behind this study. It was a noteworthy observation that sexual dimorphism emerged when assessing the anti-hyperalgesic and anti-allodynic effects of the GPR171 agonist, MS15203. Given the existence of very few such novel pain therapeutics that display sex differences *in vivo*, the mechanistic underpinnings of this effect is deserving of further investigation. This observation also highlights the drawbacks of therapeutics development without consideration of sex as a biological variable.

In this thesis, the mouse ventrolateral periaqueductal gray has been shown to exhibit heightened intracellular protein kinase activation after morphine tolerance. Several of these alterations have been demonstrated in females for first time, including differential localization of kinases and their

substrates after morphine tolerance. Manipulation of PKC activity specifically within the vlPAG has been shown for the first time *in vivo* to modulate morphine tolerance. These results advance our understanding of intracellular processes that are altered in a critical pain processing center of the brain as a result of chronic morphine treatment. Further, this thesis describes an *in vivo* application of a novel chronic pain therapeutic and advances our knowledge of the receptor GPR171 as a target for pain therapeutics.

# REFERENCES


[1] M. M. Behbehani and H. L. Fields, "Evidence that an excitatory connection between the periaqueductal gray and nucleus raphe magnus mediates stimulation produced analgesia," *Brain Research*, vol. 170, no. 1, pp. 85–93, 1979.

[2] M. M. Godoi, H. Z. Junior, J. M. da Cunha, and J. M. Zanoveli, "Mu-opioid and cb1 cannabinoid receptors of the dorsal periaqueductal gray interplay in the regulation of fear response, but not antinociception," *Pharmacology Biochemistry and Behavior*, vol. 194, p. 172938, 2020.

[3] L. F. Ferrari, J. Pei, M. Zickella, C. Rey, J. Zickella, A. Ramirez, and N. E. Taylor, "D2 receptors in the periaqueductal gray/dorsal raphe modulate peripheral inflammatory hyperalgesia via the rostral ventral medulla," *Neuroscience*, 2021.

[4] M. Morgan, M. Heinricher, and H. Fields, "Circuitry linking opioid-sensitive nociceptive modulatory systems in periaqueductal gray and spinal cord with rostral ventromedial medulla," *Neuroscience*, vol. 47, no. 4, pp. 863–871, 1992.

[5] M. S. Moss, E. J. Glazer, and A. I. Basbaum, "The peptidergic organization of the cat periaqueductal gray. i. the distribution of immunoreactive enkephalin-containing neurons and terminals," *Journal of Neuroscience*, vol. 3, no. 3, pp. 603–616, 1983.

[6] L. M. Lueptow, A. K. Fakira, and E. N. Bobeck, "The contribution of the descending pain modulatory pathway in opioid tolerance," *Frontiers in Neuroscience*, vol. 12, p. 886, 2018.

[7] W. M. Compton and N. D. Volkow, "Major increases in opioid analgesic abuse in the united states: concerns and strategies," *Drug and Alcohol Dependence*, vol. 81, no. 2, pp. 103–107, 2006.

[8] A. Koehl, H. Hu, S. Maeda, Y. Zhang, Q. Qu, J. M. Paggi, N. R. Latorraca, D. Hilger, R. Dawson, H. Matile *et al.*, "Structure of the $\mu$-opioid receptor–g i protein complex," *Nature*, vol. 558, no. 7711, pp. 547–552, 2018.

[9] M. Heinricher, I. Tavares, J. Leith, and B. Lumb, "Descending control of nociception: specificity, recruitment and plasticity," *Brain Research Reviews*, vol. 60, no. 1, pp. 214–225, 2009.

[10] E. N. Bobeck, Q. Chen, M. M. Morgan, and S. L. Ingram, "Contribution of adenylyl cyclase modulation of pre-and postsynaptic GABA neurotransmission to morphine antinociception and tolerance," *Neuropsychopharmacology*, vol. 39, no. 9, pp. 2142–2152, 2014.

[11] X. Chen, H. G. Marrero, R. Murphy, Y.-J. Lin, and J. E. Freedman, "Altered gating of opiate receptor-modulated k+ channels on amygdala neurons of morphine-dependent rats," *Proceedings of the National Academy of Sciences*, vol. 97, no. 26, pp. 14 692–14 696, 2000.

[12] J. L. Whistler and M. Von Zastrow, "Morphine-activated opioid receptors elude desensitization by $\beta$-arrestin," *Proceedings of the National Academy of Sciences*, vol. 95, no. 17, pp. 9914–9919, 1998.

[13] H. Zheng, H. H. Loh, and P.-Y. Law, "$\beta$-arrestin-dependent $\mu$-opioid receptor-activated extracellular signal-regulated kinases (ERKs) translocate to nucleus in contrast to G protein-dependent ERK activation," *Molecular Pharmacology*, vol. 73, no. 1, pp. 178–190, 2008.

[14] T. A. Macey, E. N. Bobeck, D. M. Hegarty, S. A. Aicher, S. L. Ingram, and M. M. Morgan, "Extracellular signal-regulated kinase 1/2 activation counteracts morphine tolerance in the periaqueductal gray of the rat," *Journal of Pharmacology and Experimental Therapeutics*, vol. 331, no. 2, pp. 412–418, 2009.

[15] A. Sorkin and M. Von Zastrow, "Endocytosis and signalling: intertwining molecular networks," *Nature Reviews Molecular Cell Biology*, vol. 10, no. 9, pp. 609–622, 2009.

[16] C. Mazzucchelli, C. Vantaggiato, A. Ciamei, S. Fasano, P. Pakhotin, W. Krezel, H. Welzl, D. P. Wolfer, G. Pagès, O. Valverde *et al.*, "Knockout of erk1 map kinase enhances synaptic plasticity in the striatum and facilitates striatal-mediated learning and memory," *Neuron*, vol. 34, no. 5, pp. 807–820, 2002.

[17] M. Thomas, P. Kalivas, and Y. Shaham, "Neuroplasticity in the mesolimbic dopamine system and cocaine addiction," *British Journal of Pharmacology*, vol. 154, no. 2, pp. 327–342, 2008.

[18] M. M. Morgan, R. A. Reid, and K. A. Saville, "Functionally selective signaling for morphine and fentanyl antinociception and tolerance mediated by the rat periaqueductal gray," *PloS One*, vol. 9, no. 12, p. e114269, 2014.

[19] E. N. Bobeck, S. L. Ingram, S. M. Hermes, S. A. Aicher, and M. M. Morgan, "Ligand-biased activation of extracellular signal-regulated kinase 1/2 leads to differences in opioid induced antinociception and tolerance," *Behavioural Brain Research*, vol. 298, pp. 17–24, 2016.

[20] C. C. King, M. Sastri, P. Chang, J. Pennypacker, and S. S. Taylor, "The rate of nf-$\kappa$b nuclear translocation is regulated by PKA and A kinase interacting protein 1," *PloS One*, vol. 6, no. 4, p. e18713, 2011.

[21] T. Avidor-Reiss, I. Nevo, R. Levy, T. Pfeuffer, and Z. Vogel, "Chronic opioid treatment induces adenylyl cyclase v superactivation involvement of G$\beta\gamma$," *Journal of Biological Chemistry*, vol. 271, no. 35, pp. 21 309–21 315, 1996.

[22] P. Sánchez-Blázquez, M. Rodríguez-Muñoz, and J. Garzón, "Mu-opioid receptors transiently activate the Akt-nNOS pathway to produce sustained potentiation of PKC-mediated NMDAR-CaMKII signaling," *PloS One*, vol. 5, no. 6, 2010.

[23] G. Grecksch, S. Just, C. Pierstorff, A.-K. Imhof, L. Glück, C. Doll, A. Lupp, A. Becker, T. Koch, R. Stumm *et al.*, "Analgesic tolerance to high-efficacy agonists but not to morphine is diminished in phosphorylation-deficient s375a $\mu$-opioid receptor knock-in mice," *Journal of Neuroscience*, vol. 31, no. 39, pp. 13 890–13 896, 2011.

[24] S. Illing, A. Mann, and S. Schulz, "Heterologous regulation of agonist-independent $\mu$-opioid receptor phosphorylation by protein kinase c," *British journal of pharmacology*, vol. 171, no. 5, pp. 1330–1340, 2014.

[25] A. Mann, S. Illing, E. Miess, and S. Schulz, "Different mechanisms of homologous and heterologous $\mu$-opioid receptor phosphorylation," *British journal of pharmacology*, vol. 172, no. 2, pp. 311–316, 2015.

[26] R. A. Wise and G. F. Koob, "The development and maintenance of drug addiction," *Neuropsychopharmacology*, vol. 39, no. 2, pp. 254–262, 2014.

[27] N. Volkow, H. Benveniste, and A. T. McLellan, "Use and misuse of opioids in chronic pain," *Annual Review of Medicine*, vol. 69, pp. 451–465, 2018.

[28] F. Wolfe, B. Walitt, S. Perrot, J. J. Rasker, and W. Häuser, "Fibromyalgia diagnosis and biased assessment: Sex, prevalence and bias," *PloS one*, vol. 13, no. 9, p. e0203755, 2018.

[29] T. Victor, X. Hu, J. Campbell, D. Buse, and R. Lipton, "Migraine prevalence by age and sex in the united states: a life-span study," *Cephalalgia*, vol. 30, no. 9, pp. 1065–1072, 2010.

[30] C. S. Zin, L.-C. Chen, and R. D. Knaggs, "Changes in trends and pattern of strong opioid prescribing in primary care," *European Journal of Pain*, vol. 18, no. 9, pp. 1343–1351, 2014.

[31] R. M. Shansky and A. Z. Murphy, "Considering sex as a biological variable will require a global shift in science culture," *Nature Neuroscience*, pp. 1–8, 2021.

[32] A. Manglik, H. Lin, D. K. Aryal, J. D. McCorvy, D. Dengler, G. Corder, A. Levit, R. C. Kling, V. Bernat, H. Hübner *et al.*, "Structure-based discovery of opioid analgesics with reduced side effects," *Nature*, vol. 537, no. 7619, pp. 185–190, 2016.

[33] S. Sierra, A. Gupta, I. Gomes, M. Fowkes, A. Ram, E. N. Bobeck, and L. A. Devi, "Targeting cannabinoid 1 and delta opioid receptor heteromers alleviates chemotherapy-induced neuropathic pain," *ACS Pharmacology & Translational Science*, vol. 2, no. 4, pp. 219–229, 2019.

[34] W. Fujita, I. Gomes, and L. A. Devi, "Heteromers of $\mu$-$\delta$ opioid receptors: new pharmacology and novel therapeutic possibilities," *British journal of pharmacology*, vol. 172, no. 2, pp. 375–387, 2015.

[35] C. J. Woolf, "Capturing novel non-opioid pain targets," *Biological psychiatry*, vol. 87, no. 1, pp. 74–81, 2020.

[36] M. A. Tarselli, K. M. Raehal, A. K. Brasher, J. M. Streicher, C. E. Groer, M. D. Cameron, L. M. Bohn, and G. C. Micalizio, "Synthesis of conolidine, a potent non-opioid analgesic for tonic and persistent pain," *Nature chemistry*, vol. 3, no. 6, pp. 449–453, 2011.

[37] I. Gomes, D. K. Aryal, J. H. Wardman, A. Gupta, K. Gagnidze, R. M. Rodriguiz, S. Kumar, W. C. Wetsel, J. E. Pintar, L. D. Fricker *et al.*, "Gpr171 is a hypothalamic g protein-coupled receptor for biglen, a neuropeptide involved in feeding," *Proceedings of the National Academy of Sciences*, vol. 110, no. 40, pp. 16 211–16 216, 2013.

[38] J. H. Wardman, I. Gomes, E. N. Bobeck, J. A. Stockert, A. Kapoor, P. Bisignano, A. Gupta, M. Mezei, S. Kumar, M. Filizola *et al.*, "Identification of a small-molecule ligand that activates the neuropeptide receptor gpr171 and increases food intake," *Science Signaling*, vol. 9, no. 430, pp. ra55–ra55, 2016.

[39] E. S. Lein, M. J. Hawrylycz, N. Ao, M. Ayres, A. Bensinger, A. Bernard, A. F. Boe, M. S. Boguski, K. S. Brockway, E. J. Byrnes *et al.*, "Genome-wide atlas of gene expression in the adult mouse brain," *Nature*, vol. 445, no. 7124, pp. 168–176, 2007.

[40] M. V. McDermott, L. Afrose, I. Gomes, L. A. Devi, and E. N. Bobeck, "Opioid-induced signaling and antinociception are modulated by the recently deorphanized receptor, gpr171," *Journal of Pharmacology and Experimental Therapeutics*, vol. 371, no. 1, pp. 56–62, 2019.

[41] V. Tortorici, M. M. Morgan, and H. Vanegas, "Tolerance to repeated microinjection of morphine into the periaqueductal gray is associated with changes in the behavior of off-and on-cells in the rostral ventromedial medulla of rats," *Pain*, vol. 89, no. 2-3, pp. 237–244, 2001.

[42] D. A. Lane, V. Tortorici, and M. M. Morgan, "Behavioral and electrophysiological evidence for tolerance to continuous morphine administration into the ventrolateral periaqueductal gray," *Neuroscience*, vol. 125, no. 1, pp. 63–69, 2004.

[43] M. M. Morgan, C. C. Clayton, and D. A. Lane, "Behavioral evidence linking opioid-sensitive GABAergic neurons in the ventrolateral periaqueductal gray to morphine tolerance," *Neuroscience*, vol. 118, no. 1, pp. 227–232, 2003.

[44] H. Fields, "State-dependent opioid control of pain," *Nature Reviews Neuroscience*, vol. 5, no. 7, pp. 565–575, 2004.

[45] S. L. Ingram, C. W. Vaughan, E. E. Bagley, M. Connor, and M. J. Christie, "Enhanced opioid efficacy in opioid dependence is caused by an altered signal transduction pathway," *Journal of Neuroscience*, vol. 18, no. 24, pp. 10 269–10 276, 1998.

[46] N. Mittal, M. Tan, O. Egbuta, N. Desai, C. Crawford, C.-W. Xie, C. Evans, and W. Walwyn, "Evidence that behavioral phenotypes of morphine in $\beta$-arr2-/- mice are due to the unmasking of jnk signaling," *Neuropsychopharmacology*, vol. 37, no. 8, pp. 1953–1962, 2012.

[47] B. H. Gabra, C. P. Bailey, E. Kelly, F. L. Smith, G. Henderson, and W. L. Dewey, "Pretreatment with a PKC or PKA inhibitor prevents the development of morphine tolerance but not physical dependence in mice," *Brain Research*, vol. 1217, pp. 70–77, 2008.

[48] E. J. Melief, M. Miyatake, M. R. Bruchas, and C. Chavkin, "Ligand-directed c-Jun N-terminal kinase activation disrupts opioid receptor signaling," *Proceedings of the National Academy of Sciences*, vol. 107, no. 25, pp. 11 608–11 613, 2010.

[49] R. E. Bartok and R. M. Craft, "Sex differences in opioid antinociception," *Journal of Pharmacology and Experimental Therapeutics*, vol. 282, no. 2, pp. 769–778, 1997.

[50] D. R. Loyd, M. M. Morgan, and A. Z. Murphy, "Sexually dimorphic activation of the periaqueductal gray–rostral ventromedial medullary circuit during the development of tolerance to morphine in the rat," *European Journal of Neuroscience*, vol. 27, no. 6, pp. 1517–1524, 2008.

[51] E. E. Abdelhamid, M. Sultana, P. Portoghese, and A. Takemori, "Selective blockage of delta opioid receptors prevents the development of morphine tolerance and dependence in mice." *Journal of Pharmacology and Experimental Therapeutics*, vol. 258, no. 1, pp. 299–303, 1991.

[52] H. Ueda, T. Yamaguchi, S. Tokuyama, M. Inoue, M. Nishi, and H. Takeshima, "Partial loss of tolerance liability to morphine analgesia in mice lacking the nociceptin receptor gene," *Neuroscience letters*, vol. 237, no. 2-3, pp. 136–138, 1997.

[53] L. M. Bohn, R. J. Lefkowitz, and M. G. Caron, "Differential mechanisms of morphine antinociceptive tolerance revealed in $\beta$arrestin-2 knock-out mice," *Journal of Neuroscience*, vol. 22, no. 23, pp. 10 494–10 500, 2002.

[54] J. A. Morón, S. Gullapalli, C. Taylor, A. Gupta, I. Gomes, and L. A. Devi, "Modulation of opiate-related signaling molecules in morphine-dependent conditioned behavior: conditioned place preference to morphine induces creb phosphorylation," *Neuropsychopharmacology*, vol. 35, no. 4, pp. 955–966, 2010.

[55] C. A. Fairbanks and G. L. Wilcox, "Spinal antinociceptive synergism between morphine and clonidine persists in mice made acutely or chronically tolerant to morphine," *Journal of Pharmacology and Experimental Therapeutics*, vol. 288, no. 3, pp. 1107–1116, 1999.

[56] G. Paxinos and K. B. Franklin, *The mouse brain in stereotaxic coordinates*. Academic Press, 2019.

[57] S. K. Suckow, E. L. Deichsel, S. L. Ingram, M. M. Morgan, and S. A. Aicher, "Columnar distribution of catecholaminergic neurons in the ventrolateral periaqueductal gray and their relationship to efferent pathways," *Synapse*, vol. 67, no. 2, pp. 94–108, 2013.

[58] M. M. Morgan, K. L. Whittier, D. M. Hegarty, and S. A. Aicher, "Periaqueductal gray neurons project to spinally projecting gabaergic neurons in the rostral ventromedial medulla," *Pain*, vol. 140, no. 2, pp. 376–386, 2008.

[59] E. E. Bagley and S. L. Ingram, "Endogenous opioid peptides in the descending pain modulatory circuit," *Neuropharmacology*, vol. 173, p. 108131, 2020.

[60] R. Levine, M. M. Morgan, J. T. Cannon, and J. C. Liebeskind, "Stimulation of the periaqueductal gray matter of the rat produces a preferential ipsilateral antinociception," *Brain Research*, vol. 567, no. 1, pp. 140–144, 1991.

[61] P. Marek, R. Yirmiya, and J. C. Liebeskind, "Stimulation-produced analgesia in the mouse: evidence for laterality of opioid mediation," *Brain Research*, vol. 541, no. 1, pp. 154–156, 1991.

[62] A. Gupta, W. Fujita, I. Gomes, E. Bobeck, and L. A. Devi, "Endothelin-converting enzyme 2 differentially regulates opioid receptor activity," *British Journal of Pharmacology*, vol. 172, no. 2, pp. 704–719, 2015.

[63] S. Eitan, C. D. Bryant, N. Saliminejad, Y. C. Yang, E. Vojdani, D. Keith, R. Polakiewicz, and C. J. Evans, "Brain region-specific mechanisms for acute morphine-induced mitogen-activated protein kinase modulation and distinct patterns of activation during analgesic tolerance and locomotor sensitization," *Journal of Neuroscience*, vol. 23, no. 23, pp. 8360–8369, 2003.

[64] M. Tanowitz and M. von Zastrow, "A novel endocytic recycling signal that distinguishes the membrane trafficking of naturally occurring opioid receptors," *Journal of Biological Chemistry*, vol. 278, no. 46, pp. 45 978–45 986, 2003.

[65] K. Niikura, M. Narita, E. R. Butelman, M. J. Kreek, and T. Suzuki, "Neuropathic and chronic pain stimuli downregulate central $\mu$-opioid and dopaminergic transmission," *Trends in Pharmacological Sciences*, vol. 31, no. 7, pp. 299–305, 2010.

[66] S. Civciristov, C. Huang, B. Liu, E. A. Marquez, A. B. Gondin, R. B. Schittenhelm, A. M. Ellisdon, M. Canals, and M. L. Halls, "Ligand-dependent spatiotemporal signaling profiles of the $\mu$-opioid receptor are controlled by distinct protein-interaction networks," *Journal of Biological Chemistry*, vol. 294, no. 44, pp. 16 198–16 213, 2019.

[67] T. A. Macey, E. N. Bobeck, K. Suchland, M. M. Morgan, and S. L. Ingram, "Change in functional selectivity of morphine with the development of antinociceptive tolerance," *British Journal of Pharmacology*, vol. 172, no. 2, pp. 549–561, 2015.

[68] D. Calebiro, V. O. Nikolaev, L. Persani, and M. J. Lohse, "Signaling by internalized G-protein-coupled receptors," *Trends in Pharmacological Sciences*, vol. 31, no. 5, pp. 221–228, 2010.

[69] Y. Daaka, L. M. Luttrell, S. Ahn, G. J. Della Rocca, S. S. Ferguson, M. G. Caron, and R. J. Lefkowitz, "Essential role for G protein-coupled receptor endocytosis in the activation of mitogen-activated protein kinase," *Journal of Biological Chemistry*, vol. 273, no. 2, pp. 685–688, 1998.

[70] A. C. Hanyaloglu and M. v. Zastrow, "Regulation of gpcrs by endocytic membrane trafficking and its potential implications," *Annu. Rev. Pharmacol. Toxicol.*, vol. 48, pp. 537–568, 2008.

[71] N. N. Jimenez-Vargas, J. Gong, M. J. Wisdom, D. D. Jensen, R. Latorre, A. Hegron, S. Teng, J. J. DiCello, P. Rajasekhar, N. A. Veldhuis *et al.*, "Endosomal signaling of delta opioid receptors is an endogenous mechanism and therapeutic target for relief from inflammatory pain," *Proceedings of the National Academy of Sciences*, vol. 117, no. 26, pp. 15 281–15 292, 2020.

[72] Z. Y. Weinberg, A. S. Zajac, T. Phan, D. J. Shiwarski, and M. A. Puthenveedu, "Sequence-specific regulation of endocytic lifetimes modulates arrestin-mediated signaling at the $\mu$ opioid receptor," *Molecular Pharmacology*, vol. 91, no. 4, pp. 416–427, 2017.

[73] K. Touhara, B. E. Hawes, T. van Biesen, and R. J. Lefkowitz, "G protein beta gamma subunits stimulate phosphorylation of shc adapter protein," *Proceedings of the National Academy of Sciences*, vol. 92, no. 20, pp. 9284–9287, 1995.

[74] A. Mestek, J. H. Hurley, L. S. Bye, A. D. Campbell, Y. Chen, M. Tian, J. Liu, H. Schulman, and L. Yu, "The human mu opioid receptor: modulation of functional desensitization by calcium/calmodulin-dependent protein kinase and protein kinase C," *Journal of Neuroscience*, vol. 15, no. 3, pp. 2396–2406, 1995.

[75] C. D. Mandyam, D. R. Thakker, J. L. Christensen, and K. M. Standifer, "Orphanin fq/nociceptin-mediated desensitization of opioid receptor-like 1 receptor and $\mu$ opioid receptors involves protein kinase C: a molecular mechanism for heterologous cross-talk," *Journal of Pharmacology and Experimental Therapeutics*, vol. 302, no. 2, pp. 502–509, 2002.

[76] J. Zhang, S. S. Ferguson, L. S. Barak, S. R. Bodduluri, S. A. Laporte, P.-Y. Law, and M. G. Caron, "Role for G protein-coupled receptor kinase in agonist-specific regulation of $\mu$-opioid receptor responsiveness," *Proceedings of the National Academy of Sciences*, vol. 95, no. 12, pp. 7157–7162, 1998.

[77] A. K. Finn and J. L. Whistler, "Endocytosis of the mu opioid receptor reduces tolerance and a cellular hallmark of opiate withdrawal," *Neuron*, vol. 32, no. 5, pp. 829–839, 2001.

[78] L. Martini and J. L. Whistler, "The role of mu opioid receptor desensitization and endocytosis in morphine tolerance and dependence," *Current Opinion in Neurobiology*, vol. 17, no. 5, pp. 556–564, 2007.

[79] L. C. Hull, J. Llorente, B. H. Gabra, F. L. Smith, E. Kelly, C. Bailey, G. Henderson, and W. Dewey, "The effect of protein kinase C and G protein-coupled receptor kinase inhibition on tolerance induced by $\mu$-opioid agonists of different efficacy," *Journal of Pharmacology and Experimental Therapeutics*, vol. 332, no. 3, pp. 1127–1135, 2010.

[80] D. A. Pena, M. L. Duarte, D. T. Pramio, L. A. Devi, and D. Schechtman, "Exploring morphine-triggered PKC-targets and their interaction with signaling pathways leading to pain via TrkA," *Proteomes*, vol. 6, no. 4, p. 39, 2018.

[81] C. P. Bailey, S. Oldfield, J. Llorente, C. J. Caunt, A. Teschemacher, L. Roberts, C. McArdle, F. Smith, W. Dewey, E. Kelly *et al.*, "Involvement of PKC$\alpha$ and G-protein-coupled receptor kinase 2 in agonist-selective desensitization of $\mu$-opioid receptors in mature brain neurons," *British Journal of Pharmacology*, vol. 158, no. 1, pp. 157–164, 2009.

[82] F. L. Smith, B. H. Gabra, P. A. Smith, M. C. Redwood, and W. L. Dewey, "Determination of the role of conventional, novel and atypical PKC isoforms in the expression of morphine tolerance in mice," *Pain*, vol. 127, no. 1-2, pp. 129–139, 2007.

[83] H. Ueda, M. Inoue, and T. Matsumoto, "Protein kinase c-mediated inhibition of $\mu$-opioid receptor internalization and its involvement in the development of acute tolerance to peripheral $\mu$-agonist analgesia," *Journal of Neuroscience*, vol. 21, no. 9, pp. 2967–2973, 2001.

[84] V. Rubovitch, M. Gafni, and Y. Sarne, "The mu opioid agonist damgo stimulates camp production in sk-n-sh cells through a plc–pkc–ca++ pathway," *Molecular brain research*, vol. 110, no. 2, pp. 261–266, 2003.

[85] S. K. Sharma, W. A. Klee, and M. Nirenberg, "Dual regulation of adenylate cyclase accounts for narcotic dependence and tolerance," *Proceedings of the National Academy of Sciences*, vol. 72, no. 8, pp. 3092–3096, 1975.

[86] A. Bonci and J. T. Williams, "Increased probability of GABA release during withdrawal from morphine," *Journal of Neuroscience*, vol. 17, no. 2, pp. 796–803, 1997.

[87] L. He, J. Fong, M. Von Zastrow, and J. L. Whistler, "Regulation of opioid receptor trafficking and morphine tolerance by receptor oligomerization," *Cell*, vol. 108, no. 2, pp. 271–282, 2002.

[88] M. Sastri, D. M. Barraclough, P. T. Carmichael, and S. S. Taylor, "A-kinase-interacting protein localizes protein kinase A in the nucleus," *Proceedings of the National Academy of Sciences*, vol. 102, no. 2, pp. 349–354, 2005.

[89] R. M. Craft, J. A. Stratmann, R. E. Bartok, T. I. Walpole, and S. J. King, "Sex differences in development of morphine tolerance and dependence in the rat," *Psychopharmacology*, vol. 143, no. 1, pp. 1–7, 1999.

[90] A. C. Barrett, C. D. Cook, J. M. Terner, R. M. Craft, and M. J. Picker, "Importance of sex and relative efficacy at the $\mu$ opioid receptor in the development of tolerance and cross-tolerance to the antinociceptive effects of opioids," *Psychopharmacology*, vol. 158, no. 2, pp. 154–164, 2001.

[91] H. H. Doyle, L. N. Eidson, D. M. Sinkiewicz, and A. Z. Murphy, "Sex differences in microglia activity within the periaqueductal gray of the rat: a potential mechanism driving the dimorphic effects of morphine," *Journal of Neuroscience*, vol. 37, no. 12, pp. 3202–3214, 2017.

[92] S. C. Roerig, S. M. O'Brien, J. M. Fujimoto, and G. L. Wilcox, "Tolerance to morphine analgesia: decreased multiplicative interaction between spinal and supraspinal sites," *Brain Research*, vol. 308, no. 2, pp. 360–363, 1984.

[93] B. C. Yoburn, K. Lutfy, S. Azimuddin, and V. Sierra, "Differentiation of spinal and supraspinal opioid receptors by morphine tolerance," *Life Sciences*, vol. 46, no. 5, pp. 343–350, 1990.

[94] V. Jokinen, Y. Sidorova, H. Viisanen, I. Suleymanova, H. Tiilikainen, Z. Li, T. Lilius, K. Mätlik, J. Anttila, M. Airavaara, L. Tian, P. Rauhala, and E. Kalso, "Differential spinal and supraspinal activation of glia in a rat model of morphine tolerance," *Neuroscience*, vol. 375, pp. 10–24, 2018.

[95] E. Valjent, C. Pagès, D. Hervé, J.-A. Girault, and J. Caboche, "Addictive and non-addictive drugs induce distinct and specific patterns of ERK activation in mouse brain," *European Journal of Neuroscience*, vol. 19, no. 7, pp. 1826–1836, 2004.

[96] M. D. Sanna, C. Ghelardini, and N. Galeotti, "Regionally selective activation of ERK and JNK in morphine paradoxical hyperalgesia: a step toward improving opioid pain therapy," *Neuropharmacology*, vol. 86, pp. 67–77, 2014.

[97] E. J. Wagner, O. K. Rønnekleiv, and M. J. Kelly, "Protein kinase a maintains cellular tolerance tomu opioid receptor agonists in hypothalamic neurosecretory cells with chronic morphine treatment: Convergence on a common pathway with estrogen in modulating mu opioid receptor/effector coupling," *Journal of Pharmacology and Experimental Therapeutics*, vol. 285, no. 3, pp. 1266–1273, 1998.

[98] P. E. Micevych and M. J. Kelly, "Membrane estrogen receptor regulation of hypothalamic function," *Neuroendocrinology*, vol. 96, no. 2, pp. 103–110, 2012.

[99] J. Qiu, M. A. Bosch, S. C. Tobias, D. K. Grandy, T. S. Scanlan, O. K. Rønnekleiv, and M. J. Kelly, "Rapid signaling of estrogen in hypothalamic neurons involves a novel G-protein-coupled estrogen receptor that activates protein kinase C," *Journal of Neuroscience*, vol. 23, no. 29, pp. 9529–9540, 2003.

[100] A. H. Lagrange, O. K. Rønnekleiv, and M. J. Kelly, "Modulation of G protein-coupled receptors by an estrogen receptor that activates protein kinase A," *Molecular Pharmacology*, vol. 51, no. 4, pp. 605–612, 1997.

[101] M. Bruchas, B. Land, and C. Chavkin, "The dynorphin/kappa opioid system as a modulator of stress-induced and pro-addictive behaviors," *Brain research*, vol. 1314, pp. 44–55, 2010.

[102] M. Chattopadhyay, M. Mata, and D. J. Fink, "Continuous $\delta$-opioid receptor activation reduces neuronal voltage-gated sodium channel (nav1. 7) levels through activation of protein kinase c in painful diabetic neuropathy," *Journal of Neuroscience*, vol. 28, no. 26, pp. 6652–6658, 2008.

[103] E. A. Johnson, S. Oldfield, E. Braksator, A. Gonzalez-Cuello, D. Couch, K. J. Hall, S. J. Mundell, C. P. Bailey, E. Kelly, and G. Henderson, "Agonist-selective mechanisms of $\mu$-opioid receptor desensitization in human embryonic kidney 293 cells," *Molecular Pharmacology*, vol. 70, no. 2, pp. 676–685, 2006.

[104] F. L. Smith, R. Javed, M. J. Elzey, S. P. Welch, D. Selley, L. Sim-Selley, and W. L. Dewey, "Prolonged reversal of morphine tolerance with no reversal of dependence by protein kinase c inhibitors," *Brain Research*, vol. 958, no. 1, pp. 28–35, 2002.

[105] H.-J. Lee, L.-Y. Chang, Y.-C. Ho, S.-F. Teng, L.-L. Hwang, K. Mackie, and L.-C. Chiou, "Stress induces analgesia via orexin 1 receptor-initiated endocannabinoid/cb1 signaling in the mouse periaqueductal gray," *Neuropharmacology*, vol. 105, pp. 577–586, 2016.

[106] E. N. Bobeck, R. A. Haseman, D. Hong, S. L. Ingram, and M. M. Morgan, "Differential development of antinociceptive tolerance to morphine and fentanyl is not linked to efficacy in the ventrolateral periaqueductal gray of the rat," *The Journal of Pain*, vol. 13, no. 8, pp. 799–807, 2012.

[107] M. A. Bernstein and S. P. Welch, "$\mu$-opioid receptor down-regulation and camp-dependent protein kinase phosphorylation in a mouse model of chronic morphine tolerance," *Molecular Brain Research*, vol. 55, no. 2, pp. 237–242, 1998.

[108] J. E. Zadina, S. L. Chang, L. Ge, and A. J. Kastin, "Mu opiate receptor down-regulation by morphine and up-regulation by naloxone in sh-sy5y human neuroblastoma cells." *Journal of Pharmacology and Experimental Therapeutics*, vol. 265, no. 1, pp. 254–262, 1993.

[109] J. Xu, A. J. Faskowitz, G. C. Rossi, M. Xu, Z. Lu, Y.-X. Pan, and G. W. Pasternak, "Stabilization of morphine tolerance with long-term dosing: association with selective upregulation of mu-opioid receptor splice variant mrnas," *Proceedings of the National Academy of Sciences*, vol. 112, no. 1, pp. 279–284, 2015.

[110] G. Fabian, B. Bozo, M. Szikszay, G. Horvath, C. Coscia, and M. Szücs, "Chronic morphine-induced changes in $\mu$-opioid receptors and g proteins of different subcellular loci in rat brain," *Journal of Pharmacology and Experimental Therapeutics*, vol. 302, no. 2, pp. 774–780, 2002.

[111] F. L. Smith, R. R. Javed, M. J. Elzey, and W. L. Dewey, "The expression of a high level of morphine antinociceptive tolerance in mice involves both pkc and pka," *Brain research*, vol. 985, no. 1, pp. 78–88, 2003.

[112] C. P. Bailey, F. L. Smith, E. Kelly, W. L. Dewey, and G. Henderson, "How important is protein kinase c in $\mu$-opioid receptor desensitization and morphine tolerance?" *Trends in pharmacological sciences*, vol. 27, no. 11, pp. 558–565, 2006.

[113] J.-G. Liu and K. Anand, "Protein kinases modulate the cellular adaptations associated with opioid tolerance and dependence," *Brain Research Reviews*, vol. 38, no. 1-2, pp. 1–19, 2001.

[114] E. F. Fullerton, H. H. Doyle, and A. Z. Murphy, "Impact of sex on pain and opioid analgesia: a review," *Current opinion in behavioral sciences*, vol. 23, pp. 183–190, 2018.

[115] J. Dahlhamer, J. Lucas, C. Zelaya, R. Nahin, S. Mackey, L. DeBar, R. Kerns, M. Von Korff, L. Porter, and C. Helmick, "Prevalence of chronic pain and high-impact chronic pain among adults—united states, 2016," *Morbidity and Mortality Weekly Report*, vol. 67, no. 36, p. 1001, 2018.

[116] N. E. Burma, H. Leduc-Pessah, C. Y. Fan, and T. Trang, "Animal models of chronic pain: advances and challenges for clinical translation," *Journal of Neuroscience Research*, vol. 95, no. 6, pp. 1242–1256, 2017.

[117] J. S. Mogil, "Sex differences in pain and pain inhibition: multiple explanations of a controversial phenomenon," *Nature Reviews Neuroscience*, vol. 13, no. 12, pp. 859–866, 2012.

[118] K. J. Tonsfeldt, K. L. Suchland, K. A. Beeson, J. D. Lowe, M.-h. Li, and S. L. Ingram, "Sex differences in gabaa signaling in the periaqueductal gray induced by persistent inflammation," *Journal of Neuroscience*, vol. 36, no. 5, pp. 1669–1681, 2016.

[119] M. de Mos, A. De Bruijn, F. Huygen, J. Dieleman, B. C. Stricker, and M. Sturkenboom, "The incidence of complex regional pain syndrome: a population-based study," *Pain*, vol. 129, no. 1-2, pp. 12–20, 2007.

[120] C. Barnabe, L. Bessette, C. Flanagan, S. LeClercq, A. Steiman, F. Kalache, T. Kung, J. E. Pope, B. Haraoui, J. Hochman *et al.*, "Sex differences in pain scores and localization in inflammatory arthritis: a systematic review and metaanalysis," *The Journal of Rheumatology*, vol. 39, no. 6, pp. 1221–1230, 2012.

[121] M. T. Hannan, "Epidemiologic perspectives on women and arthritis: an overview," *Arthritis & Rheumatism: Official Journal of the American College of Rheumatology*, vol. 9, no. 6, pp. 424–434, 1996.

[122] R. B. Fillingim, C. D. King, M. C. Ribeiro-Dasilva, B. Rahim-Williams, and J. L. Riley III, "Sex, gender, and pain: a review of recent clinical and experimental findings," *The Journal of Pain*, vol. 10, no. 5, pp. 447–485, 2009.

[123] E. V. Shekunova and A. Y. Bespalov, "Estrous cycle stage-dependent expression of acute tolerance to morphine analgesia in rats," *European Journal of Pharmacology*, vol. 486, no. 3, pp. 259–264, 2004.

[124] L. Gottesman-Katz, R. Latorre, S. Vanner, B. L. Schmidt, and N. W. Bunnett, "Targeting g protein-coupled receptors for the treatment of chronic pain in the digestive system," *Gut*, 2020.

[125] O. Cabral-Marques, A. Marques, L. M. Giil, R. De Vito, J. Rademacher, J. Günther, T. Lange, J. Y. Humrich, S. Klapa, S. Schinke *et al.*, "Gpcr-specific autoantibody signatures are associated with physiological and pathological immune homeostasis," *Nature Communications*, vol. 9, no. 1, pp. 1–14, 2018.

[126] K. A. Jacobson, L. A. Giancotti, F. Lauro, F. Mufti, and D. Salvemini, "Treatment of chronic neuropathic pain: Purine receptor modulation," *Pain*, vol. 161, no. 7, pp. 1425–1441, 2020.

[127] P. A. Insel, K. Sriram, M. W. Gorr, S. Z. Wiley, A. Michkov, C. Salmerón, and A. M. Chinn, "Gpcromics: an approach to discover gpcr drug targets," *Trends in Pharmacological Sciences*, vol. 40, no. 6, pp. 378–387, 2019.

[128] A. S. Hauser, M. M. Attwood, M. Rask-Andersen, H. B. Schiöth, and D. E. Gloriam, "Trends in gpcr drug discovery: new agents, targets and indications," *Nature reviews Drug discovery*, vol. 16, no. 12, pp. 829–842, 2017.

[129] P. E. Khoonsari, S. Musunri, S. Herman, C. I. Svensson, L. Tanum, T. Gordh, and K. Kultima, "Systematic analysis of the cerebrospinal fluid proteome of fibromyalgia patients," *Journal of Proteomics*, vol. 190, pp. 35–43, 2019.

[130] D. A. Krishna, N. Yang, E. V. Romanova, S. S. Rubakhin, A. Tipton, I. Dripps, Z. Sheets, J. V. Sweedler, and A. A. Pradhan, "Pacap and other neuropeptide targets link chronic migraine and opioid-induced hyperalgesia in mouse models," *Molecular & Cellular Proteomics*, vol. 18, no. 12, pp. 2447–2458, 2019.

[131] S. M. Mack, I. Gomes, and L. A. Devi, "Neuropeptide pen and its receptor gpr83: distribution, signaling, and regulation," *ACS Chemical Neuroscience*, vol. 10, no. 4, pp. 1884–1891, 2019.

[132] A. Wilson-Poe, M. Morgan, S. Aicher, and D. Hegarty, "Distribution of cb1 cannabinoid receptors and their relationship with mu-opioid receptors in the rat periaqueductal gray," *Neuroscience*, vol. 213, pp. 191–200, 2012.

[133] H. Wang and M. Wessendorf, "$\mu$-and $\delta$-opioid receptor mrnas are expressed in periaqueductal gray neurons projecting to the rostral ventromedial medulla," *Neuroscience*, vol. 109, no. 3, pp. 619–634, 2002.

[134] Y. Chen, M. K. Boettger, A. Reif, A. Schmitt, N. Üçeyler, and C. Sommer, "Nitric oxide synthase modulates cfa-induced thermal hyperalgesia through cytokine regulation in mice," *Molecular Pain*, vol. 6, no. 1, pp. 1–11, 2010.

[135] M. Cheah, J. W. Fawcett, and M. R. Andrews, "Assessment of thermal pain sensation in rats and mice using the hargreaves test," *Bio-protocol*, vol. 7, no. 16, 2017.

[136] L. Deng, B. L. Cornett, K. Mackie, and A. G. Hohmann, "Cb1 knockout mice unveil sustained cb2-mediated antiallodynic effects of the mixed cb1/cb2 agonist cp55, 940 in a mouse model of paclitaxel-induced neuropathic pain," *Molecular Pharmacology*, vol. 88, no. 1, pp. 64–74, 2015.

[137] M. L. Duarte, N. A. Trimbake, A. Gupta, C. Tumanut, X. Fan, C. Woods, A. Ram, I. Gomes, E. N. Bobeck, D. Schechtman *et al.*, "High-throughput screening and validation of antibodies against synaptic proteins to explore opioid signaling dynamics," *Communications Biology*, vol. 4, no. 1, pp. 1–13, 2021.

[138] R. A. McCloy, S. Rogers, C. E. Caldon, T. Lorca, A. Castro, and A. Burgess, "Partial inhibition of cdk1 in g2 phase overrides the sac and decouples mitotic events," *Cell Cycle*, vol. 13, no. 9, pp. 1400–1412, 2014.

[139] P. S. Cho, H. K. Lee, Y. I. Choi, S. I. Choi, J. Y. Lim, M. Kim, H. Kim, S. J. Jung, and S. W. Hwang, "Gpr171 activation modulates nociceptor functions, alleviating pathologic pain," *Biomedicines*, vol. 9, no. 3, p. 256, 2021.

[140] J. Cheriyan and P. L. Sheets, "Altered excitability and local connectivity of mpfc-pag neurons in a mouse model of neuropathic pain," *Journal of Neuroscience*, vol. 38, no. 20, pp. 4829–4839, 2018.

[141] F. Knerlich-Lukoschus, M. Noack, B. von der Ropp-Brenner, R. Lucius, H. M. Mehdorn, and J. Held-Feindt, "Spinal cord injuries induce changes in cb1 cannabinoid receptor and cc chemokine expression in brain areas underlying circuitry of chronic pain conditions," *Journal of Neurotrauma*, vol. 28, no. 4, pp. 619–634, 2011.

[142] R. Kuner and H. Flor, "Structural plasticity and reorganisation in chronic pain," *Nature Reviews Neuroscience*, vol. 18, no. 1, p. 20, 2017.

[143] Y. Liu, A. Beyer, and R. Aebersold, "On the dependency of cellular protein levels on mrna abundance," *Cell*, vol. 165, no. 3, pp. 535–550, 2016.

[144] S. J. Thompson, M. H. Pitcher, L. S. Stone, F. Tarum, G. Niu, X. Chen, D. O. Kiesewetter, P. Schweinhardt, and M. C. Bushnell, "Chronic neuropathic pain reduces opioid receptor availability with associated anhedonia in rat," *Pain*, vol. 159, no. 9, p. 1856, 2018.

[145] S. Chakrabarti, L. A. Pattison, K. Singhal, J. R. Hockley, G. Callejo, and E. S. J. Smith, "Acute inflammation sensitizes knee-innervating sensory neurons and decreases mouse digging behavior in a trpv1-dependent manner," *Neuropharmacology*, vol. 143, pp. 49–62, 2018.

[146] H. Meziane, A.-M. Ouagazzal, L. Aubert, M. Wietrzych, and W. Krezel, "Estrous cycle effects on behavior of c57bl/6j and balb/cbyj female mice: implications for phenotyping strategies," *Genes, Brain and Behavior*, vol. 6, no. 2, pp. 192–200, 2007.

[147] D. R. Loyd, X. Wang, and A. Z. Murphy, "Sex differences in $\mu$-opioid receptor expression in the rat midbrain periaqueductal gray are essential for eliciting sex differences in morphine analgesia," *Journal of Neuroscience*, vol. 28, no. 52, pp. 14 007–14 017, 2008.

[148] R. E. Sorge, M. L. LaCroix-Fralish, A. H. Tuttle, S. G. Sotocinal, J.-S. Austin, J. Ritchie, M. L. Chanda, A. C. Graham, L. Topham, S. Beggs *et al.*, "Spinal cord toll-like receptor 4 mediates inflammatory and neuropathic hypersensitivity in male but not female mice," *Journal of Neuroscience*, vol. 31, no. 43, pp. 15 450–15 454, 2011.

[149] R. E. Sorge, J. C. Mapplebeck, S. Rosen, S. Beggs, S. Taves, J. K. Alexander, L. J. Martin, J.-S. Austin, S. G. Sotocinal, D. Chen *et al.*, "Different immune cells mediate mechanical pain hypersensitivity in male and female mice," *Nature Neuroscience*, vol. 18, no. 8, pp. 1081–1083, 2015.

[150] L. N. Eidson and A. Z. Murphy, "Blockade of toll-like receptor 4 attenuates morphine tolerance and facilitates the pain relieving properties of morphine," *Journal of Neuroscience*, vol. 33, no. 40, pp. 15 952–15 963, 2013.

[151] M. J. Patil, S. B. Ruparel, M. A. Henry, and A. N. Akopian, "Prolactin regulates trpv1, trpa1, and trpm8 in sensory neurons in a sex-dependent manner: Contribution of prolactin receptor to inflammatory pain," *American Journal of Physiology-Endocrinology and Metabolism*, vol. 305, no. 9, pp. E1154–E1164, 2013.

[152] X. Luo, Y. Gu, X. Tao, C. N. Serhan, and R.-R. Ji, "Resolvin d5 inhibits neuropathic and inflammatory pain in male but not female mice: distinct actions of d-series resolvins in chemotherapy-induced peripheral neuropathy," *Frontiers in Pharmacology*, vol. 10, p. 745, 2019.

[153] W. P. Staff, "The opioid files: Follow the post's investigation of the epidemic," *The Washington Post*.

[154] A. Gillis, A. Kliewer, E. Kelly, G. Henderson, M. J. Christie, S. Schulz, and M. Canals, "Critical assessment of g protein-biased agonism at the $\mu$-opioid receptor," *Trends in Pharmacological Sciences*, 2020.

[155] E. Kelly, "Efficacy and ligand bias at the $\mu$-opioid receptor," *British journal of pharmacology*, vol. 169, no. 7, pp. 1430–1446, 2013.

CURRICULUM VITAE

# Akila Ram

## EDUCATION

**Utah State University, Logan, UT** *August 2016 - August 2021*

Ph.D. Candidate in Biology

Dissertation: The Periaqueductal Gray in Opioid Tolerance and Chronic Pain.

Advisor: Dr. Erin N. Bobeck

**Kyoto University, Japan** *April 2014 - March 2016*

M.Sc. in Cellular and Molecular Biology

Dissertation: Transformed Cells are Sensitized to Cell Growth Arrest via FLASH Depletion.

Advisor: Dr. Shin Yonehara

**Anna University, India** *September 2009 - April 2013*

B.Tech. in Biotechnology

Thesis: Cloning of Pigment Epithelium Derived Factor and Immunoprecipitation from Human Umbilical Vein Endothelial Cells

## PEER-REVIEWED PUBLICATIONS

1. Salvador Sierra, Achla Gupta, Ivone Gomes, Mary Fowkes, **Akila Ram**, Erin N. Bobeck, and Lakshmi A. Devi. Targeting cannabinoid 1 and delta opioid receptor heteromers alleviates chemotherapy-induced neuropathic pain. *ACS Pharmacology & Translational Science* (2019).

2. Mariana L. Duarte, Nikita A. Trimbake, Achla Gupta, Xiaomin Fan, Catherine Woods, **Akila Ram**, Ivone Gomes, Erin N. Bobeck, Deborah Schechtman, and Lakshmi A. Devi. High

throughput functional screening for the development and validation of antibodies to synaptic proteins: A focus on opioid receptor signaling. *Communications Biology* (2021).

## MANUSCRIPTS UNDER REVISION

1. **Akila Ram**, Taylor M. Edwards, Ashley McCarty, Max V. McDermott, and Erin N. Bobeck. Morphine-induced Kinase Activation and Localization in the Periaqueductal Gray of Male and Female Mice.

2. **Akila Ram**, Taylor M. Edwards, Ashley McCarty, Leela Afrose, Max V. McDermott, and Erin N. Bobeck. GPR171 Agonist Reduces Chronic Neuropathic and Inflammatory Pain in Male, but not Female Mice.